



**WICHITA STATE  
UNIVERSITY**

**UNIVERSITY LIBRARIES**

**Strength and failure mode analysis of composite-  
to-composite and composite-to-metal single  
lap joints with different surface treatments**

Item Type	Thesis
Authors	Paranjpe, Nikhil
Publisher	Wichita State University
Rights	Copyright 2016 by Nikhil Paranjpe
Download date	2026-05-19 22:51:21
Link to Item	<a href="http://hdl.handle.net/10057/12872">http://hdl.handle.net/10057/12872</a>

STRENGTH AND FAILURE MODE ANALYSIS OF COMPOSITE-TO-COMPOSITE AND  
COMPOSITE-TO-METAL SINGLE LAP JOINTS WITH DIFFERENT SURFACE  
TREATMENTS

A Thesis by

Nikhil Paranjpe

Bachelor of Engineering, Rajiv Gandhi Proudyogiki Vishwavidyalaya, 2013

Submitted to the Department of Mechanical Engineering  
and the faculty of the Graduate School of  
Wichita State University  
in partial fulfillment of  
the requirements for the degree of  
Master of Science

July 2016

© Copyright 2016 by Nikhil Paranjpe  
All Rights Reserved

STRENGTH AND FAILURE MODE ANALYSIS OF COMPOSITE-TO-COMPOSITE AND  
COMPOSITE-TO-METAL SINGLE LAP JOINTS WITH DIFFERENT SURFACE  
TREATMENTS

The following faculty members have examined the final copy of this thesis for form and content, and recommend that it be accepted in partial fulfillment of the requirement for the degree of Master of Science with a major in Mechanical Engineering.

---

Ramazan Asmatulu, Committee Chair

---

Zheng Chen, Committee Member

---

Rajeev Nair, Committee Member

## DEDICATION

To my parents, my brother, my family, my teachers, and all my friends

## ACKNOWLEDGEMENTS

I express my sincere thanks to my advisor and committee chair, Dr. Ramazan Asmatulu, for providing me an opportunity to work under him as a research assistant. I deeply appreciate his continued guidance and support during the time of my research. I would also like to thank Dr. Zheng Chen and Dr. Rajeev Nair for serving as members of my thesis defense committee.

I am grateful to Royal Lovingfoss, Jeffery Gilchrist, and the National Institute of Aviation Research (NIAR) for helping me out with the tensile testing.

I am grateful to all my friends who motivated, guided, and helped me during my research work.

Lastly, I thank my parents and family for their support and inspiration, which led the way to the successful fulfilment of this research.

## ABSTRACT

Adhesives are widely utilized as a part of aviation, automotive, and marine industries. Adhesives are the glue-like materials used to join two surfaces together. Adhesive joints are gradually supplanting mechanical fasteners because they are lightweight structures and thus make an assembly lighter. They also act as a sealant to prevent a structural joint from galvanic corrosion. Adhesive bonds provide high joint strength because the load is distributed uniformly, while in mechanical joints, the load is concentrated at one point, thus leading to stress at that point and in turn causing joint failure.

This research concentrated on the analysis of bond strength and failure modes in an adhesive joint. The goal here was to prepare a joint with higher strength. In order to achieve a bond of the highest quality, it is important to consider all parameters required for adhesive bonding. Test results show that a composite-to-composite joint provides higher bond strength compared to a composite-to-aluminum joint. It was concluded that a combination of surface treatments gives better results than only one surface treatment method. Also, it was observed that surface sanding plays a predominant role in enhancing the bond strength. In addition, when plasma treatment of the composite surface and ultraviolet (UV) treatment of the metal surface were combined with surface sanding, the joint strength increased 36.57% in the case of a composite-to-aluminum joint when the aluminum surface was sanded and UV treated for eight days. On the other hand, in the case of a composite-to-composite joint, the joint strength increased 46.02% when the surface was sanded and plasma treated for 12 minutes. Thus, the combination of different surface preparations with sanding, rather than only one type of surface treatment, provides an ideal joint quality.

## TABLE OF CONTENTS

Chapter	Page
1. INTRODUCTION .....	1
1.1 Background.....	1
1.1.1 Composites.....	1
1.1.2 Adhesive Bonding.....	2
1.1.3 Adhesive Joints vs. Mechanical Joints.....	3
1.2 Motivation.....	4
1.3 Research Objective .....	4
2. LITERATURE REVIEW .....	6
2.1 Adhesion.....	6
2.1.1 Specific Adhesion.....	6
2.1.2 Mechanical Adhesion.....	6
2.2 Single Lap Joint .....	7
2.3 Mechanical Interlocking .....	8
2.4 Surface Preparation.....	9
2.4.1 Passive Surface Treatments .....	10
2.4.1.1 Mechanical Abrasion.....	10
2.4.1.2 Chemical Treatment.....	10
2.4.1.3 Degreasing .....	10
2.4.2 Active Surface Treatments.....	11
2.4.2.1 Plasma Treatment.....	11
2.4.2.2 Conversion Coating .....	12
2.4.2.3 Ultraviolet Treatment.....	12
2.5 Previous Studies .....	13
3. MATERIALS AND EXPERIMENTAL METHODS .....	24
3.1 Materials .....	24
3.1.1 Magnolia 6380 A/B Epoxy.....	24
3.1.2 Turco Alumiprep 33.....	24
3.1.3 Alodine 1201.....	25
3.1.4 Aluminum 2024 T-3 .....	25
3.1.5 Carbon Fiber Composites .....	25
3.2 Experimental Methods.....	26
3.2.1 Preparation of Carbon Fiber Composite Panels.....	26
3.2.2 Preparation of Aluminum Panels.....	29
3.2.3 Plasma Treatment.....	29
3.2.4 Water Contact Angle Test.....	31
3.2.5 Sandpaper Abrasion .....	33

TABLE OF CONTENTS (continued)

Chapter	Page
3.2.6 Surface Preparation.....	34
3.2.7 Alodine Coating.....	35
3.2.8 Preparation of Adhesive.....	35
3.2.9 Bonding Samples .....	37
3.2.10 Shear Strength Test.....	38
4. RESULTS AND DISCUSSIONS .....	42
5. CONCLUSION .....	83
6. FUTURE WORK .....	85
REFERENCES .....	86

## LIST OF TABLES

Table	Page
1.1. Comparison between adhesive joints and mechanical joints .....	3
3.1 Surface preparations for composite-to-composite single lap joint .....	40
3.2 Surface preparations for aluminum-to-composite single lap joint .....	40
4.1 Contact angles for composite base and sanded surfaces exposed to plasma for different times .....	42
4.2 Contact angle test results for aluminum with different surface preparations and plasma exposure .....	43
4.3 Joint strength and failure load when composite surfaces only detergent cleaned only .....	46
4.4 Joint strength and failure load when composite surfaces detergent cleaned and plasma treated for 4 minutes .....	47
4.5 Joint strength and failure load when composite surfaces detergent cleaned and plasma treated for 8 minutes .....	49
4.6 Joint strength and failure load when composite surface detergent cleaned and plasma treated for 12 minutes .....	51
4.7 Joint strength and failure load values when composite surface sanded and detergent cleaned .....	53
4.8 Joint strength and failure load when composite surfaces sanded, detergent cleaned, and plasma treated for 4 minutes .....	55
4.9 Joint strength and failure load when composite surfaces sanded, detergent cleaned, and plasma treated for 8 minutes .....	57
4.10 Joint strength and failure load when composite surfaces sanded, detergent cleaned, and plasma treated for 12 minutes .....	59
4.11 Average failure load and standard deviation for composite base and plasma-treated samples .....	60
4.12 Average joint strength and standard deviation for composite base and plasma-treated samples .....	61

## LIST OF TABLES (continued)

Table	Page
4.13 Average failure load and standard deviation for composite sanded and plasma-treated samples .....	62
4.14 Average joint strength and standard deviation for composite sanded and plasma-treated samples .....	63
4.15 Joint strength and failure load when both aluminum and composite surface detergent cleaned .....	65
4.16 Joint strength and failure load when composite surface detergent cleaned and aluminum surface sanded and detergent cleaned .....	67
4.17 Joint strength and failure load when composite surface detergent cleaned and aluminum surface etched and alodine coated .....	69
4.18 Joint strength and failure load when composite surface detergent cleaned and aluminum surface sanded and plasma treated for 4 minutes .....	71
4.19 Joint strength and failure load when composite surface detergent cleaned and aluminum surface sanded and plasma treated for 8 minutes .....	73
4.20 Joint strength and failure load when composite surface detergent cleaned and aluminum surface sanded and UV treated for 4 days .....	75
4.21 Joint strength and failure load when composite surface detergent cleaned and aluminum surface sanded and UV treated for 8 days .....	77
4.22 Average failure load and standard deviation for different aluminum surface preparations .....	78
4.23 Average joint strength and standard deviation for different aluminum surface preparations .....	79

## LIST OF FIGURES

Figure	Page
1.1 Different types of adhesively bonded joints .....	3
2.1 Single lap joint modelled in CATIA V5R20 .....	7
2.2 Single bond joint configuration .....	8
2.3 Image showing poor and good wetting on a surface [10].....	9
2.4 Basic plasma cleaner setup [12].....	11
2.5 Alodine coating on metal surface [14].....	12
2.6 Tensile test results for specimens using different adhesives [17].....	14
2.7 Secondary bonded sample [17].....	14
2.8 Co-cured sample [17].....	15
2.9 Adhesive strength vs. joint strength [17] .....	16
2.10 Composite-to-aluminum bonded single lap joint configuration [18] .....	16
2.11 Load vs. displacement curves for adhesive bonded joints [18] .....	18
2.12 Strength and failure load comparison for bonded joint specimens [18] .....	19
2.13 SEM images of different samples: (a) square woven glass fabric covered with polymeric fluorinated hydrocarbon (b) light hand abrasion, (c) heavy hand abrasion, and (d) surface grit blasting [21].....	22
2.14 Interfacial failure observed on composite surface [21].....	23
2.15 Cohesive failure with some interfacial and composite failure [21] .....	23
3.1 Prepregs stacked and rolled uniformly .....	27
3.2 Vacuum bagging process for debulking .....	28
3.3 Oven used to cure prepregs .....	28

## LIST OF FIGURES (continued)

Figure	Page
3.4 Finished composite plate .....	28
3.5 Harrick Plasma Cleaner and vacuum pump .....	30
3.6 Sample placed in vacuum chamber .....	31
3.7 Sample exposed to plasma action inside chamber .....	31
3.8 Experimental setup for contact angle test [29] .....	32
3.9 Contact angle test image from CAM 100 software .....	33
3.10 Water contact angle test showing improved wettability after sanding .....	33
3.11 Sample immersed in Alumiprep 33 for 4 minutes .....	34
3.12 Alumiprep 33 (left) and Alodine process (right) carried out simultaneously .....	35
3.13 Preparation of adhesive mix for bonding .....	36
3.14 Bonding parameters for single lap joint.....	37
3.15 Single lap joint specimen prepared and cured in oven .....	38
3.16 Sample placed in MTS tensile testing machine .....	39
3.17 Samples bonded together in a single lap joint using adhesive .....	41
4.1 Bar graph representation for variation in contact angle .....	43
4.2 Bar graph showing variation in contact angle on aluminum with different surface preparations .....	44
4.3 Load vs. displacement graph for first set of samples.....	45
4.4 Stress vs. strain graph for first set of samples.....	45
4.5 Load vs. displacement graph for second set of samples .....	46
4.6 Stress vs. strain graph for second set of samples .....	47

## LIST OF FIGURES (continued)

Figure	Page
4.7 Load vs. displacement graph for third set of samples.....	48
4.8 Stress vs. strain graph for third set of samples.....	49
4.9 Load vs. displacement graph for fourth set of samples .....	50
4.10 Stress vs. strain graph for fourth set of samples .....	51
4.11 Load vs. displacement graph for fifth set of samples .....	52
4.12 Stress vs. strain graph for fifth set of samples .....	53
4.13 Load vs. displacement graph for sixth set of samples .....	54
4.14 Stress vs. Strain graph for sixth set of samples.....	55
4.15 Load vs. displacement graph for seventh set of samples .....	56
4.16 Stress vs. Strain graph for seventh set of samples .....	57
4.17 Load vs. displacement graph for eighth set of samples .....	58
4.18 Stress vs. strain graph for eighth set of samples .....	59
4.19 Bond failure analysis of composite base and plasma-treated samples .....	60
4.20 Joint strength analysis of composite base and plasma-treated samples .....	61
4.21 Failure load analysis of sanded and plasma-treated samples range .....	62
4.22 Joint strength analysis of sanded and plasma-treated samples .....	63
4.23 Load vs. displacement graph for ninth set of samples .....	64
4.24 Stress vs. strain graph for ninth set of samples.....	65
4.25 Load vs. displacement graph for tenth set of samples .....	66
4.26 Stress vs. strain graph for tenth set of samples .....	67

LIST OF FIGURES (continued)

Figure	Page
4.27 Load vs. displacement graph for eleventh set of samples.....	68
4.28 Stress vs. strain graph for eleventh set of samples.....	69
4.29 Load vs. displacement graph for twelfth set of samples.....	70
4.30 Stress vs. strain graph for twelfth set of samples.....	71
4.31 Load vs. displacement graph for thirteenth set of samples.....	72
4.32 Stress vs. strain graph for thirteenth set of samples.....	73
4.33 Load vs. displacement graph for fourteenth set of samples.....	74
4.34 Stress vs. strain graph for fourteenth set of samples.....	75
4.35 Load vs. displacement graph for fifteenth set of samples.....	76
4.36 Stress vs. strain graph for fifteenth set of samples.....	77
4.37 Variation in failure load for different aluminum surface preparations. ....	79
4.38 Variation in joint strength for different aluminum surface preparations. ....	80
4.39 Failures observed in composite-to-composite lap joint .....	81
4.40 Failures observed in aluminum-to-composite lap joint .....	81

# CHAPTER 1

## INTRODUCTION

This research primarily focused on strength and failure mode analysis of a bonded single lap joint between composites and also composite to metal. The lap joint between specimens was made using an adhesive. Analyses of the strength and failure modes were carried out on different types of surface treatments and preparations for both the composites and metal specimens.

### **1.1 Background**

#### **1.1.1 Composites**

With the progression in designing innovation, engineers have an assortment of accessible materials from which to choose. These materials are classified based on material attributes: (1) ceramics, (2) composites, (3) plastics, and (4) metals [1].

A composite is a material that is manufactured by combining two or more different materials in order to form a material with unique properties and characteristics. Thus, the main concept of a composite material lies in the presence of matrix material. When different types of reinforcement such as fibers, whiskers, or particulates are mixed with matrix materials such as metals or ceramics, a composite material is formed. The matrix of composite materials provides rigidity and environmental protection, whereas the fabric of composite materials provides stiffness and strength. Composite materials possess some special features:

- They have a high resistance to corrosion, in comparison to metals.
- Their specific stiffness is high.
- Their fatigue strength is much higher than that of metals.
- They provide engineers with greater design flexibility.
- They provide increased feasibility for employing a product design.

- They can be produced close to or alike the desired shape, which reduces production time and cost, thus eliminating various machining operations [2].

With the advantages of utilizing composite materials, there are also downsides to utilizing these materials:

- The material expense for composites is much higher than that for metals.
- They absorb moisture, thus affecting the dimensional stability of the material.
- Their temperature resistance depends on the temperature resistance of its matrix.

The composite business sector is generally spread in different areas, such as car commercial ventures, aviation, marine building, and civil structures, thus involving different mechanical applications [2].

### **1.1.2 Adhesive Bonding**

For any good engineering design, it is desirable to integrate structures together rather than joining them. A joint in a structure is the weakest connection and is largely responsible for a structure's failure under different loading conditions. The composite structure can be joined utilizing two distinctive joining methods: (a) adhesive bonding, and (b) mechanical joints [3-4]. Adhesive bonding can be characterized as using an adhesive, such as epoxy, methyl acrylate, or polyurethane, to join two substrates (adherents) together. Different types of adhesively bonded joints are shown in Figure 1.1. Among these, the single lap joints are most commonly used. In a single lap joint, shear stresses are responsible for the transfer of load between the two substrates or adherents. At the lap closures of the adhesive in a single lap joint, both normal stress and shear stress reduce the joint strength of a lap joint [3-4].

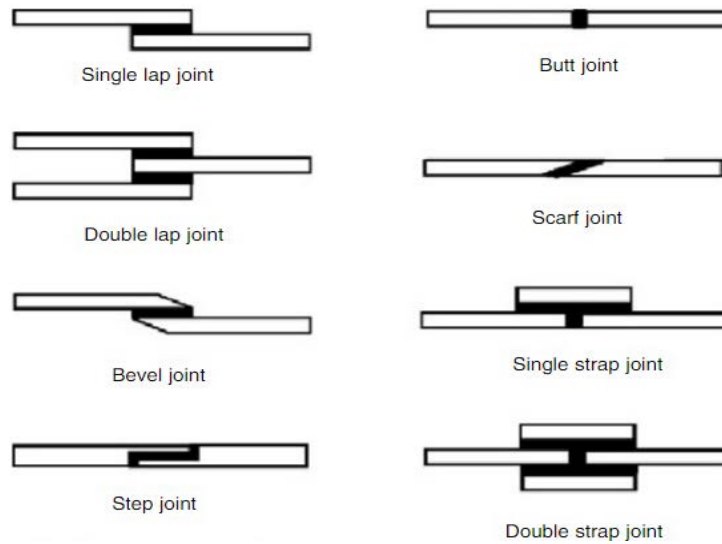


Figure 1.1. Different types of adhesively bonded joints [4].

### 1.1.3 Adhesive Joints vs. Mechanical Joints

Table 1.1 provides a comparison between adhesive joints and mechanical joints.

TABLE 1.1

COMPARISON BETWEEN ADHESIVE JOINTS AND MECHANICAL JOINTS

Serial No.	Adhesive-Bonded Joints	Mechanical Joints
1.	Load distribution over an area instead of being concentrated at a point	Concentration of load at a point causing joint failure
2.	As stress distribution is uniform, these joints are more impervious to fatigue, and flexural and vibrational stresses	Non-uniform stress distribution resulting in fatigue cracking
3.	Lightweight compared to mechanical joints	Heavy compared to adhesive joints
4.	Aside from bonding surfaces, adhesive acts as sealant, thus avoiding galvanic corrosion	Prone to galvanic corrosion
5.	Irregular surface can be easily joined.	Joining irregular surfaces is tough
6.	Smooth contours favorable while outlining streamlined shapes	Weld heads or fastener heads resulting in unsmooth contours
7.	Cheaper than mechanical joints	Expensive compared to adhesive joints
8.	Cannot be disassembled	Can be easily disassembled
9.	Difficult inspection	Easy inspection

## **1.2 Motivation**

Any product design involves a combination of different parts joined together to form an assembly. Therefore, different parts are interconnected by a joint to make a final product. The role of a joint is to exchange loads between the segments joined together. To build a superior product, it is vital that the joints be sufficiently solid. This notion is what inspired the idea to analyze the joint quality and failure mode between a composite-to-composite and a composite-to-metal single lap joint.

Because of certain issues associated with the use of mechanical joints, the adhesive bonding technique was used for this research. Adhesive bonding provides strong structures and bond quality. To a great extent, it is largely dependent on the preparation of the surface to be bonded. The motivation here was to adequately prepare a surface by using different surface-preparation methods in order to adhesively bond specimens in a single lap joint assembly.

## **1.3 Research Objective**

In order to achieve efficient bonding, surface treatment and surface preparation are the two most important techniques that must be followed. The objective of this research was to create a single lap joint using adhesives and to test them for shear strength using an MTS tensile testing machine. During this research, various surface preparations and surface treatments were applied. The overlap length and specimen width were uniform throughout. This aim of this research was to improve the joint strength of an adhesively bonded single lap joint by enhancing the surface properties of the specimens to be joined. This research focused on some key points:

- A combination of various surface treatments—detergent cleaning, sanding, chemical etching, plasma treatment, ultraviolet (UV) treatment, and conversion coating—were used

on samples prior to bonding, with the aim of preparing a surface that yields the greatest joint strength.

- It is believed that preparing/cleaning the surface suitably will enhance the adhesion and wettability of the surface, thus enhancing bond quality.

## **CHAPTER 2**

### **LITERATURE REVIEW**

#### **2.1 Adhesion**

Adhesion is the principle of holding two different adherends together by adhesive forces. In other words, two adherends are joined together using adhesives. The principle of adhesion is also involved in coating as well as priming a substrate using a liquid [5]. The phenomenon of adhesion is controlled by the state of the adherend surface. Adhesion can be broadly classified into two distinct categories: specific adhesion and mechanical adhesion. Both play vital roles in understanding the effect of surface preparation on adhesion.

##### **2.1.1 Specific Adhesion**

Specific adhesion can be defined as the adhesion between the two substrates held together by valance forces, which are responsible for cohesive failure. One theory on specific adhesion states that specific adhesion is responsible for generating some sort of attractive force between molecules and atoms that frames adhesive and adherends. Specific adhesion requires virtual contact between the adherend and the adhesive.

##### **2.1.2 Mechanical Adhesion**

Mechanical adhesion can be defined as adhesion that is the result of an interconnecting force between the adherend and the adhesive [6]. This type of adhesion occurs when an adhesive flow into the microstructure of the surfaces to be bonded. Venables produced some high-quality micrographs showing that on a microscopic level, mechanical adhesion does not leave a major impact on the adhesion as well on the resilience of the adhesive bond. Venables concluded that in the case of specific adhesion, surface preparation is a major factor to be considered in mechanical adhesion as well [7].

## 2.2 Single Lap Joint

Adhesives that are available today are not as strong as compared to the material they join together. An overlap joint is utilized to increase the load-carrying capacity of the joint. With an adhesive joint, the perfect methodology is to guarantee that the bonded joint has greater strength than the parts being joined. In the adhesively bonded single lap joint, the transfer of axial load takes place between the substrates joined together. A single lap joint is, for the most part, the least difficult and least expensive of all joints to manufacture because of its simple design [8]. Figure 2.1 shows a single lap joint assembly designed using the CATIA V5R20 software application. For shear testing a single lap joint, the most commonly used method is the ASTM D1002 test, which helps to measure the adhesive strength. Figure 2.2 shows a single lap joint configuration. All values shown in this figure are in mm: standard total length ( $L$ ) = 175 mm, bonding length ( $b$ ) = 25 mm, and width of sample ( $w$ ) = 25 mm.

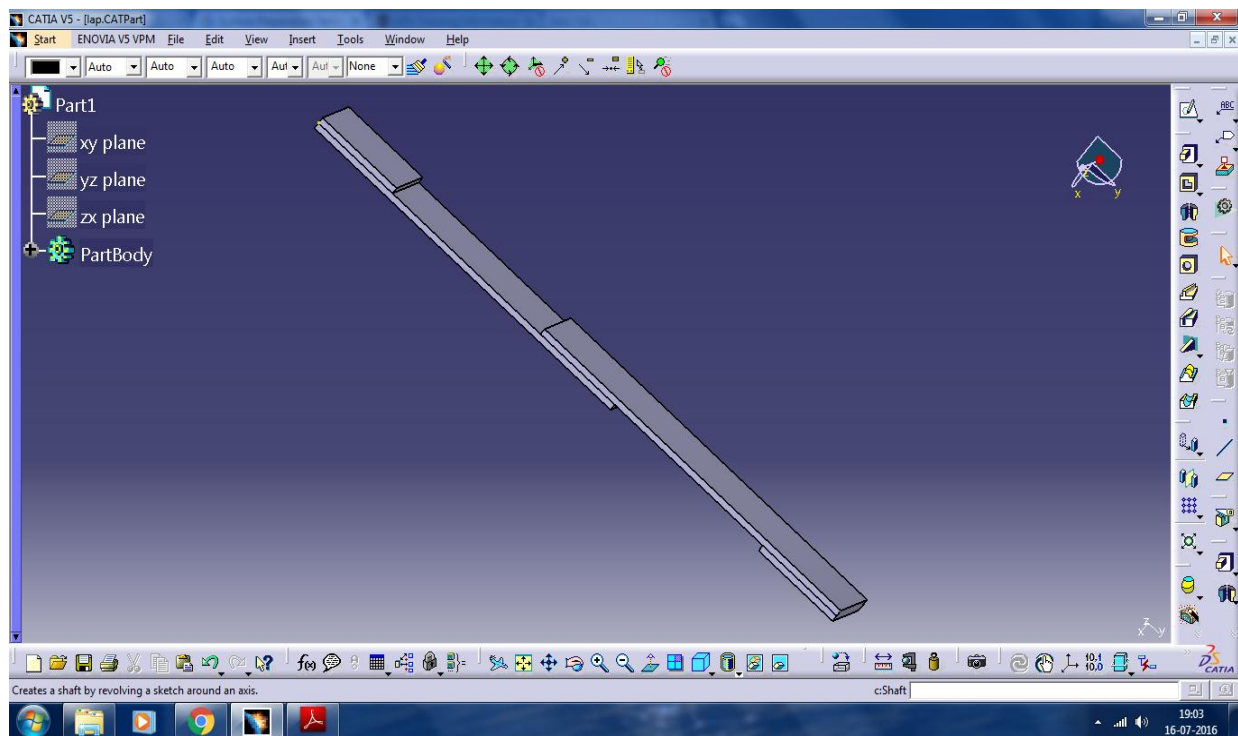


Figure 2.1. Single lap joint modelled in CATIA V5R20.

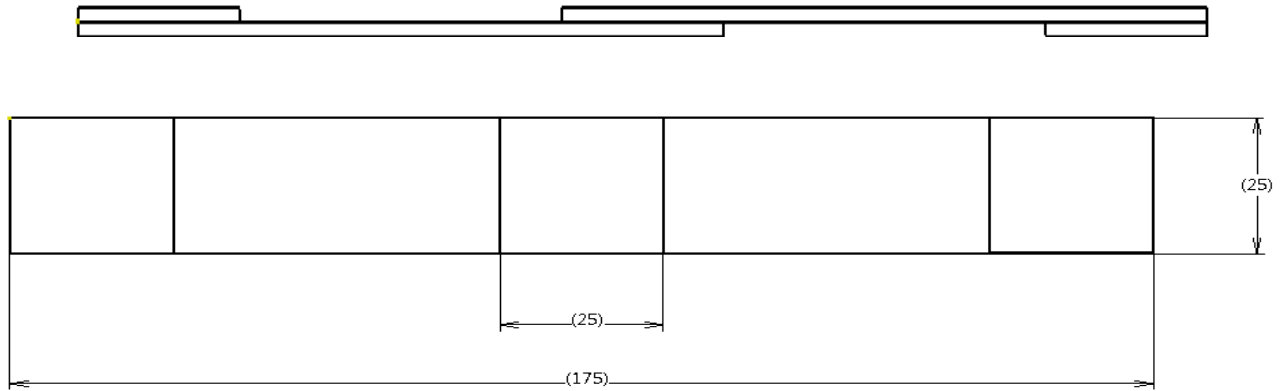


Figure 2.2. Single bond joint configuration.

### 2.3 Mechanical Interlocking

Mechanical interlocking can be defined as the interlocking between the substrate and the adhesive, which results in the formation of a bond. When a substrate is observed carefully, at no time is it smooth and flat, but rather it possesses some peaks and valleys with microcracks. At the time of a wetting process, the adhesive applied on the substrate starts penetrating into the cracks and the adhesive starts to harden. During the hardening process, the two surfaces are held together mechanically. Uniform clamping pressure is applied so that the adhesive penetrates deep inside the microcracks, thus displacing any air trapped on the interface.

When sandblasting or sanding is done on the surface of a substrate, any oils are eliminated, and the surface is prepared to be more reactive, which increases the mechanical interlocking and thus forms a larger surface area. As the surface area increases, the bond strength is enhanced due to the rise in intermolecular forces [10]. Figure 2.3 shows images of poor and good wetting on a substrate surface.

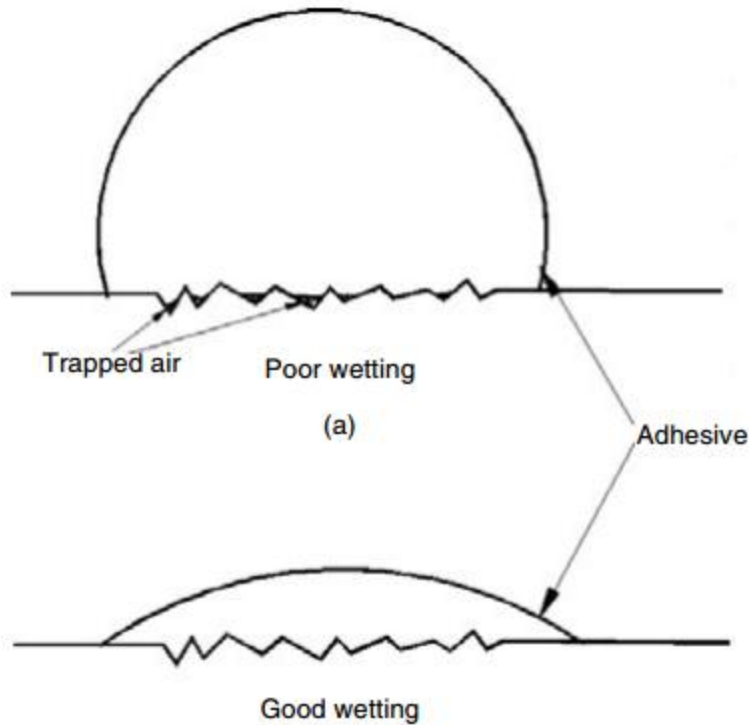


Figure 2.3. Image showing poor and good wetting on substrate surface [10].

## 2.4 Surface Preparation

Surface preparation is characterized as one or a progression of operations that includes surface cleaning, expulsion of free material, and surface modification, either physically or by utilizing chemicals in order to prepare the surface adequately for adhesive bonding. The concept behind surface preparation, particularly in the case of composites, is to enhance the wettability of the surface, expand the surface polarity, and improve the surface for adhesive bonding. In the case of metals, surface preparation improves the bonding strength so that the bond is strong and durable in a tropical environment [9]. Adhesive bond strength is largely dependent on the way the surface is prepared for bonding, which is dependent on certain factors such as required bond strength, cost, as well as production volume. Surface treatment preparation for the substrate can be classified into two distinct categories: passive and active [10].

### **2.4.1 Passive Surface Treatments**

In passive surface treatment, the surface chemistry of the substrate is not disturbed. This type of treatment only eliminates the loosely bonded layer present on the outer face of the surface [10]. Different passive surface preparation methods are explained below.

#### **2.4.1.1 Mechanical Abrasion**

With mechanical abrasion, the surface of the composite or metal is roughened so that the surface area is raised and any dust particles or contaminants are removed from the bonding area. This process involves the use of a wire brush, handheld sandpaper, and emery cloth [10]. This process is very slow and is not useful for larger surface areas. Mechanical abrasion leaves behind the surface remains after scraping as well as some contaminants that amass on the surface that is abraded. In order to achieve a bond of highest quality, it is desired that these impurities be removed by cleaning the surface with an unsoiled cloth and then applying certain solvents [11].

#### **2.4.1.2 Chemical Treatment**

Chemical treatment involves emulsification of the surface to be treated. This process entails the use of strong detergents to eliminate any sort of contamination affecting the surface [10] and typically involves dipping the surface to be cleaned in a detergent solution. When in contact with the surface, the detergent removes loose dirt, impurities, and body oil. After the surface is removed from the detergent solution, it is rinsed properly and allowed to air dry [11].

#### **2.4.1.3 Degreasing**

Degreasing involves removing any oils from the surface to be bonded. For degreasing metals, the metal surface is exposed to a stabilized vapor bath of trichloroethane for a period of 30 seconds. Trichloroethane is toxic in nature but non-flammable. In the case of composites, the surface is degreased using acetone, methyl alcohol, or some detergents [10].

## 2.4.2 Active Surface Treatments

In active surface treatment, the exposed surface of the sample is altered chemically [10]. In doing so, the surface is exposed to a highly energized charge or to some different ionic species. Different active surface treatments are explained below.

### 2.4.2.1 Plasma Treatment

Plasma cleaner is an effective method to adequately prepare a surface for bonding. Here the surface to be treated is exposed to plasma, which can be seen in the neon lights in the plasma cleaner. Plasma can be defined as an ionized gas comprised of both negative and positive charges of equal density. Plasma treatment provides a solution to the adhesion and wetting problem. Plasma treatment is predominantly used for cleaning, surface activation, deposition, and etching. Once the surface is exposed to the action of the plasma, the free radical reaction begins. This reaction occurs either as a result of the interaction of materials in the plasma, or the intercommunication of electrons and ions in the plasma with the surface. Apart from this, a surface reaction may occur as the ultraviolet light is absorbed by the exposed surface. The energy offered by species present in plasma accounts for 10S of electron volts, which proves to be sufficient to break the carbon-carbon bonds. Plasma treatment is carried out at low atmospheric pressure, and because this type of treatment proves to be costly, plasma cleaner is not one of the more frequently used methods industry [12]. Figure 2.4 shows a basic sketch of a plasma cleaner setup.

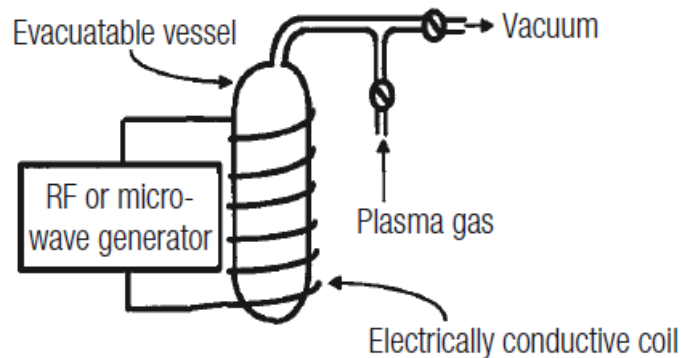


Figure 2.4. Basic plasma cleaner setup [12].

### 2.4.2.2 Conversion Coating

Conversion coating materials are applied on a metal surface to make it corrosion resistant and in turn raising the adhesion of the organic coating. For coating an aluminum surface sample, the acidic materials are either applied by brush application, spraying, or dipping the sample in the solution. As a result, a gelatinous oxide layer is formed on the aluminum surface when it reacts with the solution. Many of the conversion coating methods include the use of phosphoric acid, chromic acid, or other agents such as ferricyanide. When the surface dries out, the gelatinous layer breaks down, resulting in a conversion coating on the aluminum sample. This type of coating is uniform and smooth [13]. Figure 2.5 shows the alodine coating on a metal surface as being gold or tan in color.



Figure 2.5. Alodine coating on metal surface [14].

### 2.4.2.3 Ultraviolet Treatment

Exposure of a surface to UV radiation generates high energy. One surface treatment method uses an excimer laser to produce high-energy UV radiation. This laser is comprised of krypton fluoride, which acts as an active medium. The radiation generated carries high energy, which breaks down the covalent bonds on the surface, thus causing ablation. The use of flash lamps, which emit short but very powerful radiation, improves the surface adhesion [15-16].

## 2.5 Previous Studies

### **Failure Mode and Strength of Uni-Directional Composite Single Lap Bonded Joints with Different Bonding Methods**

Kim et al. explored the strength and failure modes in a single lap joint between uni-directional composites utilizing distinctive bonding techniques. This research was performed taking two imperative parameters into consideration. First, the impacts of various bonding methods bringing about failure were analyzed and the quality was resolved. Also, the impact of secondary bonding was researched to decide the joint strength for the secondary bonded joints [17]. This research demonstrates the strength comparison between secondary bonded joints and co-cured joints by considering distinctive bonding criteria. The specimens produced for the purpose of this research were single lap joints, which were tested under tensile loading. They were manufactured using three diverse bonding techniques: co-curing without using adhesives, co-curing with the use of adhesives, and the use of paste adhesion for secondary bonding. All samples were tested on an MTS 318 testing machine.

Results showed that out of the three different adhesives used, FM 73 yielded an exceptional ultimate stress value of 60.4 MPa, while the other two adhesives EA9309NA and EA9309.3NA, yielded stress values of about 34.5 MPa and 36.4 MPa. A combination of interfacial failure as well as cohesive failure was observed in the secondary bonded joints.

In another analysis of failure strength, it was observed that the co-cured specimen without adhesive gave the most noteworthy failure strength when contrasted with other specimens using adhesives. The specimen bonded with FM 73 provided a minimal failure strength [17]. Figure 2.6 shows a stress versus strain curve for the test conducted. The load versus displacement curve was discovered to be linear until the point of failure for specimens without adhesives. While in the event of secondary bonded joints, failure through the adhesive layer was progressive, causing a

non-linear behavior. For the co-cured sample using FM 73, delamination took place before any sort of adhesive failure [17]. Figures 2.7 and 2.8 show load versus displacement curves between a secondary bonded sample using EA930.39NA adhesive and a co-cured sample using FM73 adhesive after sanding, respectively.

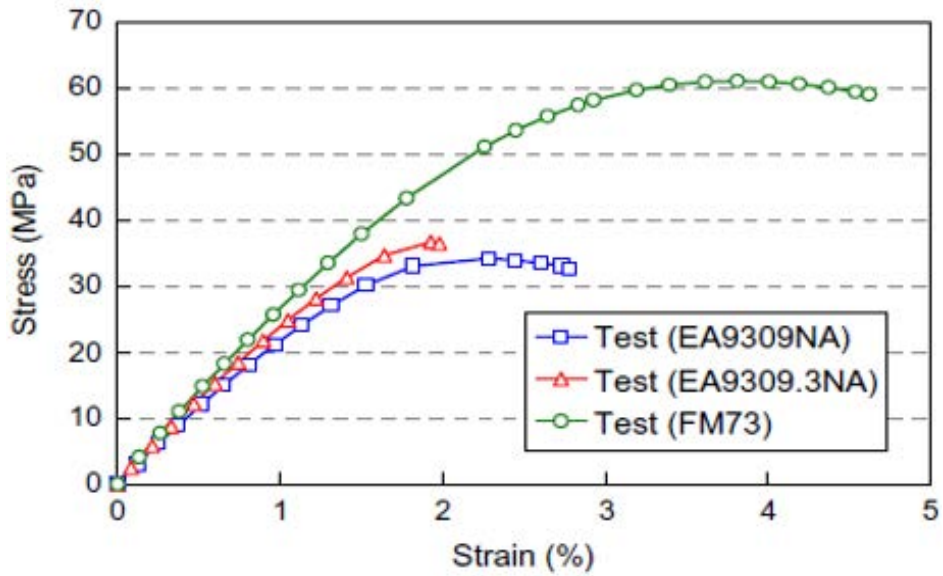


Figure 2.6. Tensile test results for specimens using different adhesives [17].

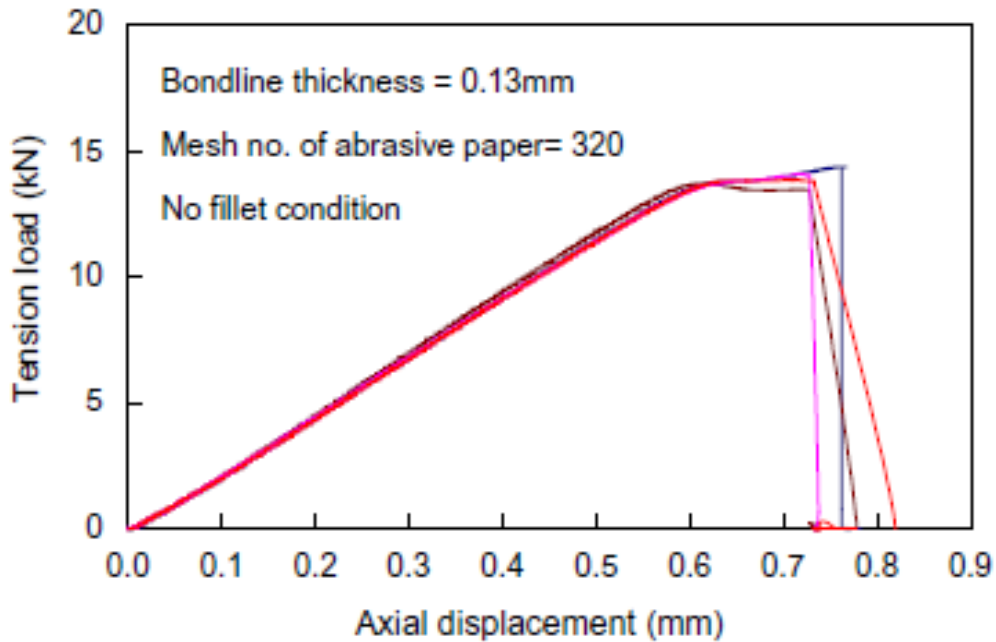


Figure 2.7. Secondary bonded sample [17].

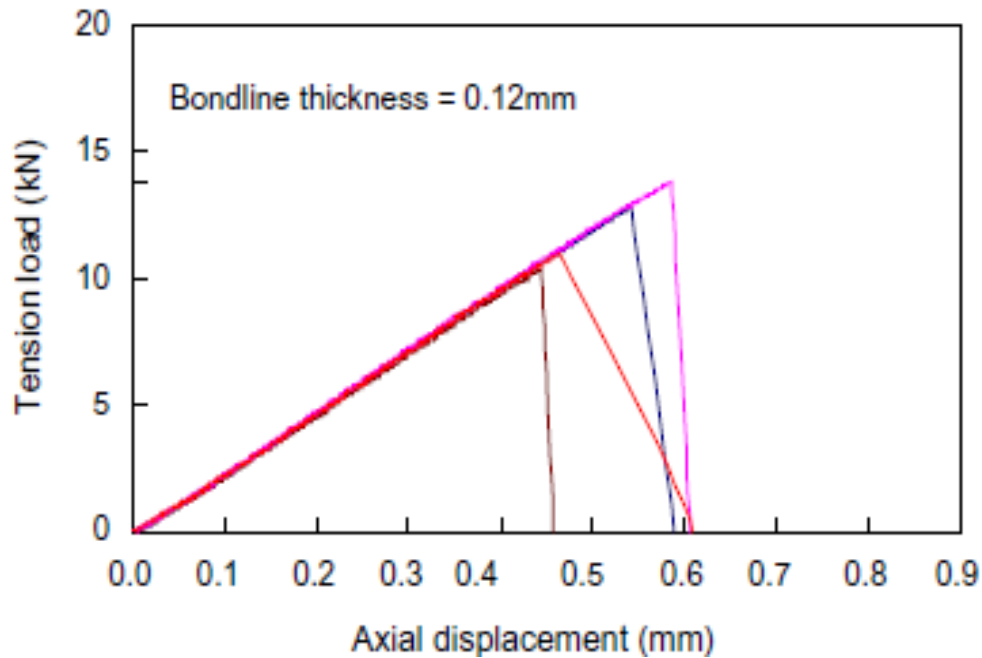


Figure 2.8. Co-cured sample [17].

Another set of analyses were conducted considering the surface roughness parameter. It was observed that as the abrasive sandpaper number increased, the surface roughness was lowered, which in turn resulted in noteworthy joint strength. Also, as the size of fillets increased, the joint strength also increased. The researchers concluded that a secondary bonded joint has a higher joint strength than co-cured specimens using adhesives, because delamination occurs at an early stage in co-cured samples through the adhesive, while in secondary bonded joints, delamination is delayed because of progressive failure of the adhesive layer [17]. Figure 2.9 shows a bar graph comparing the tensile strength of the adhesive, strength of a single lap joint for metals, and strength of a single lap joint in composites. Results indicate that the bond strength of the FM73 adhesive was greater than that of the EA9309.3NAF. Also, the bond strength was stronger for single lap joints in metals compared to single lap joints in composites.

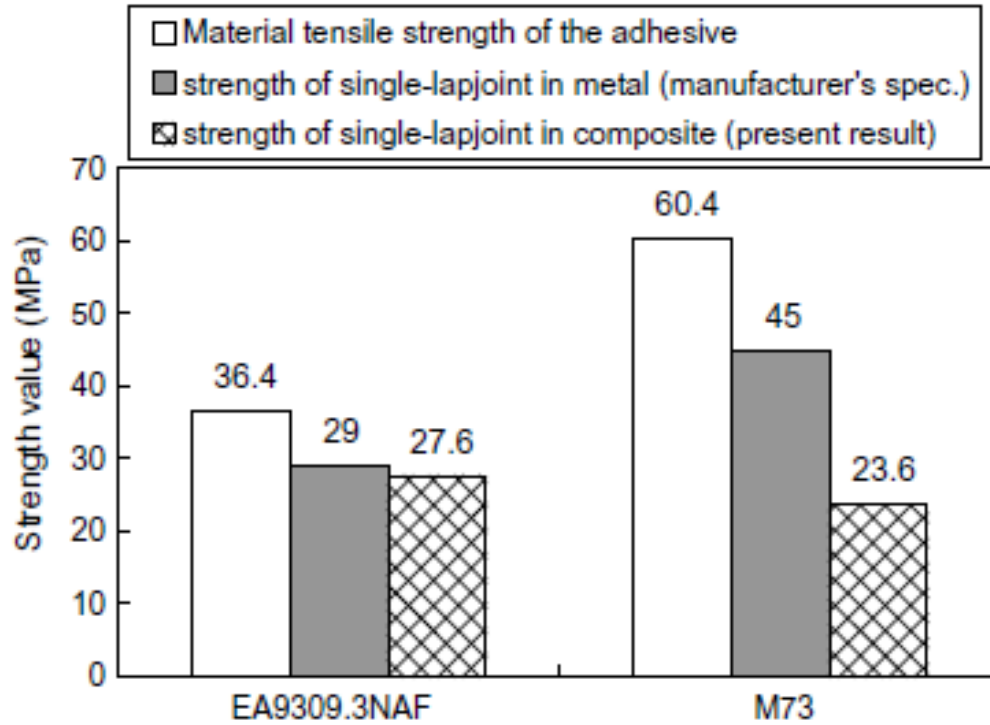


Figure 2.9. Adhesive strength vs. joint strength [17].

### Experimental Study on Effect of Overlap Length on Failure of Composite-to-Aluminum Bonded Single Lap Joints

Kim et al. conducted research to study the effect of different overlap lengths leading to failure in a composite-to-aluminum single lap joint. Figure 2.10 shows the configuration of this bonded joint specimen.

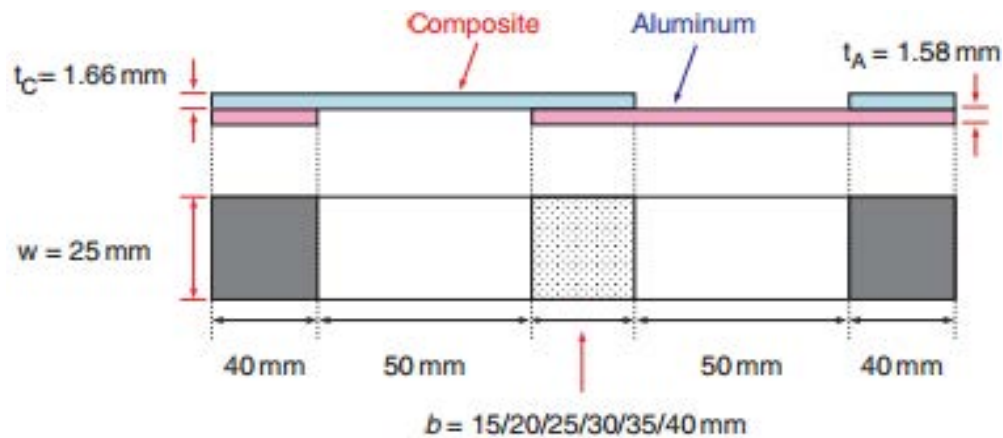


Figure 2.10. Composite-to-aluminium bonded single lap joint configuration [18].

This composite was fabricated utilizing USN125 carbon/epoxy prepregs. The stacking sequence for the composite laminate was  $[\pm 45/90/0]_{25}$ . The thickness of the aluminum plate 2024-T3 was 1.58 mm. The specimen was prepared by joining the composite to the aluminum using adhesive FM73m. Six distinct arrangements of bonding lengths were considered: 15, 20, 25, 30, 35, and 40 mm. The width of the specimen was kept constant at 25 mm. Five specimens for each bonding length were prepared and measured for thickness. An Instron 5582 machine was used to test the specimens. The initial speed rate was set up at 1.3 mm/min. Strain gauges were attached on either side of the samples [18].

Results from this study suggest that failure in the composite-to-aluminum bonded joints was seen to be marginally unique compared to the composite-to-composite joints. However, the final failure mode was the same. The failure propagated more gradually in the composite-to-aluminum joint. From these outcomes, it is inferred that failure in the bonded joints is influenced by the mix of adherends, type of loading, and perhaps thickness and stacking arrangement of the composite adherends. Also, it was found that the thickness and stacking sequence affects the final mode of failure. As the bonding length increased, a more profound level of delamination can be noticed in the composite adherends. Along these lines, it was observed that in order to attain high strength for the bonded joints, it is vital to design such a composite adherend that has a high level of imperviousness to delamination.

The load versus displacement graphs were plotted from these testing results. For specimens with the lowest bonding length of 15 mm, failure mode occurred below 13 KN. But for all other specimens with different bonding lengths, a non-linearity in behavior of the specimens was observed when they attained a load of approximately 13 KN. This suggests that bonded joints are exceptionally susceptible to variables such as spew geometry, material flaws, and different surface

treatment conditions that can influence delamination. Figure 2.11 shows load vs. displacement curves for the adhesive-bonded joints. Different bonding lengths exhibit different natures and different failure loads.

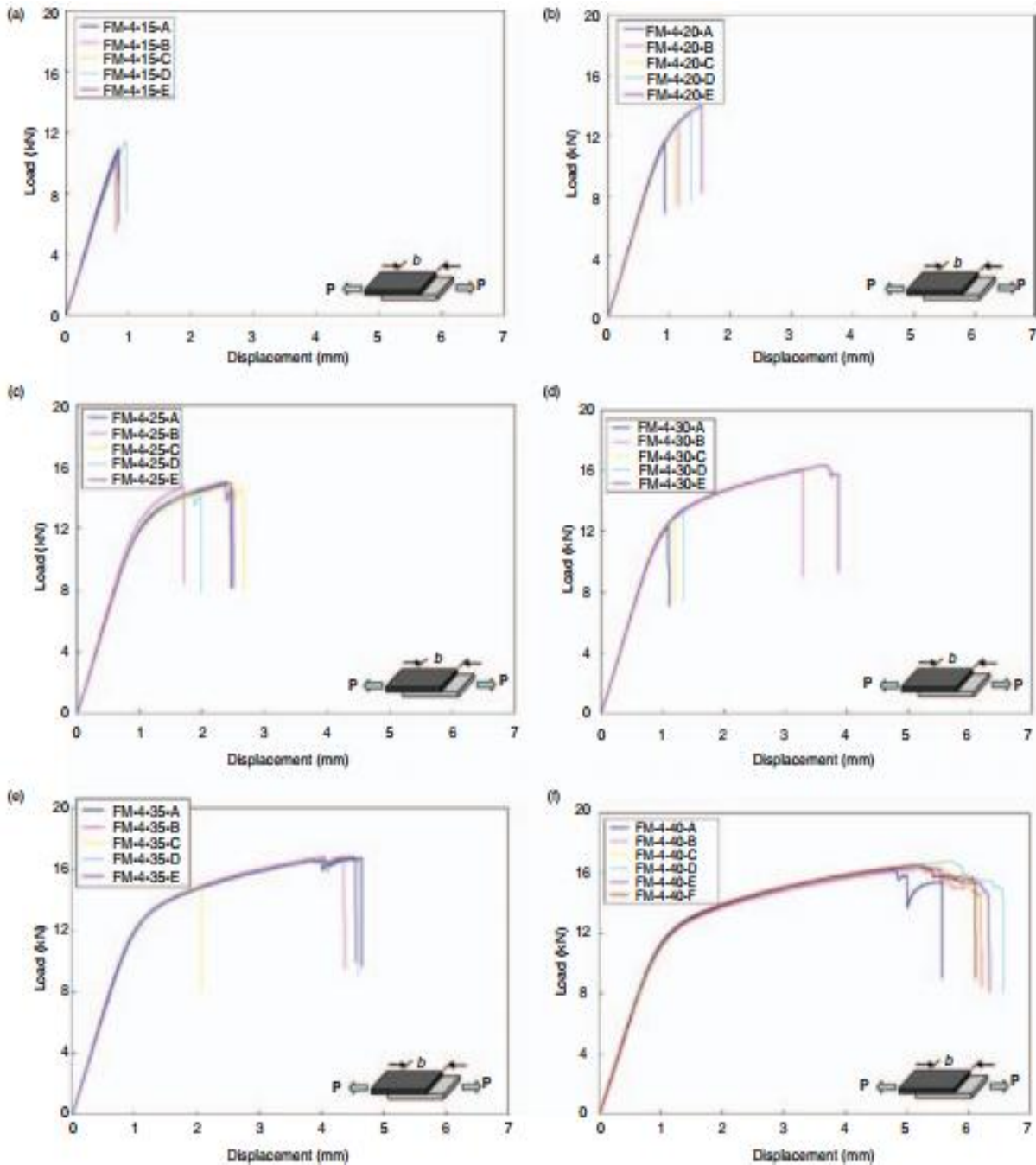


Figure 2.11. Load vs. displacement curves for adhesive bonded joints [18].

Maximum tensile stress for the aluminum panel in the bonded joint was 415 MPa for a bonding length of 40 mm, while the minimum stress of 267 MPa was observed for a bonding length of 15 mm. Additionally, a correlation was made between the joint strength results from this study to the examination directed by other researchers. Kim et al. found that the average strength for the specimen with a bonding length of 20 mm is 25.8 MPa, which is approximately 44% less than 46.1 MPa for a specimen of the same geometry [19]. When compared to the co-cured composite-to-composite joints, it was 9% higher than 23.6 MPa [17]. Figure 2.12 shows a comparison between joint strength and failure load at different bonding lengths. The overlap lengths range from 15 to 40 mm.

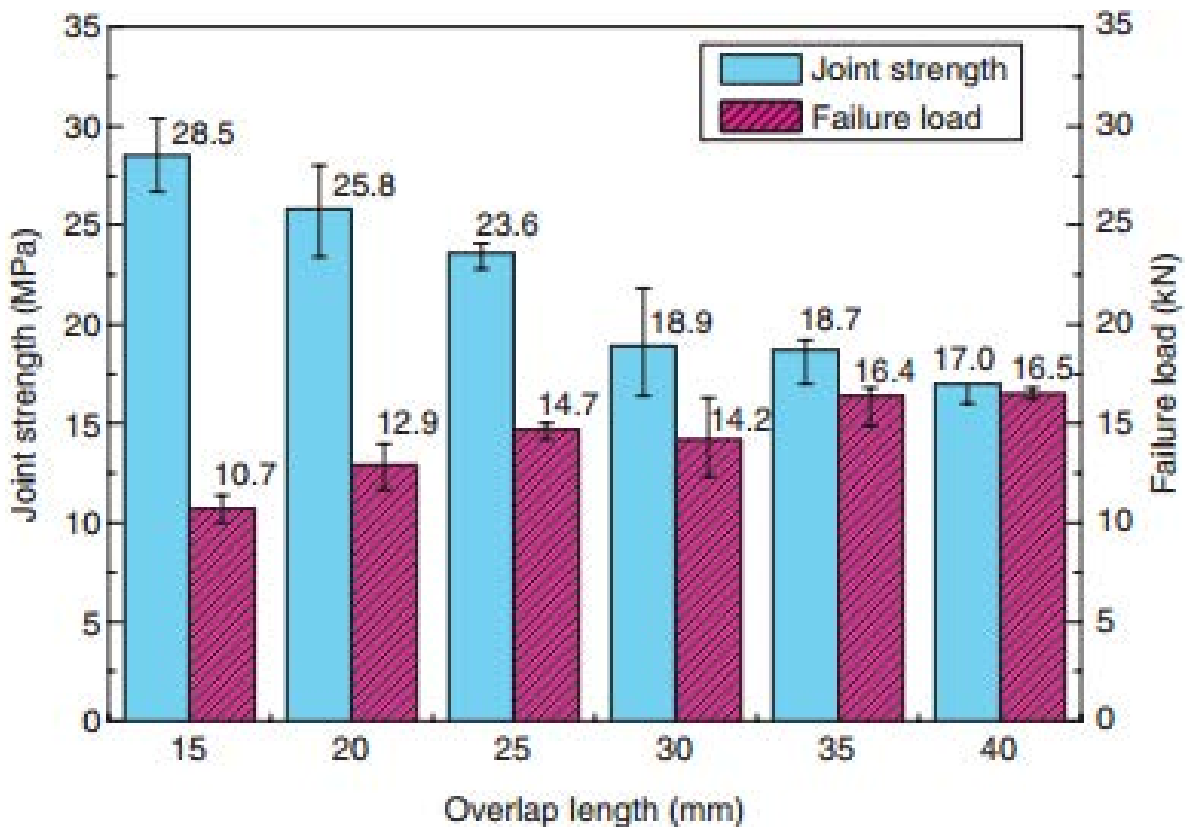


Figure 2.12. Strength and failure load comparison for bonded joint specimens [18].

Subsequently from this study, it was presumed that the joint strength values for a composite-to-aluminum lap joint were falling between the metal-to-metal and composite-to-composite lap joints. The explanation for this conclusion was the fact that the strength of adhesive was working well for the metal-to-metal joint, while in the composite-to-composite joint, failure occurred as a result of the composite overlay, hence resulting in lower strength. In this research, delamination as well as the adhesive resulted in failure. In order to utilize the maximum strength of the adhesive, it is important that the joint designed is effectively resistant to delamination [18].

### **Surface Treatment of Cured Epoxy Graphite Composites to Improve Adhesive Bonding**

Crane et al. carried out an investigation for the pre-treatment of carbon fiber-reinforced polymer (CFRP) required for adhesive bonding. This work showed that exclusive light sanding of a surface was expected to deliver a 30% expansion in joint strength, compared to a surface that was modified using a release cloth [20].

### **Surface Pre-Treatment of Carbon Fibre-Reinforced Composites for Adhesive Bonding**

Parker and Waghorne discuss the impact of surface defilement and various grating pre-treatments on the properties of adhesively bonded CFRP joints. Pre-treatments included impacting with dry alumina grit as well as a few hand abrasion techniques. Here, single lap joints were reinforced with five different epoxy adhesives and tested for joint strength, both with and without introduction to hot/damp conditions. Various failure modes for the joints were also examined. The stacking sequence for the prepregs was  $[0/\pm 45/90]_S$ . The thickness of the manufactured plate was 2 mm. Four different techniques were used to vary the lower surface of the prepregs: a business, square, woven glass fabric covered with polymeric fluorinated hydrocarbon; a silk weave material impregnated at the Royal Aircraft Establishment with polytetrafluoroethylene (PTFE); an aluminum sheet covered with a polymeric fluorinated hydrocarbon, preheated at 120°C, brush-

covered with a suspension of release agent specialist, and then air-dried for 10 minutes at 120°C while joined together; and an aluminum sheet cured for 30 minutes at 150°C and covered with a silicone-containing arrangement [21]. The surface of the prepregs was pre-treated using the following techniques:

- Surface abrading with light, medium, and heavy paper with sandpaper made of silicon carbide with either a 240 or 320 grit size.
- Surface abrading with an abrasive cloth or Scotch-Brite™ until the required surface was generated.
- Surface blasting with dry alumina grit 280.

Five epoxies were used to bond the single lap joint: (1) an epoxy film modified and cured at 120°C for 30 minutes, (2) an epoxy-nylon film cured at 175°C for 60 minutes, (3) an epoxy film modified and mixed with woven nylon cloth and cured at 175°C for 60 minutes, (4) a modified epoxy paste cured at room temperature, and (5) an epoxy paste modified at room temperature and post cured in order to achieve maximum joint strength. The surface was mopped with acetone, and the width and overlap length of the sample were fixed at 25 and 12 mm, respectively. The bondline thickness was 0.1 mm, which was controlled using shims. Joint failure analysis was done optically. Failure modes of the bonded joints were classified into three distinct categories: composite failure, composite-adhesive interface failure, and cohesive failure [21]. Scanning electron microscopy (SEM) images of different samples are shown in Figure 2.13.

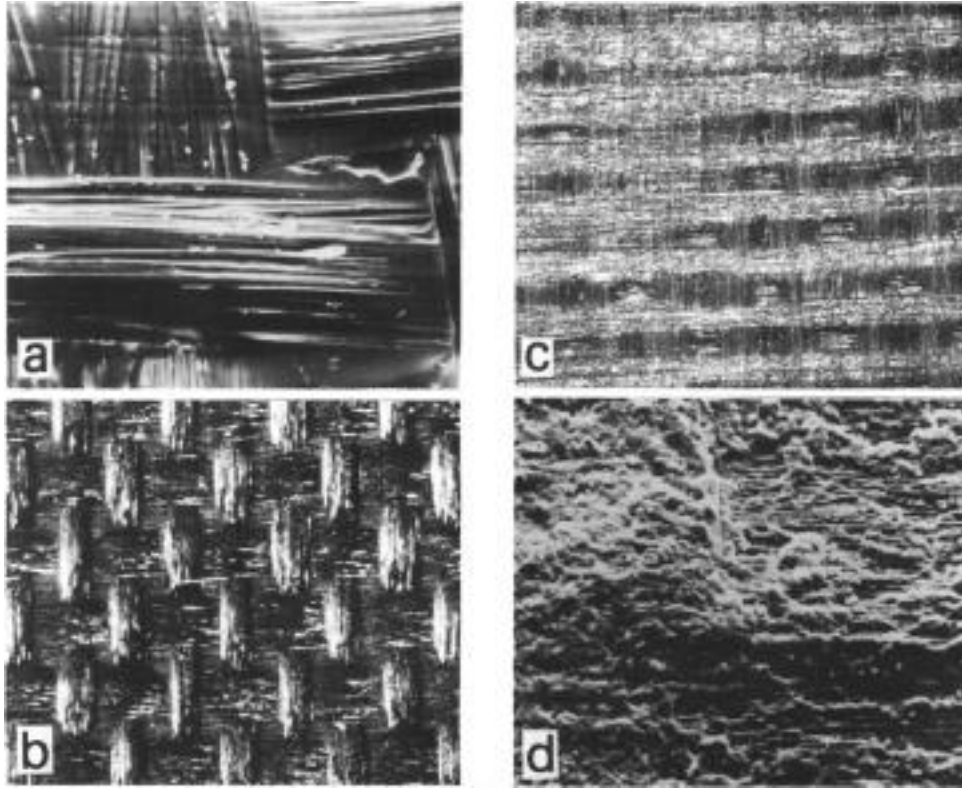


Figure 2.13. SEM images of different samples: (a) square woven glass fabric covered with polymeric fluorinated hydrocarbon, (b) light hand abrasion, (c) heavy hand abrasion, and (d) surface grit blasting [21].

Results show that as the surface contamination decreases, the joint strength increases. In the composite plate, it was observed that the carbon concentration was less than the resin matrix. Thus, as the abrasive pre-treatment level was raised, the carbon resin concentration increased, whereas the fluorine and silicon surface concentration decreased. It was evident that surface contamination produced a joint failure, particularly at the adhesive interface. From the different epoxies mentioned above, epoxies 1, 2, and 5 showed failure in the composite plate, which increased with increasing abrasion, but for epoxy 3, an increase in abrasion led to cohesive failure in the adhesive [21]. It was concluded that the abrasion process restricts the contamination of the surface but only to a certain extent. Dry alumina grit blasting proved to be useful for eliminating surface contamination but still maintaining surface roughness. It was noticed that the surface

contamination reduced the joint strength of the tested specimens. The reduction in joint strength because of surface contamination was dependent on the type of adhesive selected. Therefore, it was suggested to thoroughly prepare the surfaces before bonding [21]. The failure modes observed are shown in Figures 2.14 and 2.15

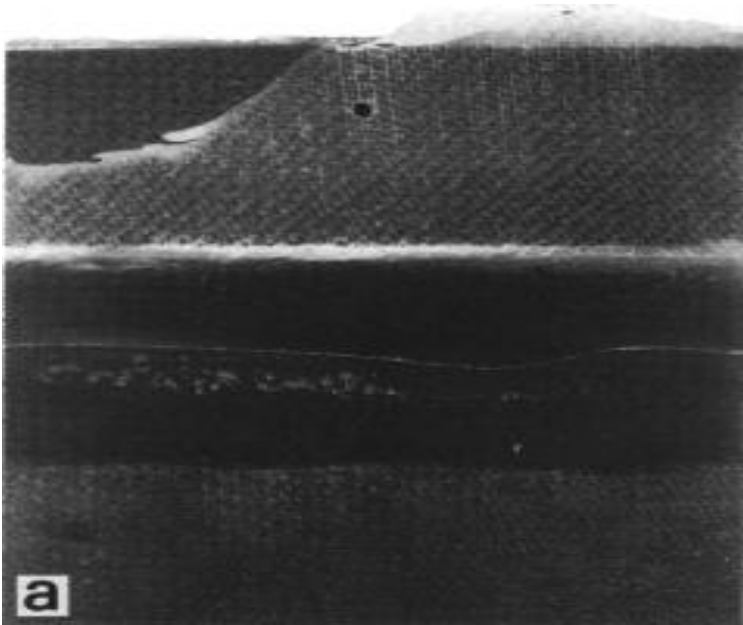


Figure 2.14. Interfacial failure observed on composite surface [21].

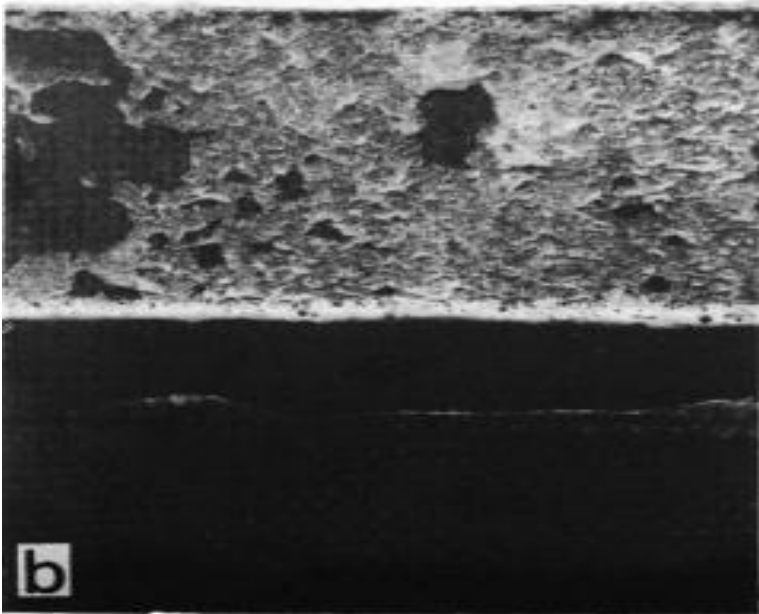


Figure 2.15. Cohesive failure with some interfacial and composite failure [21].

## CHAPTER 3

### MATERIALS AND EXPERIMENTAL METHODS

#### 3.1 Materials

##### 3.1.1 Magnolia 6380 A/B Epoxy

Magnolia 6380, or Magnobond, is a two-segment, toughened, bondline, controlled epoxy adhesive framework that is used on a wide assortment of substrates. It has good properties over an extensive variety of temperatures. This epoxy takes only six hours to set at room temperature. No metallic fillers are included in the epoxy, which results in high-quality bonding for a variety of substrates [22]. The handling strength for Magnobond is achieved after six hours when kept at room temperature, but the required properties are attained after three days. Due to the presence of glass spacers in the epoxy, a precise bondline thickness of around 5 to 7 thousandths can be achieved. The shelf life of Magnobond at 75°F or lower is 12 months.

The mixing ratio by weight for the Magnobond 6380 A/B epoxy is 100:27. To prepare an adhesive, 100 parts by weight of Magnobond 6380 part A and 27 parts by weight of Magnobond 6380 part B are mixed together. According to a technical data sheet, the pot life for the material for 3 ounces at 77°F is 90 minutes, and the specific gravity for the mixed solution is 1.2 [23].

##### 3.1.2. Turco Alumiprep 33

Alumiprep 33 is a phosphoric acid based cleaner that is non-flammable. It is used to prepare an aluminum surface which is chemically cleaned and free from corrosion. This chemical lights up the aluminum surface before any specific utilization of welding or painting processes on it. While using alumiprep 33, for every 100 parts of mixture, the mixing ratio should be 75 parts of water to 25 parts of alumiprep 33. Alumiprep 33 can be used at any temperature between room

temperature and 120°F. In case the surface treated with alumiprep 33 dries out, the surface should be rewetted with the solution before rinsing with water [24].

### **3.1.3 Alodine 1201**

Alodine 1201 is a chromic, acid-based, non-flammable chemical which is used as a coating agent on the surface of aluminum and its alloys. A chrome conversion coating fashioned by means of Alodine 1201 is gold to tan in color and becomes a part of the aluminum surface. This chromate conversion makes the surface unreactive by forming a coating that improves the adhesion properties of the substrate. The result of the coating process is a low-priced substrate that is resistant to corrosion and offers paint adhesion [25]. A few benefits of using Alodine 1201 are as follows:

- A visible conversion coating that delivers enduring paint adhesion.
- A protective layer that forms on the surface prevents corrosion.
- An aluminum surface after treatment that will be chemically stabilized.

### **3.1.4 Aluminum 2024-T3**

Sheets of aluminum 2024-T3, ordered from Online Metals, are useful for achieving a high strength-to-weight ratio. Heat treatments can be easily carried out on these sheets, which are non-magnetic in nature. The sheet ordered for this study was 12 inches by 12 inches and 1.6 mm thick. These lightweight sheets have a wide application in the mechanical and aerospace industries [26].

### **3.1.5 Carbon Fiber Composites**

The unidirectional carbon fiber prepreg roll, requested from Cytec Engineered Materials, lot number 301910285, was 24 inches wide. The thickness of the prepreg sheet was 0.15 mm. Products manufactured using carbon fibers are lightweight, flexible, and heat resistant and offer high tensile strength.

## 3.2 Experimental Methods

### 3.2.1 Preparation of Carbon Fiber Composite Panels

For the purpose of this research, carbon fiber composite plates were assembled using a prepreg lay-up methodology. This procedure includes slicing the prepreg sheet according to the required measurements and then laying the slices on the surface according to the required fiber orientation and stacking sequence. Figures 3.1 to 3.4 show the composite manufacturing process for the composite plates, which is explained below:

- The carbon fiber prepreg sheet was marked as per the required dimensions and then cut into samples using scissors.
- An aluminum metal plate was chosen as a lay-up mold for the prepregs, and the surface was made smooth utilizing different types of sandpapers beginning from P 120 to P 400 to P 600. Once the surface was made smooth, the aluminum plate was cleaned completely with water and then cleaned with acetone to remove all contaminants.
- Two-sided sticky tape was utilized to cover all four sides of the aluminum plate.
- Releasing agent was applied on the lay-up surface to make the surface smooth.
- Twelve plies of prepregs, each 0.15 mm thick, were laid on top of each other on the surface with a stacking sequence of  $[0,90,0,90]_s$  and then rolled uniformly utilizing a roller in order to stack them properly.
- After the prepregs were stacked according to the required stacking process, a sheet of resin film was used to cover the stacked prepregs. This resin film achieves high fiber volumes.
- A caul plate was placed on top of the resin film to apply pressure on the laminate in order to achieve a smooth surface.

- Then breeder material was placed on top of the caul plate to absorb the extra resin bleed from the prepregs.
- A vacuum pump hose was introduced on top of the breeder material, and the assembly was packed with a plastic sheet called a vacuum bag.
- The hose was connected to the vacuum pump, and the vacuum pump was turned on. All edges were checked for any type of leakage and appropriately sealed.
- The assembly was left for a minimum 16 hours to carry out the debulking process, which ensures that the lay-up stays in place and also guarantees that there is even solidification and air is expelled from the overlay before final curing. After debulking, the assembly was transferred to an oven for curing. The vacuum pump was connected throughout this entire process.
- The cure cycle followed to cure the laminate was in three stages. In stage 1, the temperature in the oven was raised from 25<sup>0</sup>C to 125<sup>0</sup>C in a time span of 45 minutes. In stage 2, the temperature was maintained at 125<sup>0</sup>C for 2 hours. And in stage 3, the temperature was gradually brought down to 25<sup>0</sup>C within 45 minutes. The cure time for the entire process was 3 hours and 30 minutes.



Figure 3.1. Prepregs stacked and rolled uniformly.

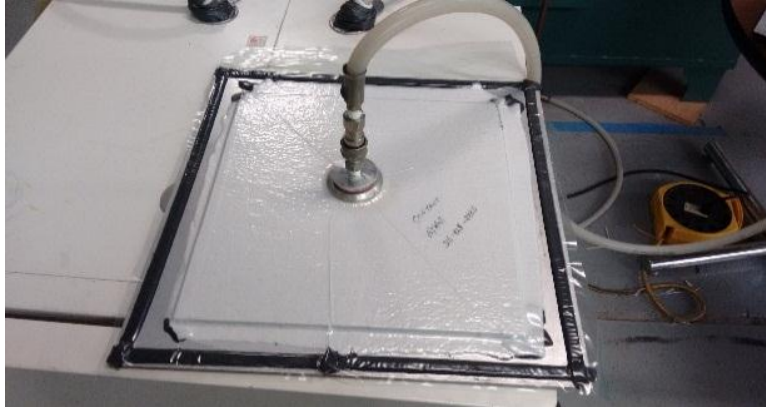


Figure 3.2. Vacuum bagging process for debulking.



Figure 3.3. Oven used to cure preregs.

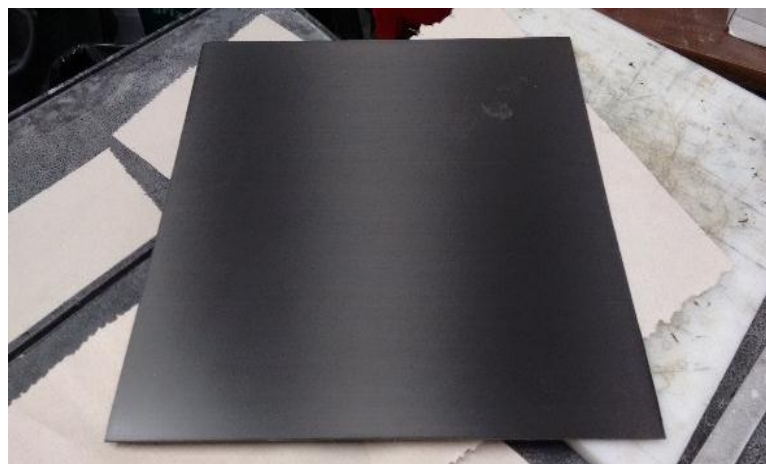


Figure 3.4. Finished composite plate.

### **3.2.2 Preparation of Aluminum Panels**

For purposes of this research, the aluminum 2024-T3 sheet was machined into rectangular pieces measuring 100 mm × 25 mm × 1.62 mm. Samples were cut into the required dimensions using the milling machine in order to obtain a proper finish on the edges of the specimen. The surface of the aluminum plate was sanded using grit size P 120, P 400, and P 600, in order to enhance the surface properties by improving the surface roughness. The surfaces were then rinsed thoroughly with distilled water and thereafter cleaned properly using acetone to remove all dust, contaminants, and any kind of foreign materials present on the surface.

### **3.2.3 Plasma Treatment**

Plasma treatment was performed on both the composite and metal samples using a Harrick Plasma Cleaner PDC-32G. The radio frequency (RF) was set to the highest level and the plasma treatment process carried out in sets of 4, 8, and 12 minutes individually. The steps involved to operate the Harrick plasma cleaner are as follows:

- The sample to be treated was placed in the plasma vacuum chamber.
- The area of the sample to be bonded was left exposed, and the remaining part of the sample was covered using aluminum foil.
- The vacuum pump for pumping non-reactive gases into the vacuum chamber was an Oerlikon Leybold Vacuum TRIVAC D 2, 5 E.
- The sample was placed in the vacuum chamber, and the chamber door was closed using a lid with an O-ring for quick opening and closing.
- The vacuum pump was turned on, and the air was evacuated from the chamber. Then non-reactive gases started to pump into the chamber. The valves on the door lid were closed

tightly to restrict gas flow outside the chamber, the device was turned on, and the RF level was set to the highest point.

- The gases entering the chamber were subjected to a solenoid coil current, which generates induced RF electric and magnetic fields inside the chamber.
- As a result of the collision that occurs, the electrons in the gas heat up and generate plasma, which can be observed as a glowing light inside the chamber.
- Once the process was completed, the device was turned off, the valve opened to eject the gases, the door of the chamber opened, and the sample removed without any bodily contact.
- After the surface was cleaned, it was tested for wettability by measuring the contact angle on the exposed area: the lower the contact angle, the greater the wettability. Figures 3.5 to 3.7 show the Harrick plasma cleaner process.



Figure 3.5. Harrick plasma cleaner and vacuum pump.



Figure 3.6. Sample placed in vacuum chamber.

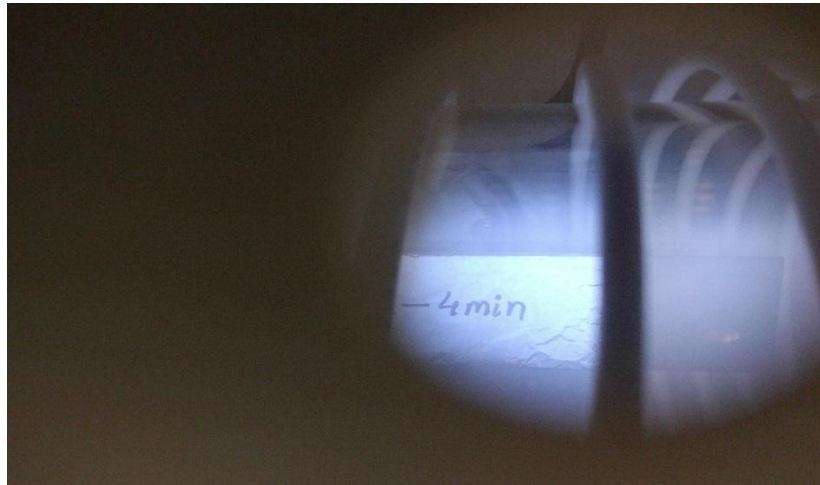


Figure 3.7. Sample exposed to plasma action inside chamber.

### 3.2.4 Water Contact Angle Test

In general, the water contact angle is measured to examine the wettability and surface adhesion of the surface that is to be bonded. The following steps were involved in the contact angle measurement process:

- This setup involved a special syringe to precisely measure the water drop which was to be measured for the contact angle.

- A high resolution camera was set to record the images and send them to the CAM 100 software for contact angle analysis.
- An adjustable stand was used to move the sample up and down as required.
- A monochromatic light was thrown from the LED source right beside the stand opposite the camera, which helped to generate a sharper image [27].
- The syringe was fixed in one of the other stands in such a way that it could be adjusted.
- The CAM 100 software calculated the contact angle.
- The LED light was turned on, and the syringe was filled with distilled water and fixed in the stand.
- The sample to be tested was placed on the stand and adjusted.
- The camera was adjusted until the image on the syringe needle became sharp and clear.
- A small drop of water was released on the surface, and using the software, the contact angle data was accumulated.

Figure 3.8 shows the experimental setup required to carry out the contact angle test. Figure 3.9 shows the contact angle calculations from measuring the water drop and the CAM 100 software used to record the data.

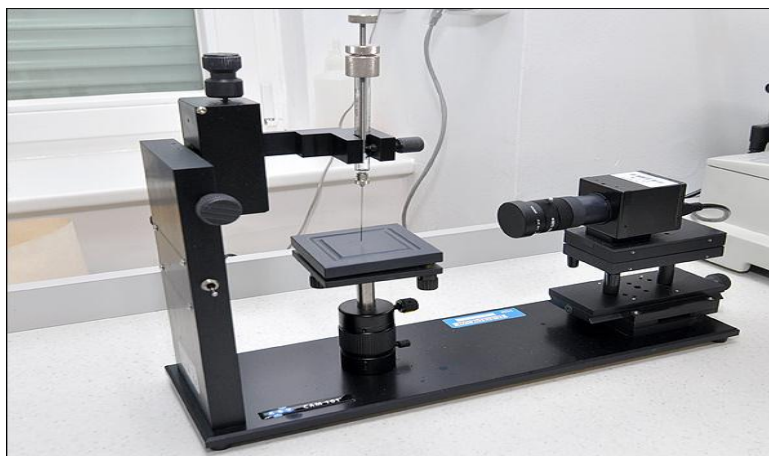


Figure 3.8. Experimental setup for contact angle test [28].

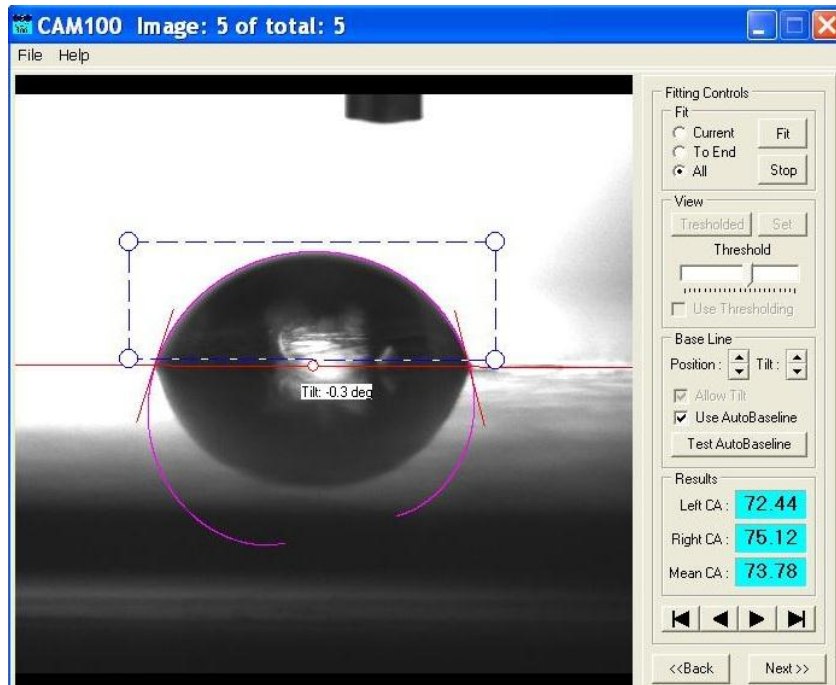


Figure 3.9. Contact angle test image from CAM 100 software.

### 3.2.5 Sandpaper Abrasion

Sandpaper was used to remove rust and paint from the surface, make the surface rougher, and increase the surface area. As a result, wettability of the surface improves which in turn provides an efficient bond strength. The drawback of using the sanding method is that debris from the surface is left behind. Thus, the surface should be thoroughly rinsed after sanding. Figure 3.10 shows a comparison of water angle test results before and after sanding.

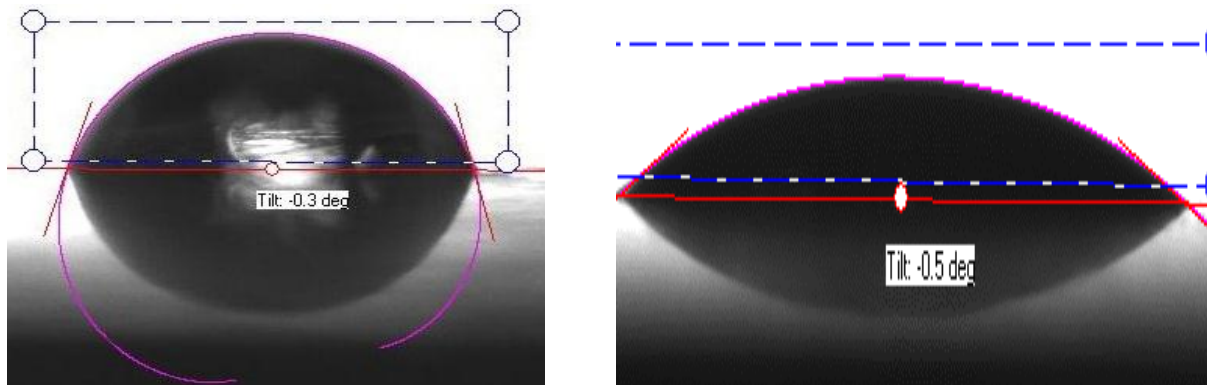


Figure 3.10. Water contact angle test showing improved wettability after sanding.

### 3.2. Surface Preparation

Alumiprep 33 was used for pre-treatment of the aluminum surface to remove the oxide layer before the Alodine coating. Alumiprep 33 is a combination of phosphoric acid, 2-Butoxyethanol, potassium phosphate, and hydrogen fluoride. Below is the step-by-step procedure used to prepare the aluminum surface before Alodine coating:

- As per the data sheet for 100 parts of bath, 75 parts of water and 25 parts of solution were mixed together [23].
- Wearing protective laboratory apparel, Alumiprep 33 was carefully poured in an aluminum tray as per the required quantity.
- The aluminum surface was immersed in the solution and left for 3–4 minutes until the contaminants and oxide layer were removed from the surface.
- During this time bubbles were observed being released from the surface, thus assuring that the surface was being cleaned.
- After 4 minutes, the sample was removed and rinsed under a water jet until all contamination was removed, whereupon the surface becomes a “water break-free surface,” thus indicating removal of all contaminants and the oxide layer [23].
- The sample was then allowed to air dry before applying the Alodine coating.

The sample preparation using alumiprep 33 is shown in Figure 3.11.

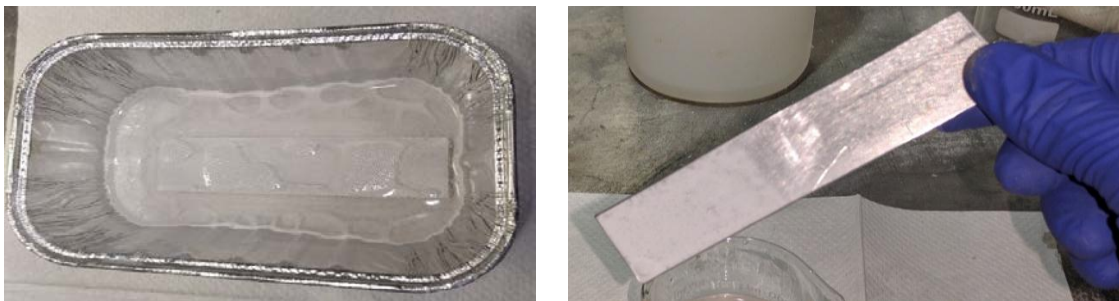


Figure 3.11. Sample immersed in alumiprep 33 for 4 minutes.

### 3.2.7 Alodine Coating

Alodine coating is a type of protective coating on an aluminum surface to improve paint adhesion and corrosion resistance. The steps involved in this process are as follows:

- Alodine 1201 solution was poured into an aluminum tray as per the required quantity.
- The sample recovered from the Alumiprep 33 solution was air dried and placed in the Alodine 1201 solution.
- The waiting time was 2–5 minutes so that the Alodine could coat on the surface.
- After 5 minutes, the sample was removed and rinsed with water immediately before drying.
- The sample was allowed to air dry. The coating formed by Alodine is a gold or tan color.

Figure 3.12 shows the sample cleaning in the Alumiprep 33 on the left, and then dipped in the Alodine for coating on the right.



Figure 3.12. Alumiprep 33 (left) and Alodine process (right) carried out simultaneously.

### 3.2.8 Preparation of Adhesive

To prepare the adhesive required for bonding the sample together, a two-part epoxy system provided by Magnolia, a high-performance epoxy system, was used. This epoxy is comprised of

two parts: Magnolia 6380 A (main epoxy) and Magnolia 6380 B (hardener). The steps involved to prepare the adhesive are as follows:

- A plastic plate was used to mix the adhesive. A Mettler Toledo weighing scale was used to measure the weight.
- A plastic plate was placed on the weighing scale and set to zero, neglecting the weight of the plate.
- The mix ratio for the adhesive was 100:27 parts by weight, meaning 100 parts by weight of Part A epoxy were mixed with 27 parts by weight of part B hardener.
- Once the weighing was done, the adhesive was slowly mixed for 5–7 minutes, in order to combine it well.
- The mixture was used before it started to harden.

Figure 3.13 shows the mixture of Magnolia 6380 Part A and Magnolia 6380 Part B, the main epoxy and hardener, respectively.



Figure 3.13. Preparation of adhesive mix for bonding.

### 3.2.9 Bonding Samples

Bonding the specimen together is a very important step in order to obtain accurate joint strength and mode of failure. Figure 3.14 shows adequate bonding parameters for a single lap joint.

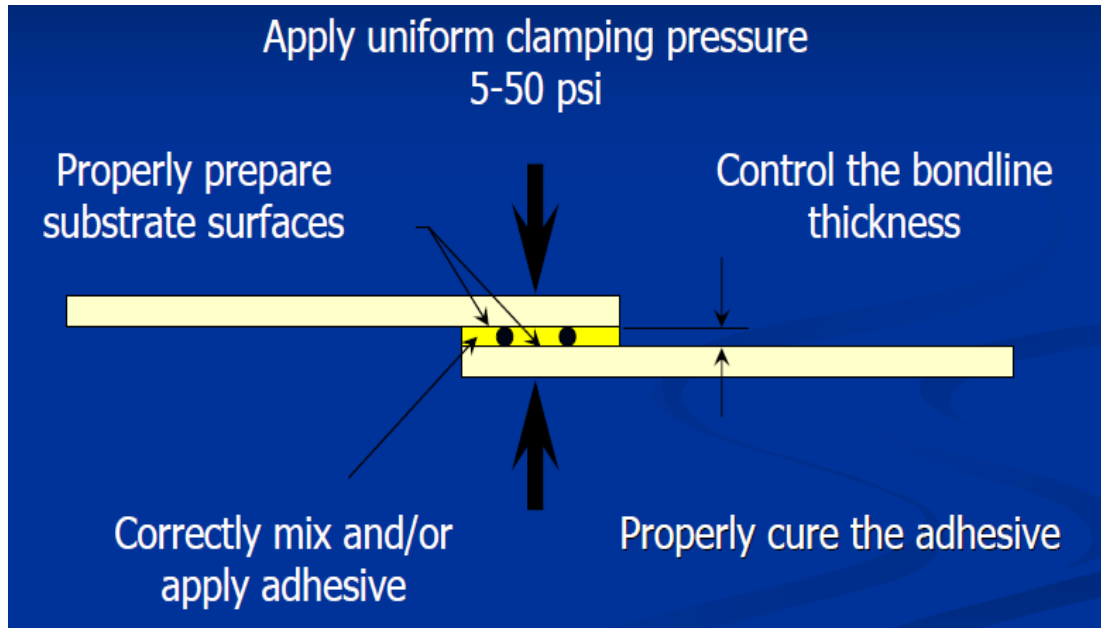


Figure 3.14. Bonding parameters for single lap joint [29].

The five parameters shown in Figure 3.14 play a vital role in deciding the strength of the single lap joint. The steps involved to bond the samples are the following:

- The surface of the sample was marked for a bonding length of 25 mm. The width of the sample was kept constant at 25 mm.
- Using a surgical metallic rod, the adhesive mix was spread over the bonding area of the surface. Another sample marked for the bonding length was placed over the first sample where the adhesive was spread.
- A helical curved jaw with a wire cutter was used as a clamp on the bond area. The pressure applied through it was 2–5 psi. This clamp was used to remove excessive adhesive between the two surfaces in order to control the bondline thickness.

- The samples were then checked for proper alignment; if not aligned properly, they were adjusted before curing of the adhesive.
- The adhesive bond was cured using a THELCO laboratory oven, with the temperature set to 80°C for a cure cycle of 2 hours.
- Composite tabs were also fixed at the ends of the samples inside the bonding to prevent the joint from failing during tensile testing as the result of twisting.

Figure 3.15 shows some of the single lap joints prepared and kept in the oven to cure.



Figure 3.15. Single lap joint specimens prepared and cured in oven.

### 3.2.10 Shear Strength Test

An MTS 318 tensile testing machine was used to calculate the joint strength and failure mode analysis of the samples made using different surface preparations. The detailed procedure is explained below:

- The jaws of the machine were aligned, and the bottom was fixed, leaving the upper jaw adjustable.
- Using machine controls, the specimen was fixed between the jaws of the machine. Both ends of the sample were set up on the X-mark line present in both jaws.

- The jaws were tightened so that the sample experienced only the shear load.
- The software used to record the data was Test Works 4.
- The load and displacement values were changed to N and mm, respectively.
- The machine began applying shearing load to the sample.
- The software recorded all raw data required for analysis.
- After a certain point, the bond broke apart, producing a sharp sound, thus indicating bond failure.
- The sample was then removed from the jaws and the raw data retrieved from the software Test Works 4.

Figure 3.16 shows the MTS tensile testing machine setup with the sample. Tables 3.1 and 3.2 show the different preparations used for preparing the composite and aluminum surfaces. Some of the prepared samples are shown in Figure 3.17.



Figure 3.16. Sample placed in MTS tensile testing machine.

TABLE 3.1

## SURFACE PREPARATIONS FOR COMPOSITE-TO-COMPOSITE SINGLE LAP JOINT

<b>Serial No.</b>	<b>Surface Preparation for Composites</b>	<b>Specimens</b>
1.	Both surfaces cleaned with detergent	3
2.	Both surfaces sanded and cleaned with detergent	3
3.	Both surfaces cleaned with detergent and plasma treated for 4 min	3
4.	Both surfaces cleaned with detergent and plasma treated for 8 min	3
5.	Both surfaces cleaned with detergent and plasma treated for 12 min	3
6.	Both surfaces sanded, cleaned with detergent, and plasma treated for 4 min	3
7.	Both surfaces sanded, cleaned with detergent, and plasma treated for 8 min	3
8.	Both surface sanded, cleaned with detergent, and plasma treated for 12 min	3

TABLE 3.2

## SURFACE PREPARATIONS FOR ALUMINUM-TO-COMPOSITE SINGLE LAP JOINT

<b>Serial No.</b>	<b>Surface Preparation for Composites</b>	<b>Surface Preparation for Aluminum</b>	<b>Specimens</b>
1.	Surface cleaned with detergent	Surface cleaned with detergent	3
2.	Surface cleaned with detergent	Surface sanded and cleaned with detergent	3
3.	Surface cleaned with detergent	Surface etched (Alumiprep 33) and Alodine coated	3
4.	Surface cleaned with detergent	Surface sanded, cleaned with detergent, and plasma treated for 4 min	3
5.	Surface cleaned with detergent.	Surface sanded, cleaned with detergent, and plasma treated for 8 min	3
6.	Surface cleaned with detergent.	Surface sanded, cleaned with detergent, and UV treated for 4 days	3
7.	Surface cleaned with detergent.	Surface sanded, cleaned with detergent, and UV treated for 8 days	3

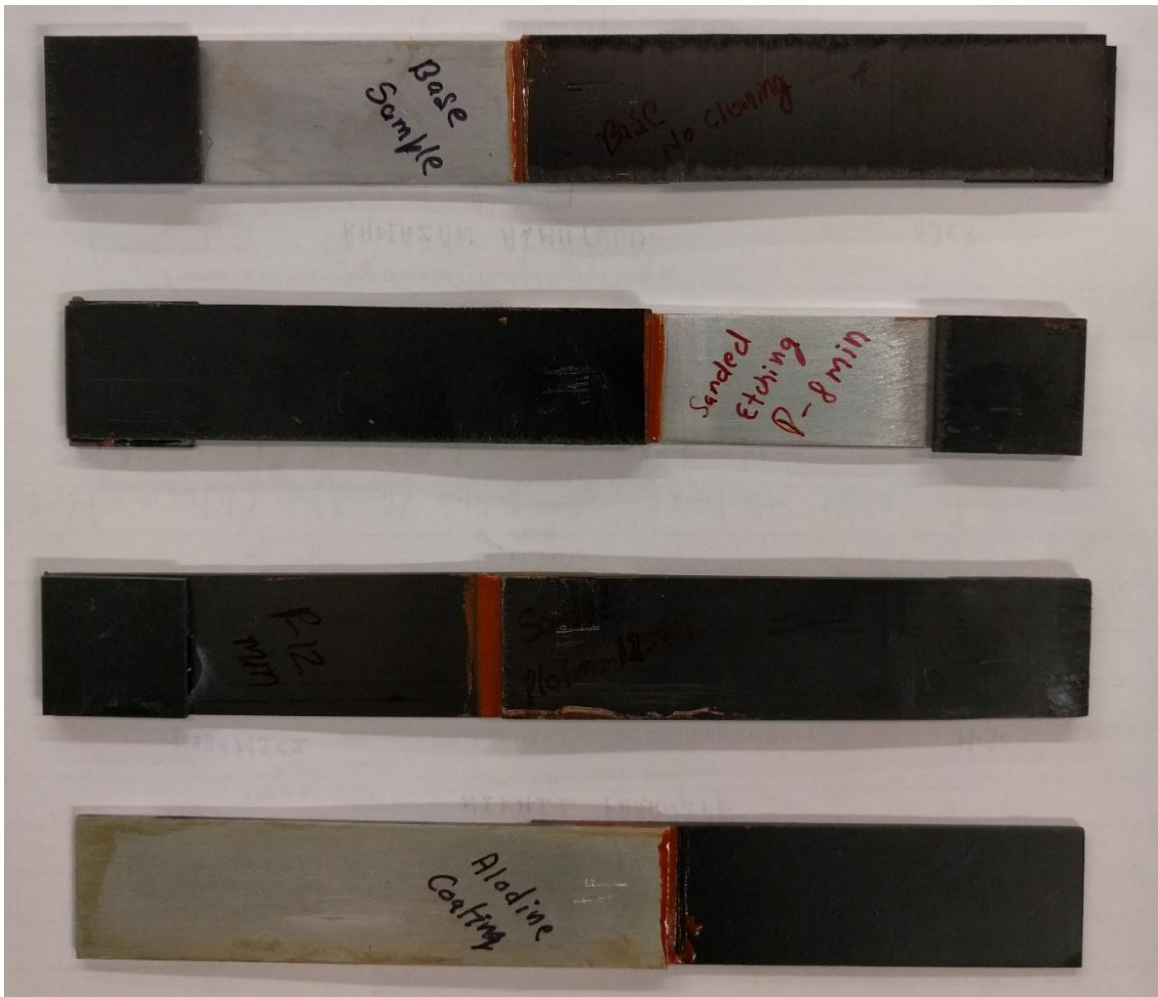


Figure 3.17. Samples bonded together in a single lap joint using adhesive.

## CHAPTER 4

### RESULTS AND DISCUSSIONS

Samples were produced using a combination of 15 different types of surface preparations. They were bonded together using a high-performance aerospace epoxy, Magnolia 6380 A/B. Testing was conducted on an MTS 318 tensile testing machine. Analyses were performed using raw data from this machine. The data were formulated in Microsoft Excel and used to plot load versus displacement graphs, as well as stress-strain values. The results of contact angle tests on composites after sanding and plasma treatments are shown in Table 4.1. It can be seen that as the plasma-exposure time on the surface was increased, the contact angle decreased. Figure 4.1 shows the variation in contact angle at different exposure time intervals for plasma cleaning. It can be seen that when the surface was treated with plasma, the contact angle was lowered significantly. Also, when the sample was sanded, the contact angle dropped further. Therefore, it can be concluded that as the sanded surface was exposed to plasma, the contact angle decreased, in turn improving the wettability and adhesion of the surface and increasing the bond strength of the joint.

TABLE 4.1

CONTACT ANGLES FOR COMPOSITE BASE AND SANDED SURFACES EXPOSED TO PLASMA FOR DIFFERENT TIMES

<b>Surface Type</b>	<b>No Plasma</b>	<b>Plasma 4 Minutes</b>	<b>Plasma 8 Minutes</b>	<b>Plasma 12 Minutes</b>
Base	74.83	46.29	42.91	39.58
Sanded	61.51	33.25	28.64	23.89

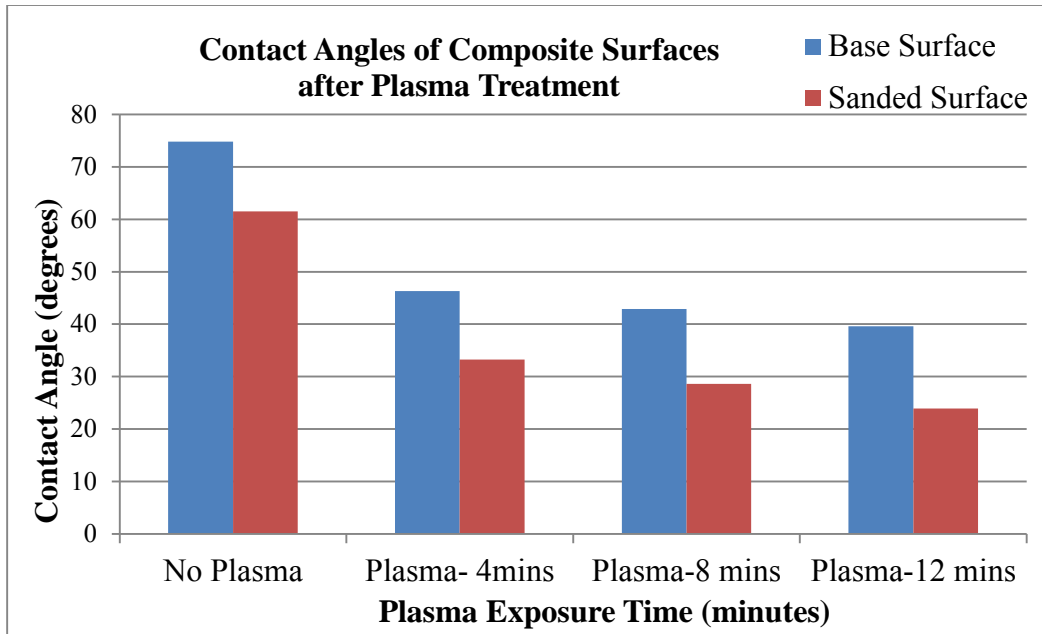


Figure 4.1. Bar graph representation of variation in contact angle.

Table 4.2 shows contact angle test results for different surface preparations on an aluminium surface. Figure 4.2 shows the variation in contact angles for different surface treatments on aluminum at different plasma-exposure times. All values recorded in Tables 4.1 and 4.2 were taken from CAM 100 software that measured the contact angle for all samples. For each set of samples, five readings were recorded, and the average of all five is represented.

TABLE 4.2

CONTACT ANGLE TEST RESULTS FOR ALUMINUM WITH DIFFERENT SURFACE PREPARATIONS AND PLASMA EXPOSURE

Surface Type	No Plasma	Plasma 4 Minutes	Plasma 8 Minutes	Plasma 12 Minutes
Base	77.93	42.09	37.68	33.48
Sanded	60.59	30.12	26.98	23.04
UV-Treated	68.42	48.21	44.61	40.94
Plasma-Treated	70.74	52.19	47.91	40.45
Alodine-Coated	72.22	60.74	51.89	47.28

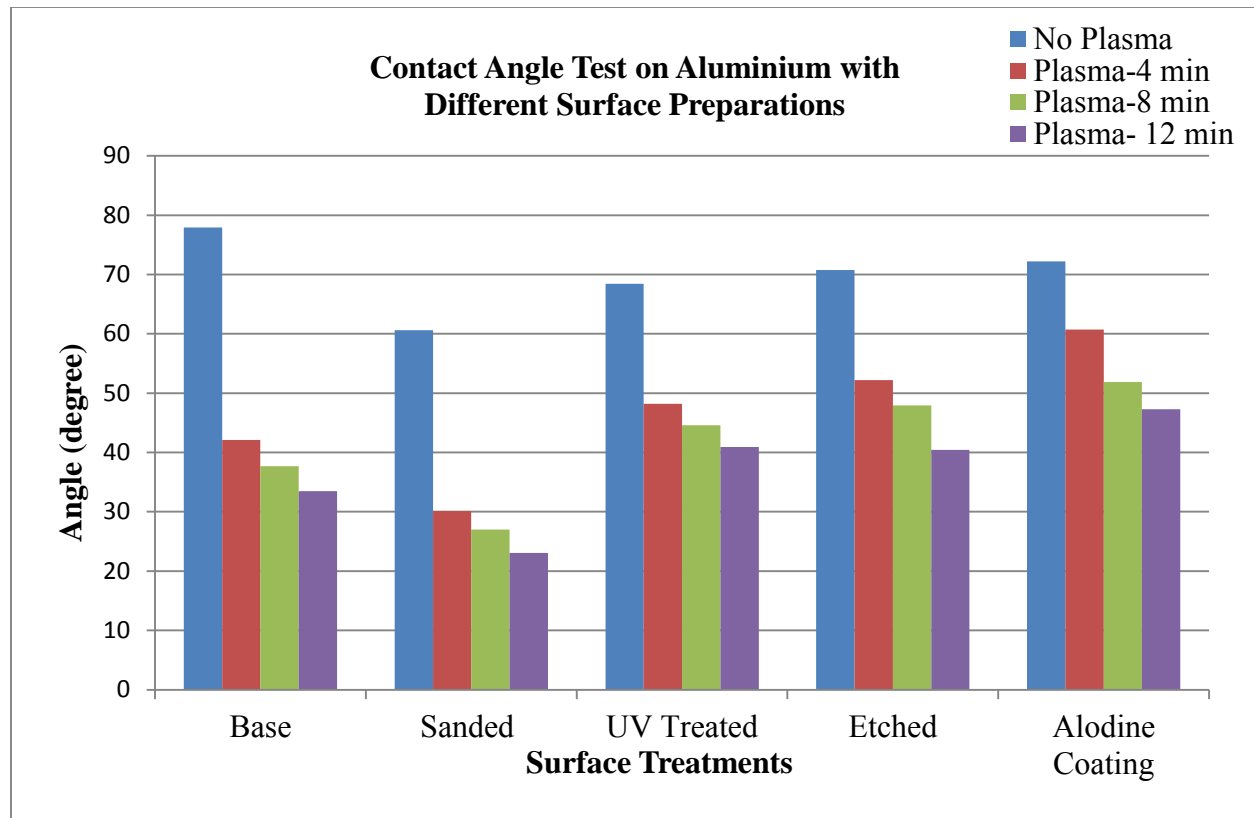


Figure 4.2. Bar graph showing variation in contact angle on aluminium with different surface preparations.

The first set of samples prepared were single lap joints between composites. Three specimens were prepared. Both surfaces to be joined were cleaned with detergent. These samples were analysed as base results for further comparisons. The overlap length was fixed at 25 mm. Figure 4.3 shows the maximum failure load, that is, the maximum load at which the joint failed. It can be seen that the graph in Figure 4.3 is not linear. The failure modes for all three samples tested varied from 11.1 kN to 11.8 kN. The sample with only detergent cleaning gave the least joint strength and bond failure load. Figure 4.4, which shows the stress versus strain graph to obtain the maximum joint strength, indicates that the average joint strength for the base samples was 18.76 MPa, with the range being between 18.62 MPa and 18.86 MPa. Table 4.3 shows the values for failure load and joint strength for the base samples.

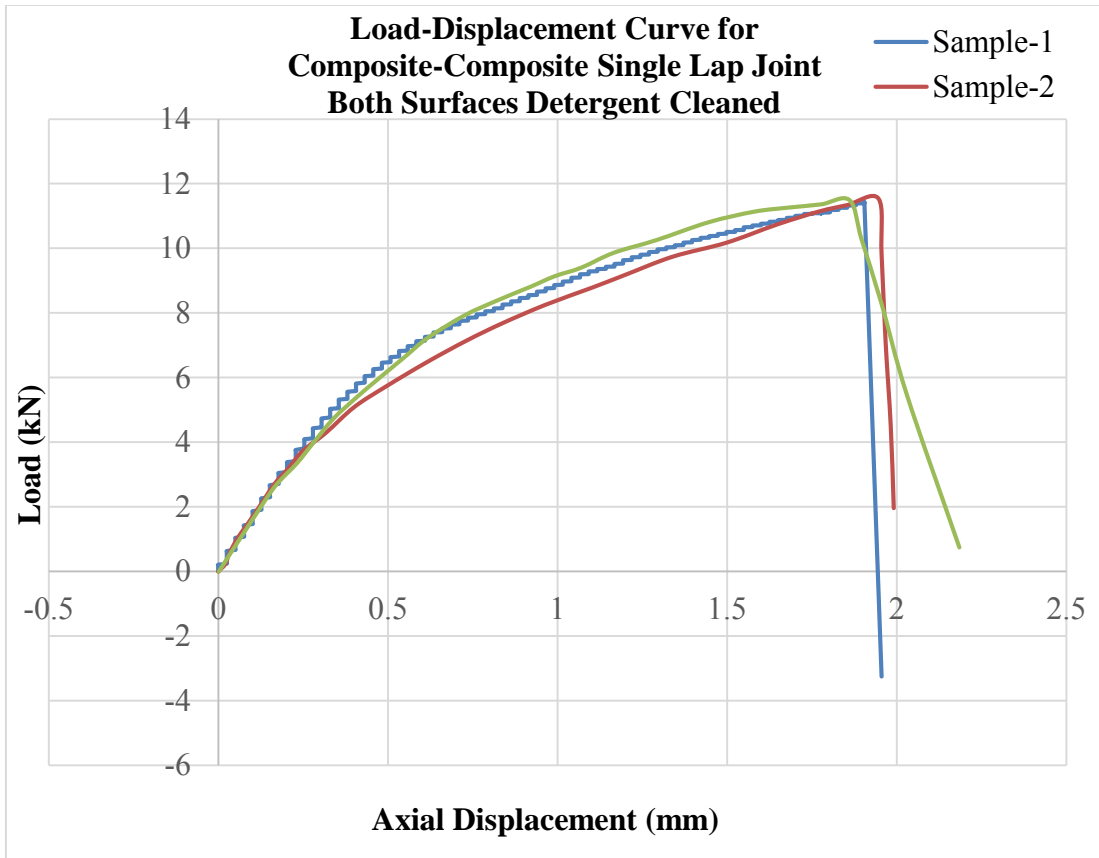


Figure 4.3. Load vs. displacement graph for first set of samples.

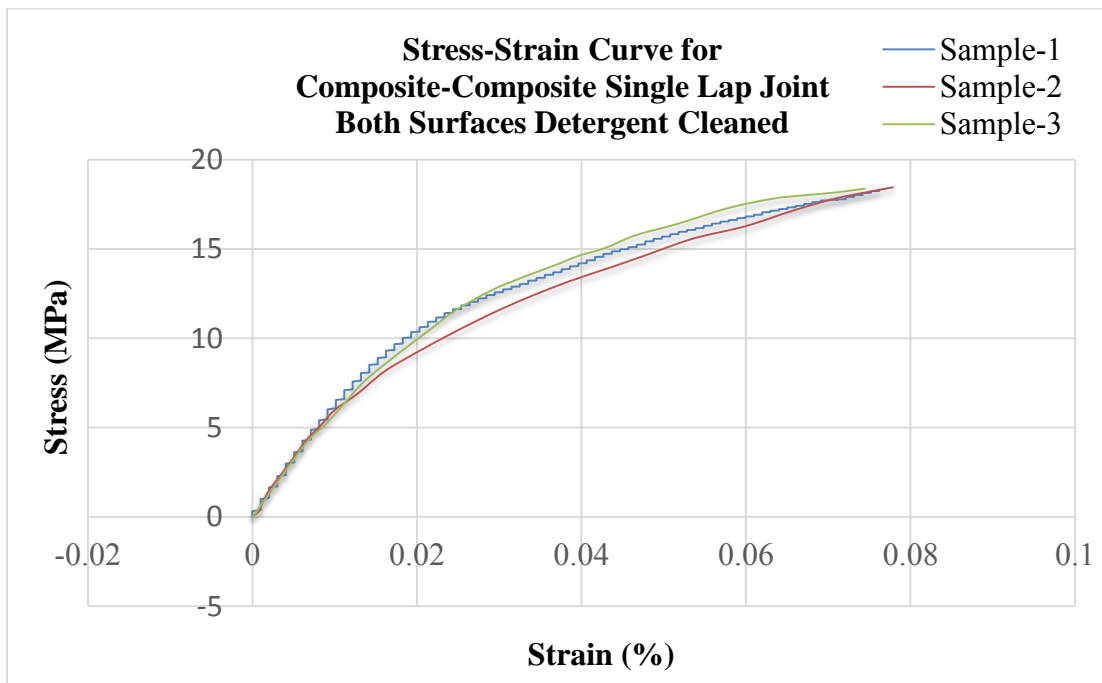


Figure 4.4. Stress vs. strain graph for first set of samples.

TABLE 4.3  
JOINT STRENGTH AND FAILURE LOAD WHEN COMPOSITE SURFACES  
DETERGENT CLEANED ONLY

Sample ID	Failure Load (kN)	Joint Strength (MPa)
1	11.14	17.82
2	11.79	18.86
3	11.62	18.59
Average	11.51	18.42
Standard Deviation	0.38	0.54

The second set of samples prepared were single lap joints between composites. Three specimens were prepared. Both surfaces to be joined were cleaned with detergent and then plasma treated for 4 minutes. The overlap length was fixed at 25 mm. The graphical representation of failure load, that is, the load at which the joint failed, is shown in Figure 4.5. It can be seen that the nature of the graph is linear. The failure mode for all three samples tested varied from 13 kN to 13.8 kN. Figure 4.6 shows the stress versus strain graph to obtain the maximum joint strength.

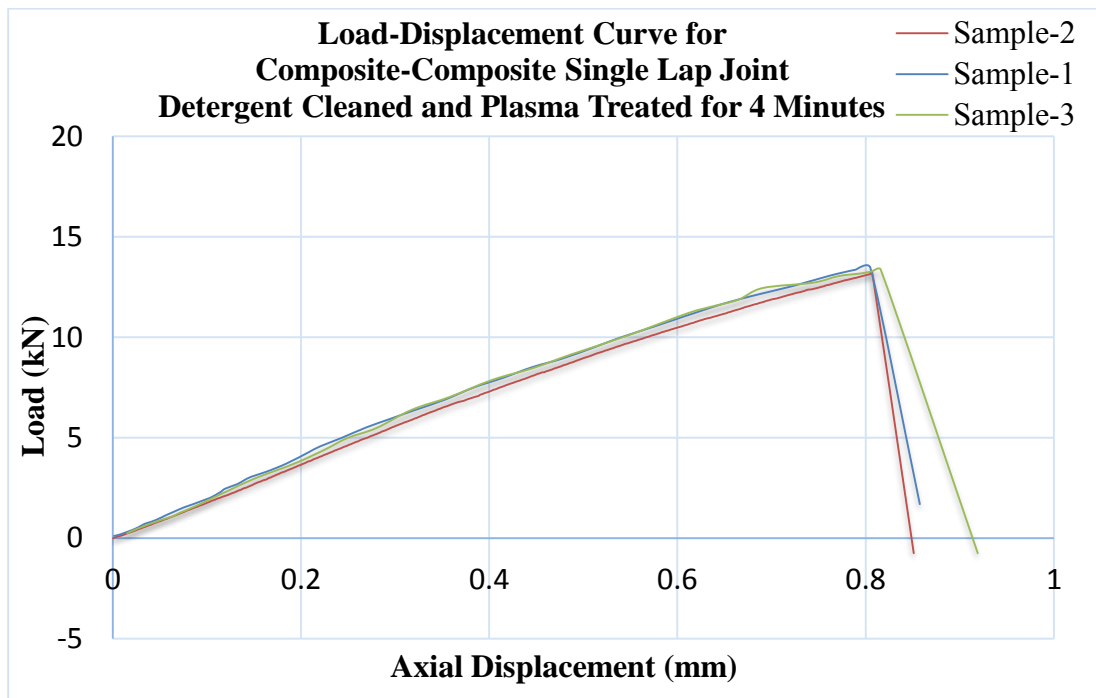


Figure 4.5. Load vs. displacement graph for second set of samples.

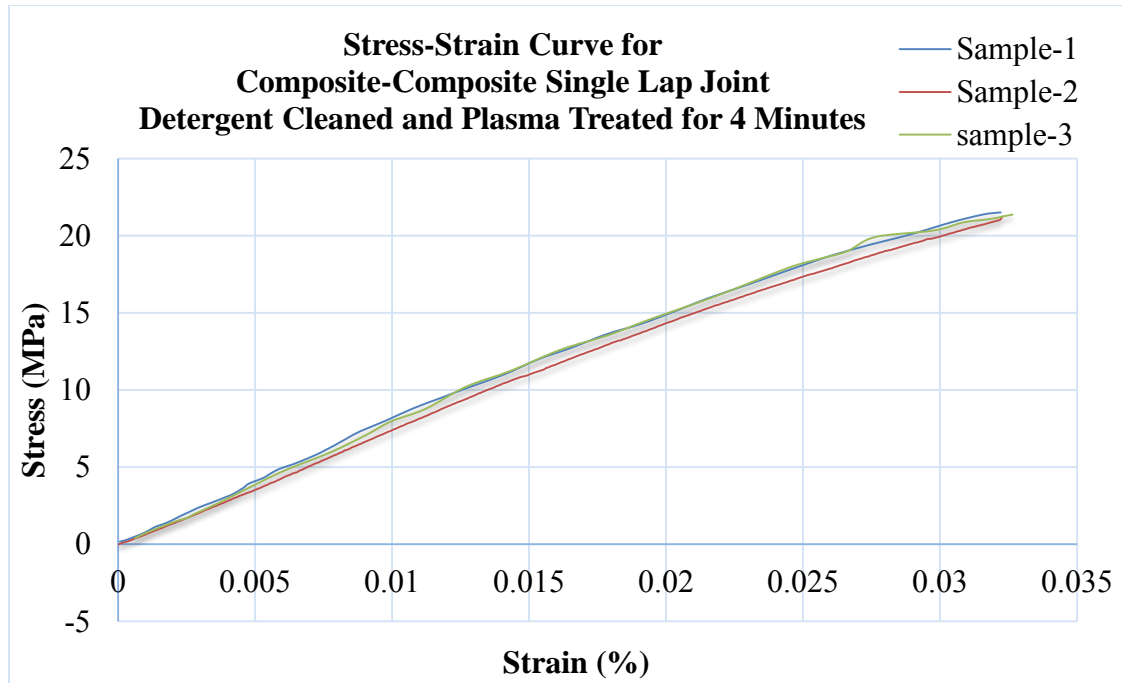


Figure 4.6. Stress vs. strain graph for second set of samples.

From Figure 4.6, it can be seen that the joint strength for all the three samples tested varied from 21 MPa to 22 MPa, with an average strength of 21.59 MPa. The samples after treating in plasma cleaner showed improved bond strength and failure mode. Table 4.4 shows the values for joint strength and failure load when the composite surface was detergent cleaned and plasma treated for 4 minutes.

TABLE 4.4

JOINT STRENGTH AND FAILURE LOAD WHEN COMPOSITE SURFACES  
DETERGENT CLEANED AND PLASMA TREATED FOR 4 MINUTES

Sample ID	Failure Load (kN)	Joint Strength (MPa)
1	13.78	22.05
2	13.14	21.02
3	13.38	21.41
Average	13.43	21.49
Standard Deviation	0.32	0.52

The third set of samples prepared were single lap joints between composites. Both surfaces were cleaned with detergent and plasma treated for 8 minutes. The overlap length was fixed at 25 mm. The graphical representation shown in Figure 4.7 indicates the failure load, that is, the load at which the joint failed. It can be seen that the nature of the graph is linear. The failure mode for all three samples tested varied from 15 kN to 16 kN. The average failure load observed was 15.12 kN. Figure 4.8 shows the stress versus strain graph to obtain the maximum joint strength.

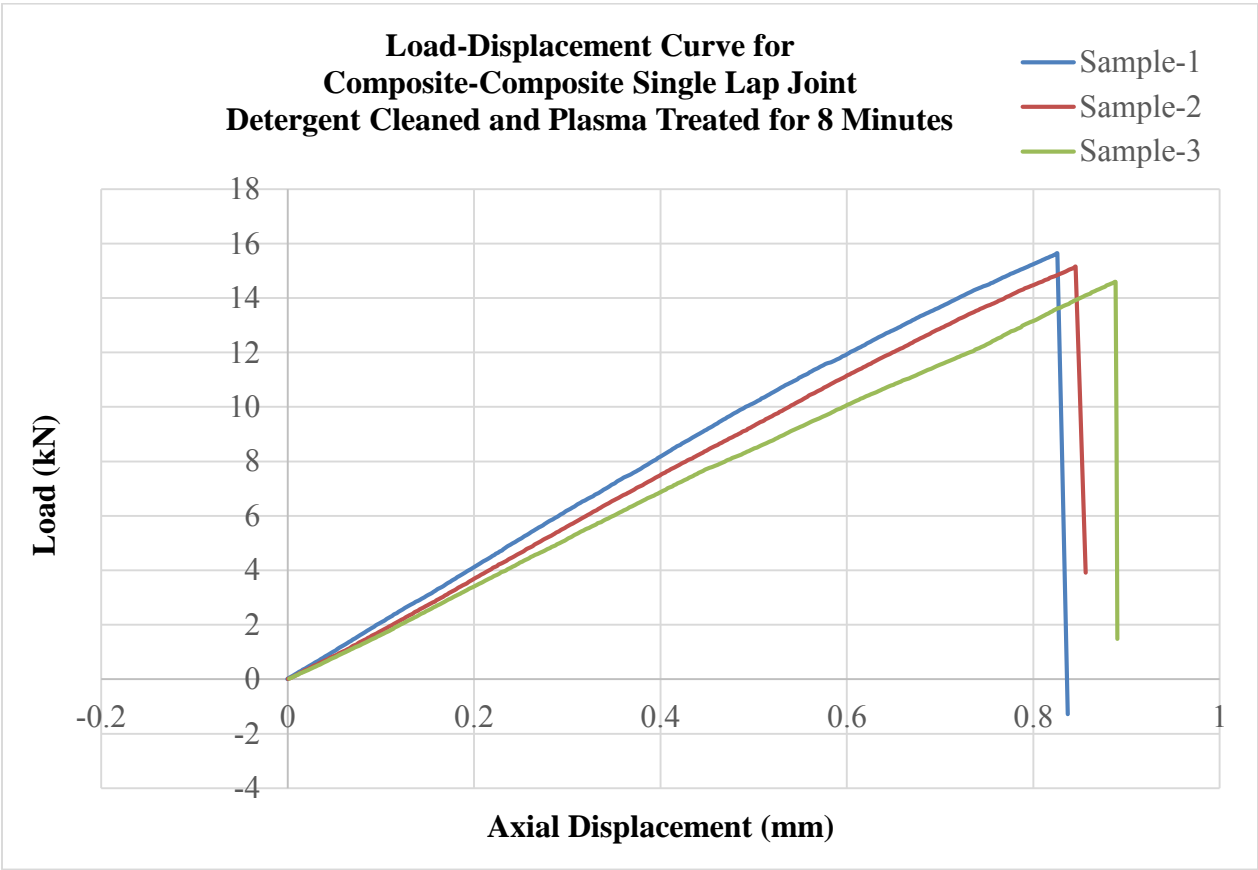


Figure 4.7. Load vs. displacement graph for third set of samples.

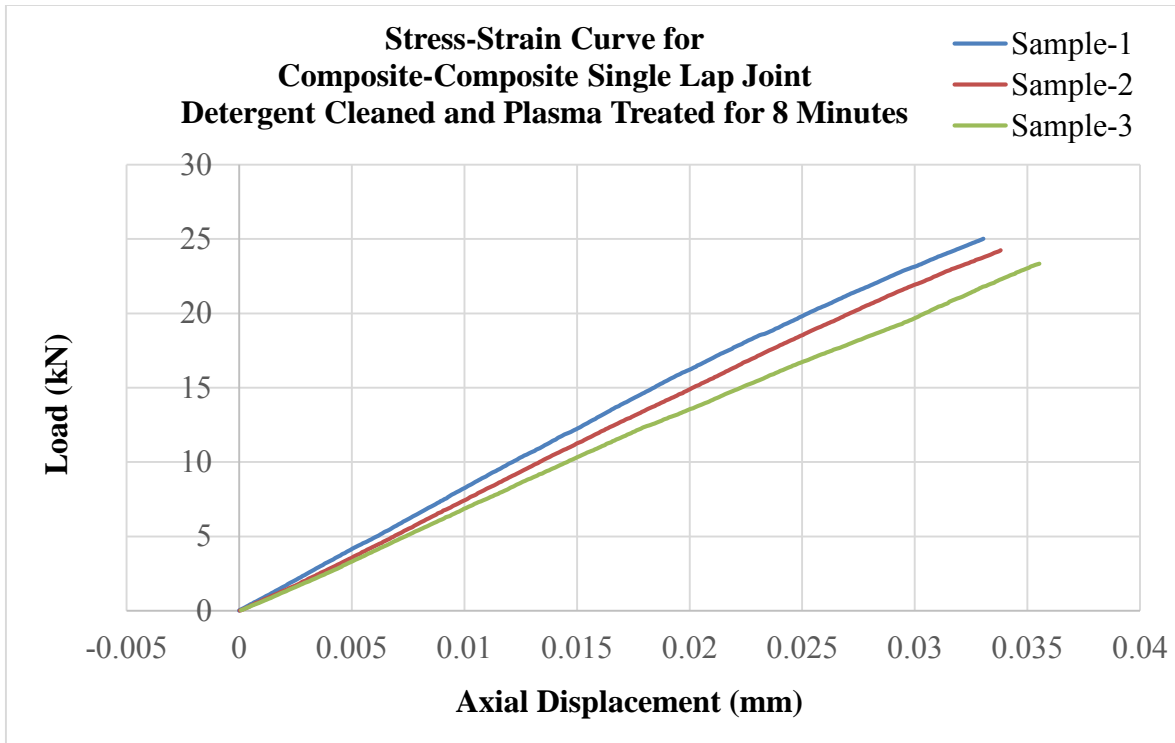


Figure 4.8. Stress vs. strain graph for third set of samples.

From Figure 4.8, it can be seen that the joint strength varied between 23 MPa and 25.1 MPa, with an average strength of 24.2 MPa. Table 4.5 shows the values for joint strength and failure load when the composite surface was detergent cleaned and plasma treated for 8 minutes.

TABLE 4.5

JOINT STRENGTH AND FAILURE LOAD WHEN COMPOSITE SURFACES  
DETERGENT CLEANED AND PLASMA TREATED FOR 8 MINUTES

Sample ID	Failure Load (kN)	Joint Strength (MPa)
1	15.64	25.02
2	15.15	24.24
3	14.56	23.30
Average	15.12	24.19
Standard Deviation	0.54	0.86

The fourth set of samples prepared were single lap joints between composites. Both surfaces were cleaned with detergent and plasma treated for 12 minutes. The overlap length was fixed at 25 mm. The graphical representation shown in Figure 4.9 indicates the failure load, that is, the load at which the joint failed. It can be seen that the nature of the graph is linear. The failure mode for all three samples tested varied from 14.8 kN to 16.3 kN. The average failure load observed was 15.45 kN. Figure 4.10 shows the stress versus strain graph to obtain maximum joint strength.

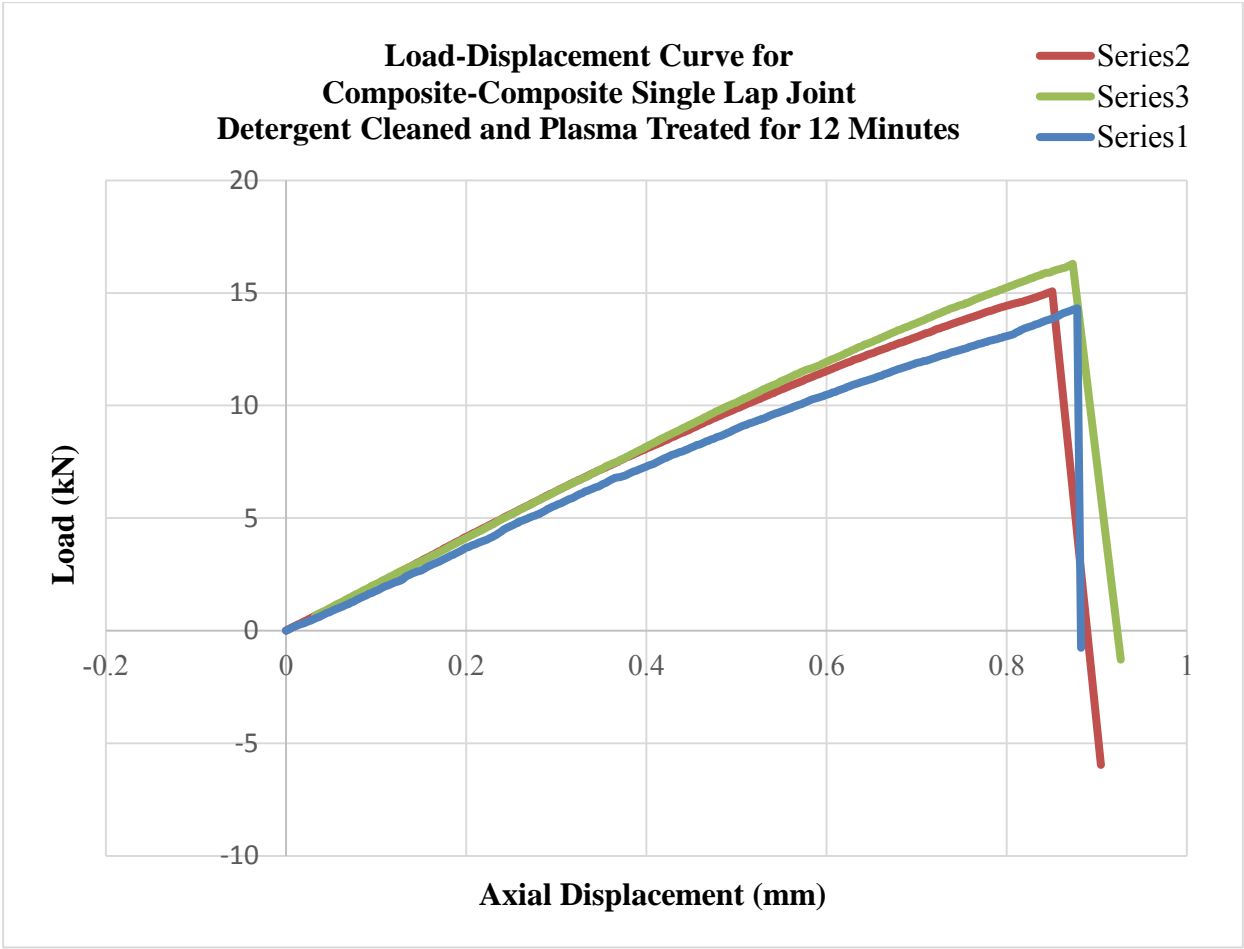


Figure 4.9. Load vs. displacement graph for fourth set of samples.

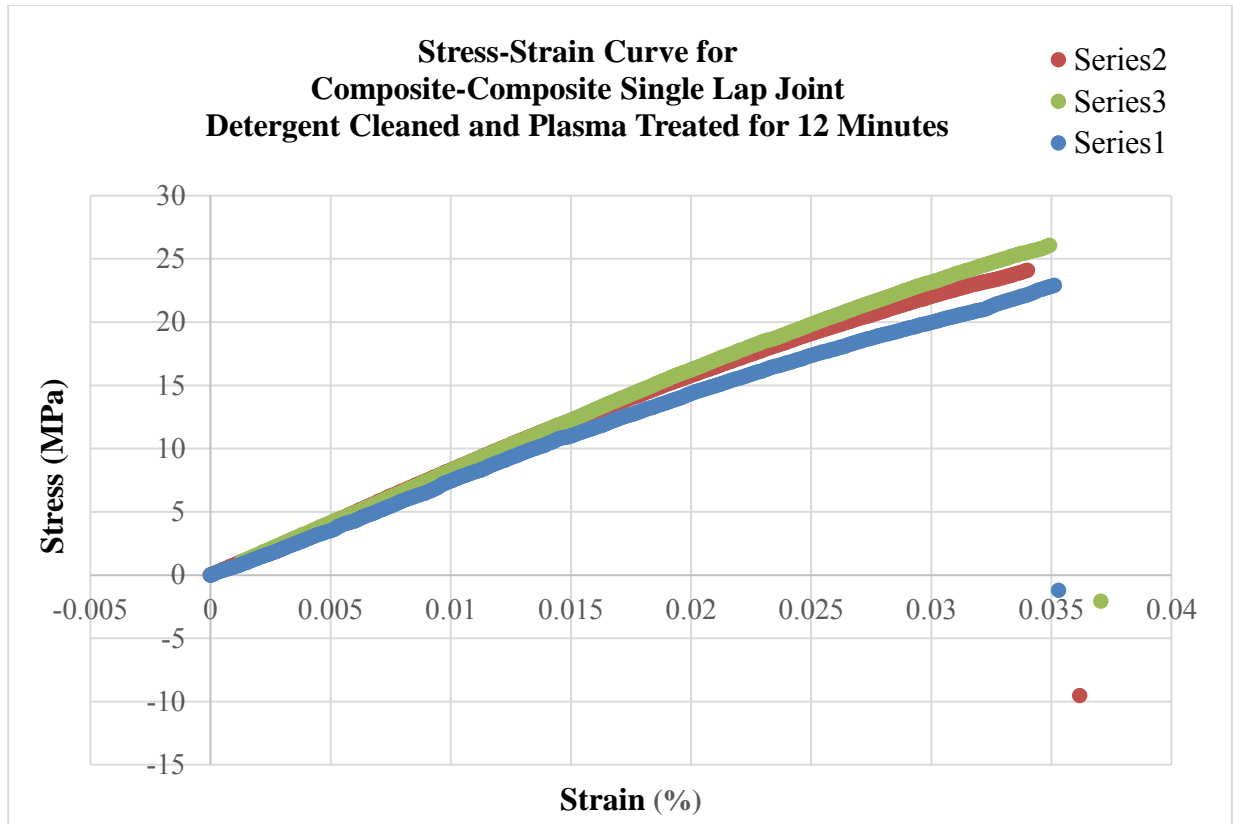


Figure 4.10. Stress vs. strain graph for fourth set of samples.

From Figure 4.10, it can be seen that the joint strength varied between 23.5 MPa and 26.1 MPa, with an average strength of 24.72 MPa. Table 4.6 shows the values for joint strength and failure loads when the composite surface was detergent cleaned and plasma treated for 12 minutes.

TABLE 4.6

JOINT STRENGTH AND FAILURE LOAD WHEN COMPOSITE SURFACES  
DETERGENT CLEANED AND PLASMA TREATED FOR 12 MINUTES

Sample ID	Failure Load (kN)	Joint Strength (MPa)
1	14.81	23.70
2	15.25	24.40
3	16.29	26.06
Average	15.45	24.72
Standard Deviation	0.76	1.21

The fifth set of samples prepared were single lap joints between composites. Both surfaces were sanded using sandpaper P 400 and cleaned with detergent. The overlap length was fixed at 25 mm. The graphical representation shown in Figure 4.11 indicates that the failure load, that is, the load at which the joint failed. It can be seen that the nature of the graph is not linear. The failure mode for all three samples tested varied from 13 kN to 14.2 kN. The average failure load was 13.67 kN. Figure 4.12 show the stress versus strain graph to obtain maximum joint strength.

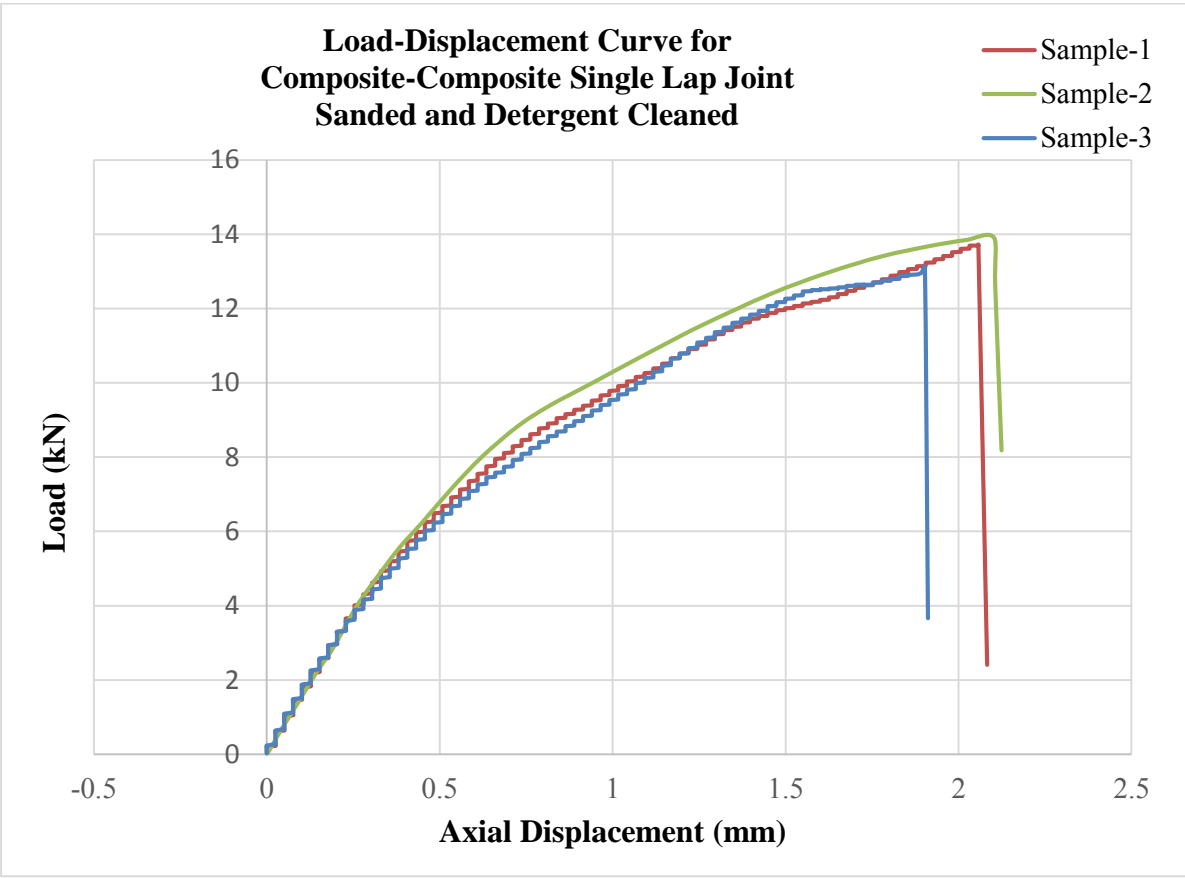


Figure 4.11. Load vs. displacement graph for fifth set of samples.

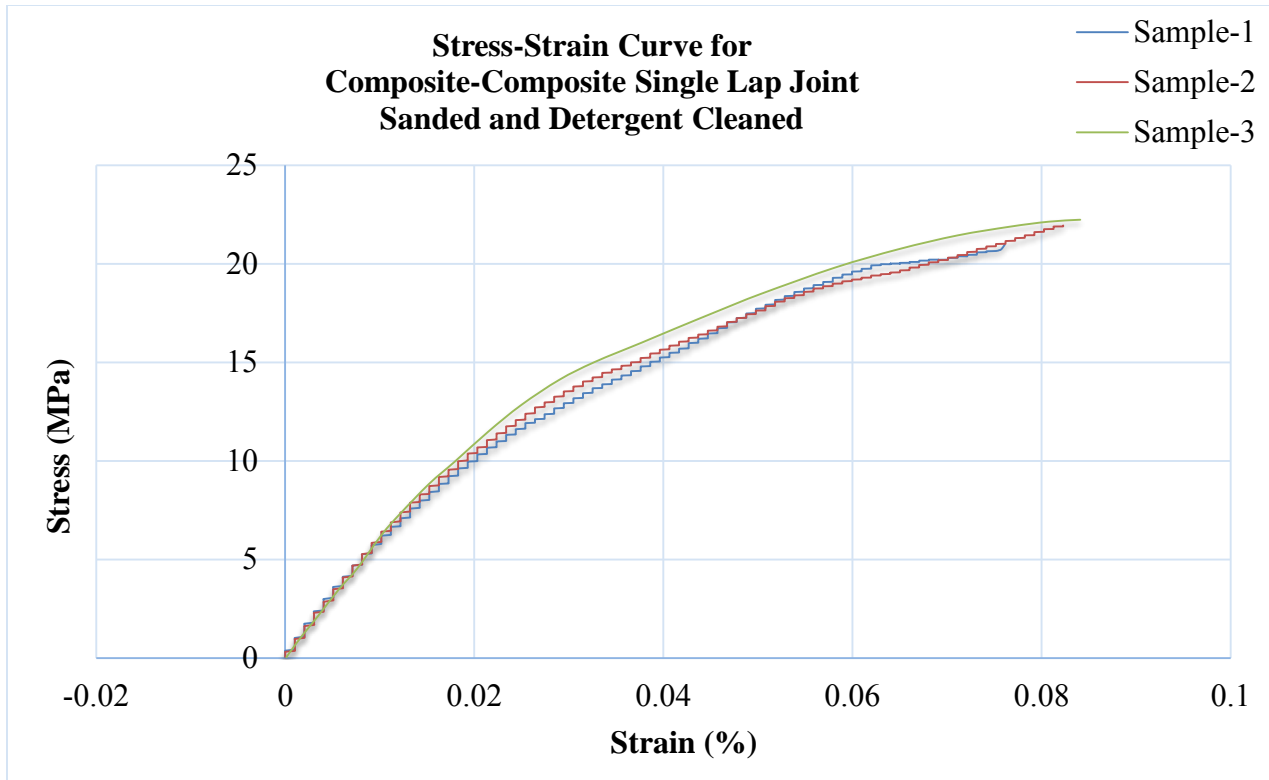


Figure 4.12. Stress vs. strain graph for fifth set of samples.

From Figure 4.12, it can be concluded that the joint strength varied between 21.13 MPa and 22.5 MPa, with an average strength of 21.86 MPa. Table 4.7 shows the values for joint strength and failure load when the composite surface was sanded and detergent cleaned.

TABLE 4.7

JOINT STRENGTH AND FAILURE LOAD VALUES WHEN COMPOSITE SURFACES SANDED AND DETERGENT CLEANED

Sample ID	Failure Load (kN)	Joint Strength (MPa)
1	13.21	21.13
2	13.78	22.06
3	13.99	22.40
Average	13.66	21.86
Standard Deviation	0.40	0.66

The sixth set of samples prepared were single lap joints between composites. Both surfaces were sanded using sandpaper P 400, cleaned with detergent, and plasma treated for 4 minutes. The overlap length was fixed at 25 mm. The graphical representation shown in Figure 4.15 indicates the failure load, that is, the load at which the joint failed. It can be seen that the nature of the graph is linear. The failure mode for all three samples tested varied from 13 kN to 16.2 kN. The average failure load calculated was 14.84 kN. Figure 4.16 show the stress versus strain graph to obtain maximum joint strength.

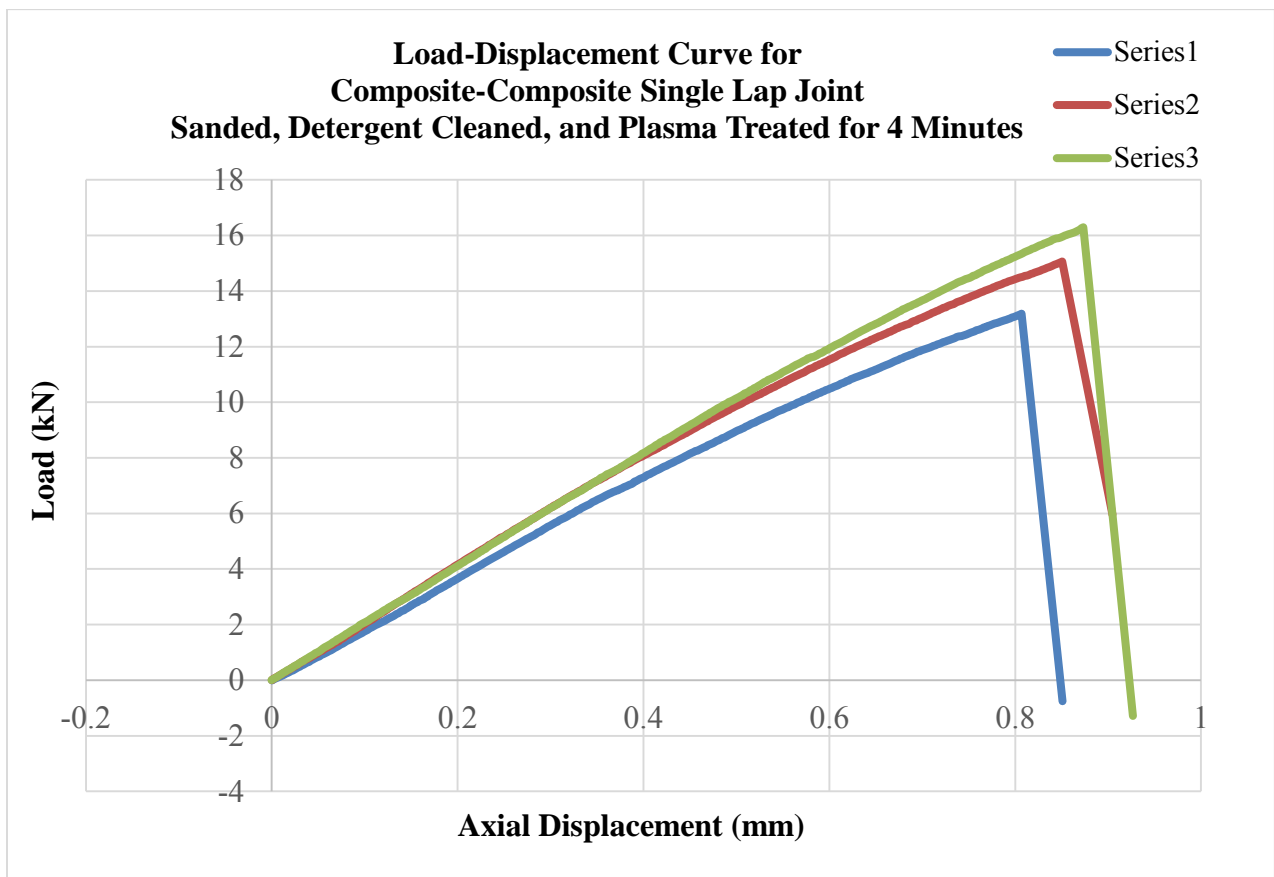


Figure 4.15. Load vs. displacement graph for sixth set of samples.

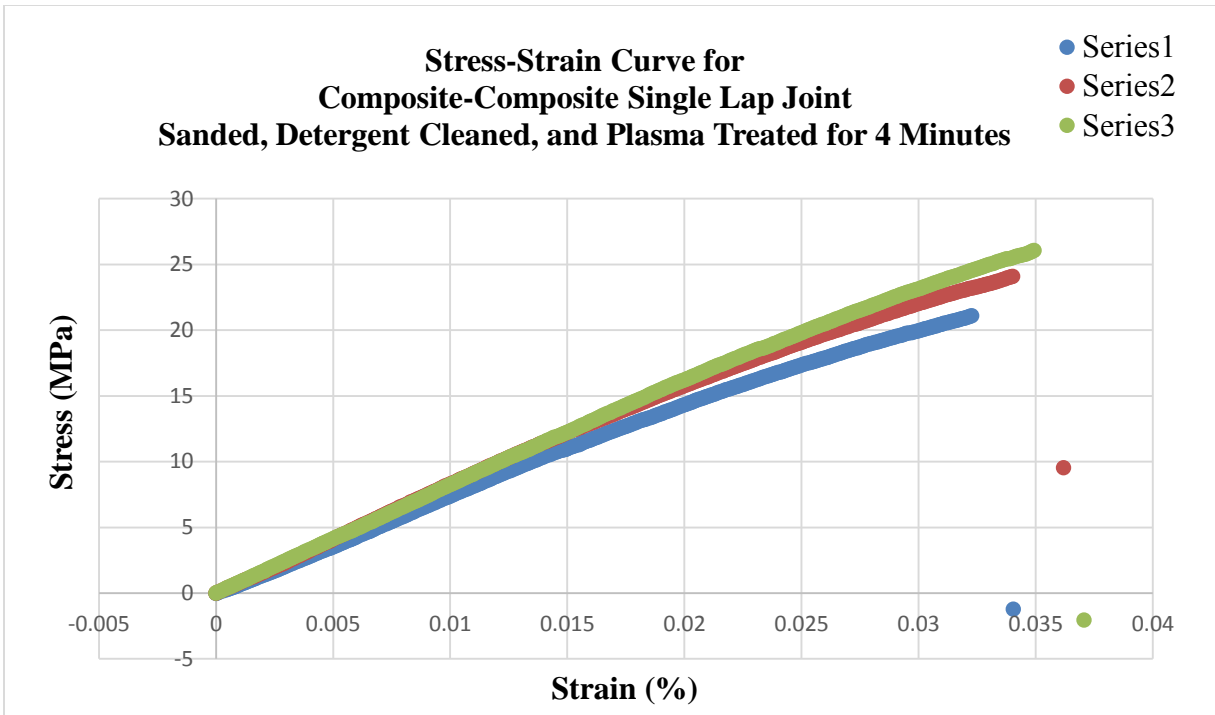


Figure 4.16. Stress vs. strain graph for sixth set of samples.

From Figure 4.16, it can be seen that the joint strength varied between 23.5 MPa and 24.2 MPa, with an average strength of 23.75 MPa. Table 4.8 shows the values for joint strength and failure load and when the composite surface was sanded, detergent cleaned, and plasma treated for 4 minutes.

TABLE 4.8

JOINT STRENGTH AND FAILURE LOAD WHEN COMPOSITE SURFACES SANDED, DETERGENT CLEANED, AND PLASMA TREATED FOR 4 MINUTES

Sample ID	Failure Load (kN)	Joint Strength (MPa)
1	13.18	21.10
2	15.07	24.11
3	16.28	26.05
Average	14.84	23.75
Standard Deviation	1.56	2.49

The seventh set of samples prepared were single lap joints between composites. Both surfaces were sanded using sandpaper P 400, cleaned with detergent, and plasma treated for 8 minutes. The overlap length was fixed at 25 mm. The graphical representation shows the failure load, that is, the load at which the joint failed. It can be seen that the nature of the graph is linear. The failure mode for all three samples tested varied from 14.8 kN to 16.4 kN. The average failure load calculated was 15.45 kN. Figure 4.14 show the stress versus strain graph to obtain the maximum joint strength.

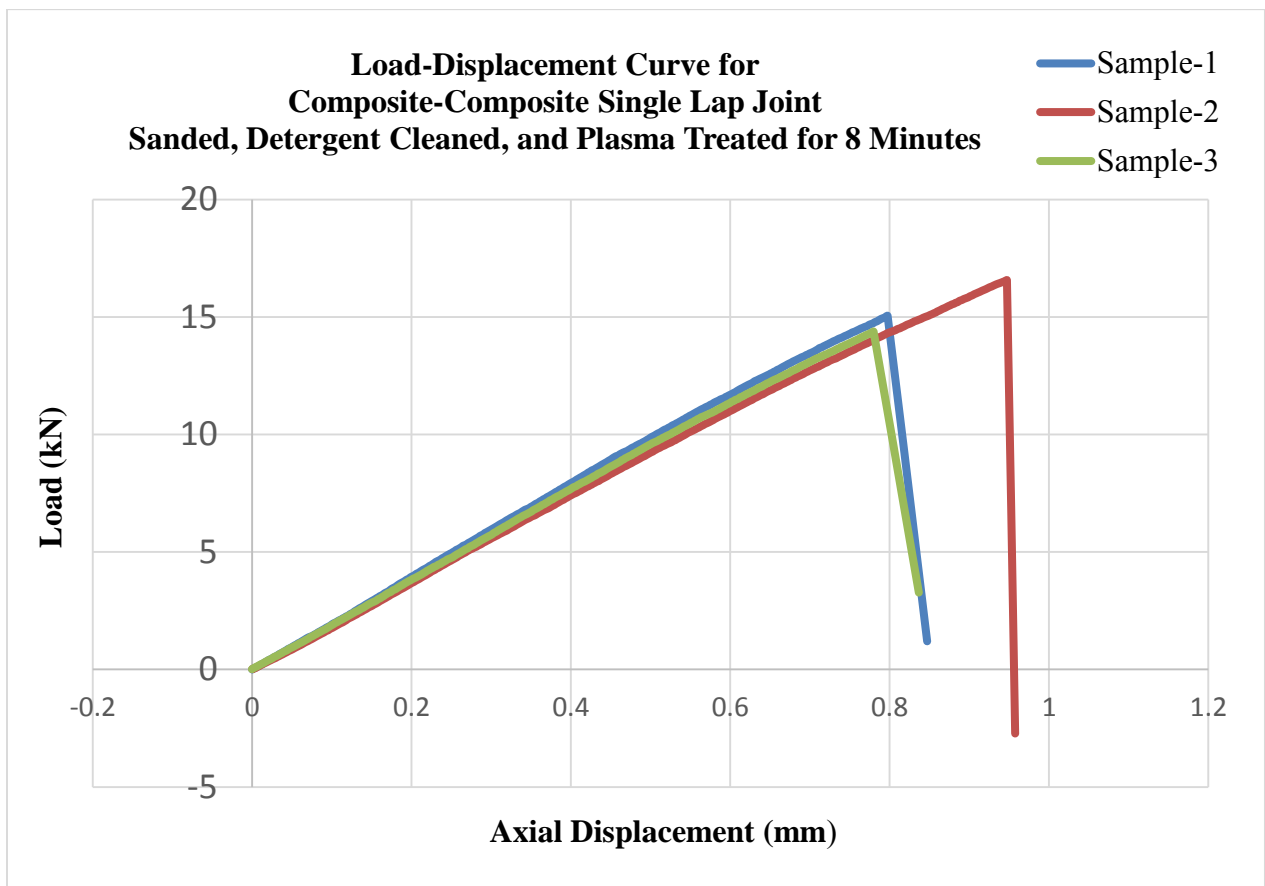


Figure 4.13. Load vs. displacement graph for seventh set of samples.

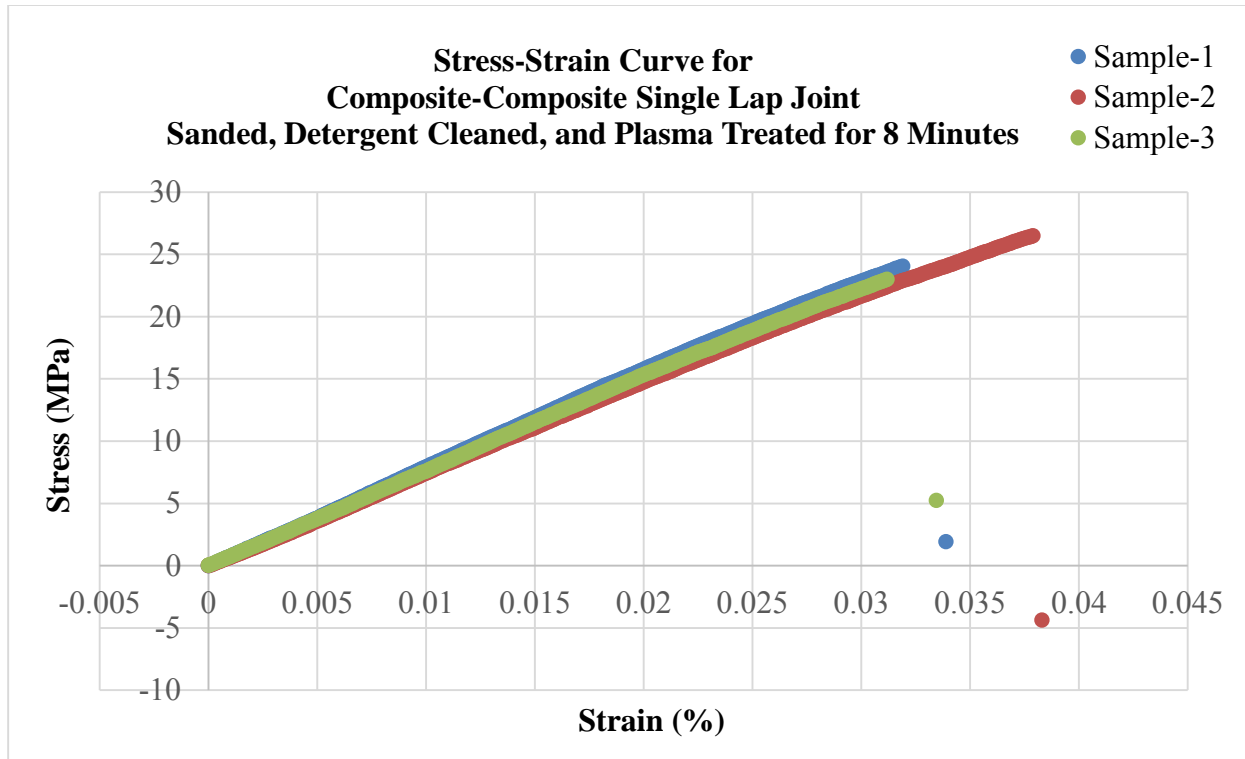


Figure 4.14. Stress vs. strain graph for seventh set of samples.

From Figure 4.14, it can be seen that the joint strength varied from 23.6 MPa to 26.2 MPa, with an average strength of 24.72 MPa. Table 4.9 shows the values for joint strength and failure load when the composite surface was sanded, detergent cleaned, and plasma treated for 8 minutes.

TABLE 4.9

JOINT STRENGTH AND FAILURE LOAD WHEN COMPOSITE SURFACES SANDED, DETERGENT CLEANED, AND PLASMA TREATED FOR 8 MINUTES

Sample ID	Failure Load (kN)	Joint Strength (MPa)
1	14.81	23.70
2	15.18	24.29
3	16.37	26.19
Average	15.45	24.72
Standard Deviation	0.82	1.30

The eighth set of samples prepared were single lap joints between composites. Both surfaces were sanded using sandpaper P 400, cleaned using detergent, and plasma treated for 12 minutes. The overlap length was fixed at 25 mm. The graphical representation shows the failure load, that is, the load at which the joint failed. It can be seen that the nature of the graph is linear. The failure mode for all three samples tested varied from 15.4 kN to 16.2 kN. The average failure load calculated was 15.82 kN. Figure 4.18 show the stress versus strain graph to obtain maximum joint strength.

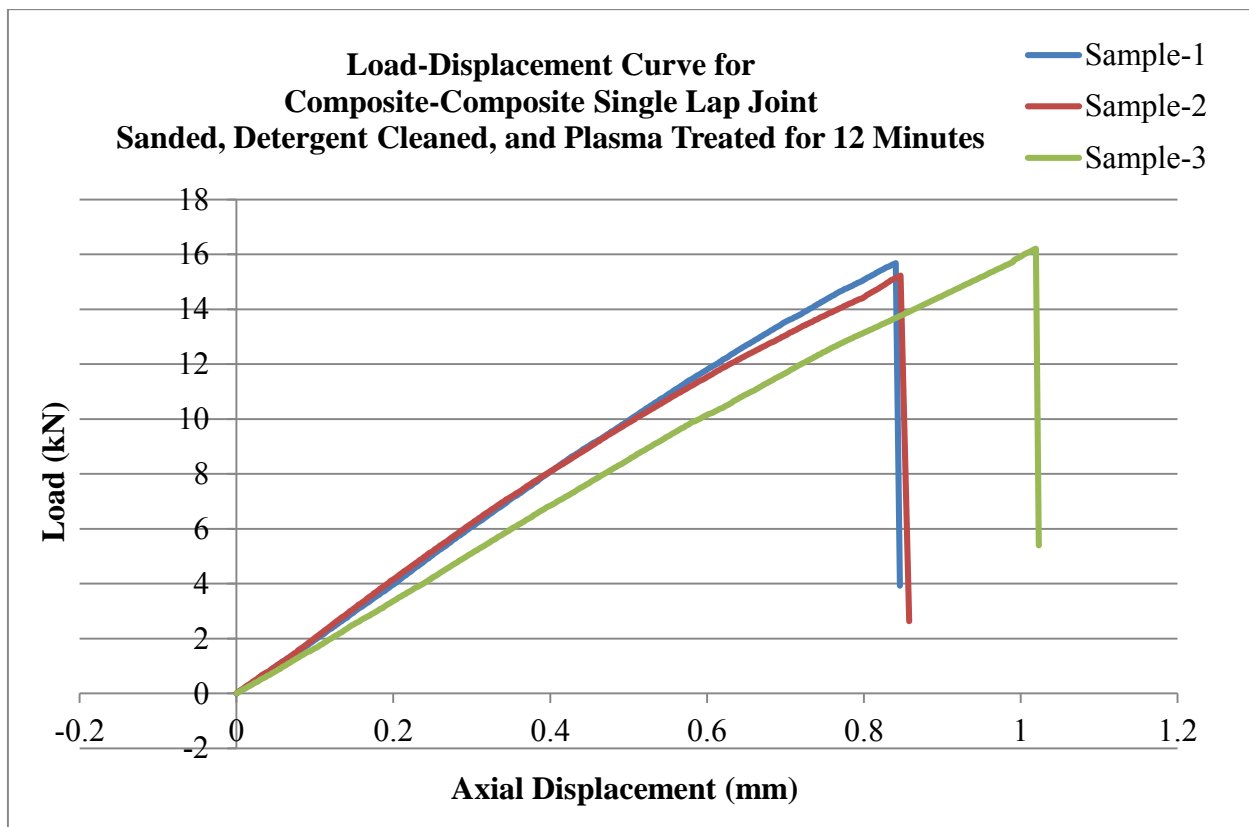


Figure 4.17. Load vs. displacement graph for eighth set of samples.

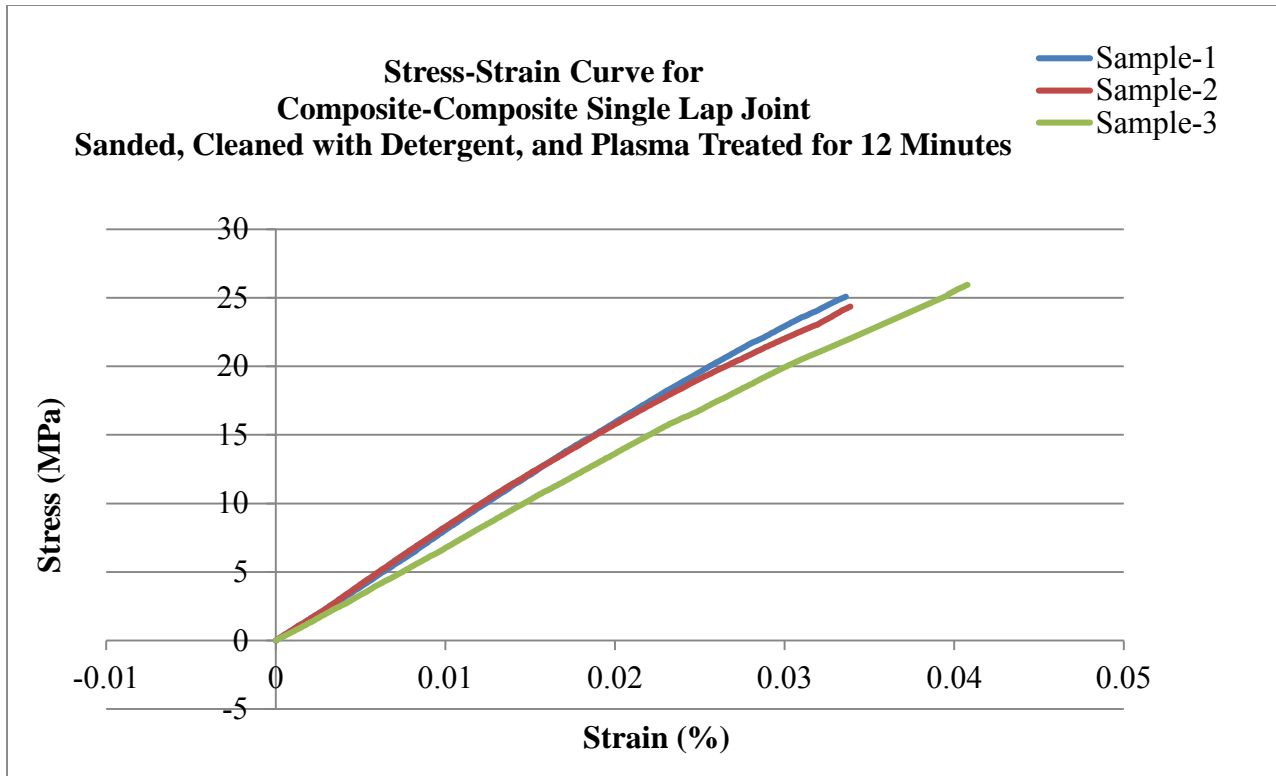


Figure 4.18. Stress vs. strain graph for eight set of samples.

From Figure 4.18, it was concluded that the joint strength varied from 24.7 MPa to 26 MPa, with an average strength of 25.31 MPa. Table 4.10 shows the values for joint strength and failure load when the composite surface was sanded, detergent cleaned, and plasma treated for 12 minutes.

TABLE 4.10

JOINT STRENGTH AND FAILURE LOAD WHEN COMPOSITE SURFACES SANDED, DETERGENT CLEANED, AND PLASMA TREATED FOR 12 MINUTES

Sample ID	Failure Load (kN)	Joint Strength (MPa)
1	15.83	25.33
2	15.48	24.77
3	16.15	25.84
Average	15.82	25.31
Standard Deviation	0.34	0.54

Failure loads were measured in a composite-to-composite single lap joint where the first sample was detergent cleaned only, while the other three samples were detergent cleaned and plasma treated for 4, 8, and 12 minutes. Table 4.11 shows the average load and standard deviation for different plasma-treatment times on the base composite samples. Figure 4.19 is a bar graph representation of failure load analysis with standard deviations at different plasma-treatment times. The analysis shows that as the plasma exposure time increased, the failure load also increased, in turn enhancing the bond strength.

TABLE 4.11

AVERAGE FAILURE LOAD AND STANDARD DEVIATION FOR COMPOSITE BASE AND PLASMA-TREATED SAMPLES

	<b>Base (No Plasma)</b>	<b>Plasma 4 Minutes</b>	<b>Plasma 8 Minutes</b>	<b>Plasma 12 Minutes</b>
Average Failure Load	11.51	13.43	15.12	15.45
Standard Deviation	0.38	0.32	0.54	0.76

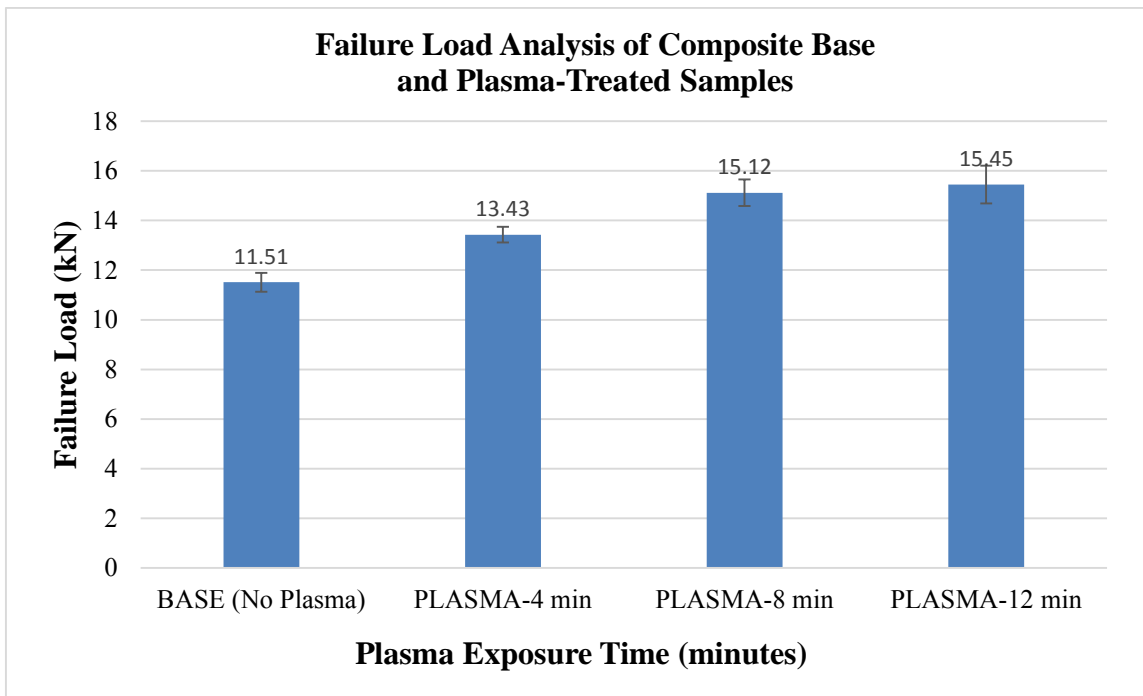


Figure 4.19. Bond failure analysis of base and plasma-treated samples.

Table 4.12 shows the average joint strength and standard deviation for different plasma-exposure times on the base composite samples. Figure 4.20 is a bar graph of joint strength analysis and standard deviation for different plasma-treatment times. The analysis shows that as the plasma exposure time increased, the joint strength also increased, in turn increasing the bond strength.

TABLE 4.12

AVERAGE JOINT STRENGTH AND STANDARD DEVIATION FOR COMPOSITE BASE AND PLASMA-TREATED SAMPLES

	<b>Base (No Plasma)</b>	<b>Plasma 4 Minutes</b>	<b>Plasma 8 Minutes</b>	<b>Plasma 12 Minutes</b>
Average Joint Strength	18.42	21.49	24.19	24.72
Standard Deviation	0.54	0.52	0.86	1.21

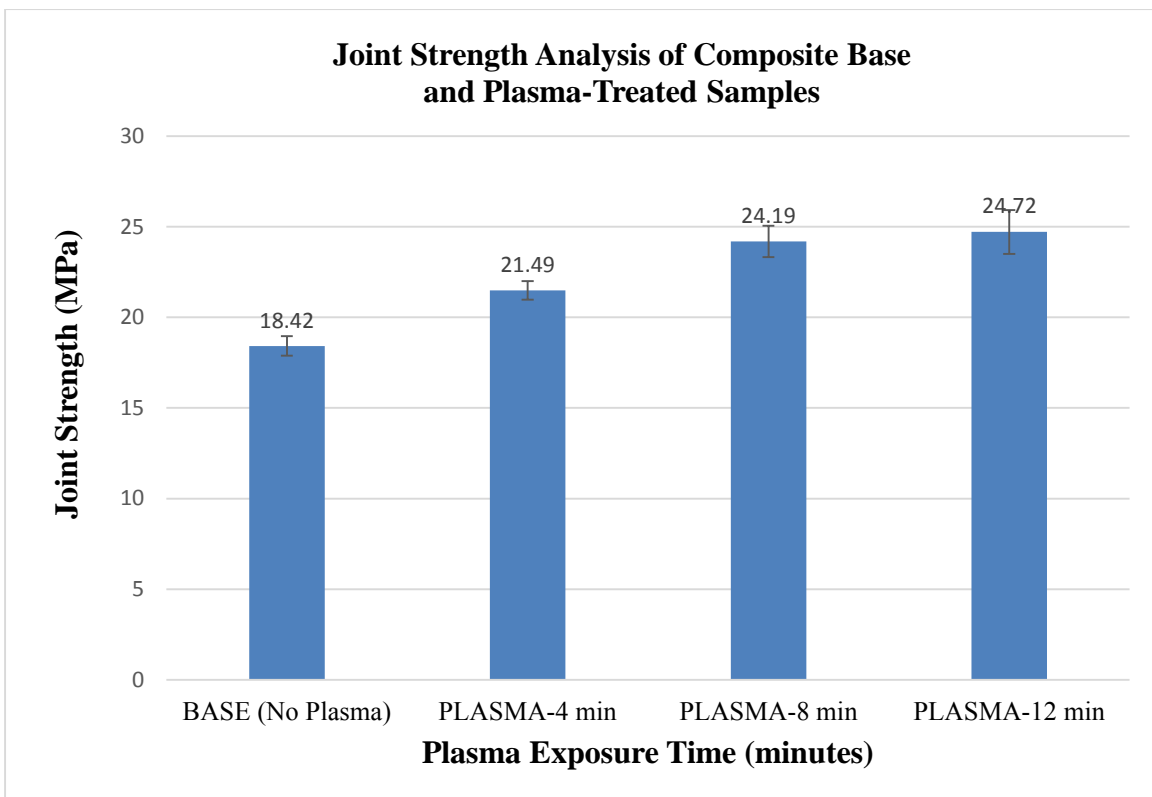


Figure 4.20. Joint strength analysis of composite base and plasma-treated samples.

Table 4.13 shows the average load and standard deviation calculations for different plasma exposure times on sanded composite samples. Figure 4.21 is a bar graph representation of failure load with standard deviation at different plasma-exposure times.

TABLE 4.13

AVERAGE FAILURE LOAD AND STANDARD DEVIATION FOR COMPOSITE SANDED AND PLASMA-TREATED SAMPLES

	<b>Base (No Plasma)</b>	<b>Plasma 4 Minutes</b>	<b>Plasma 8 Minutes</b>	<b>Plasma 12 Minutes</b>
Average Failure Load	13.66	14.84	15.45	15.82
Standard Deviation	0.40	1.56	0.82	0.34

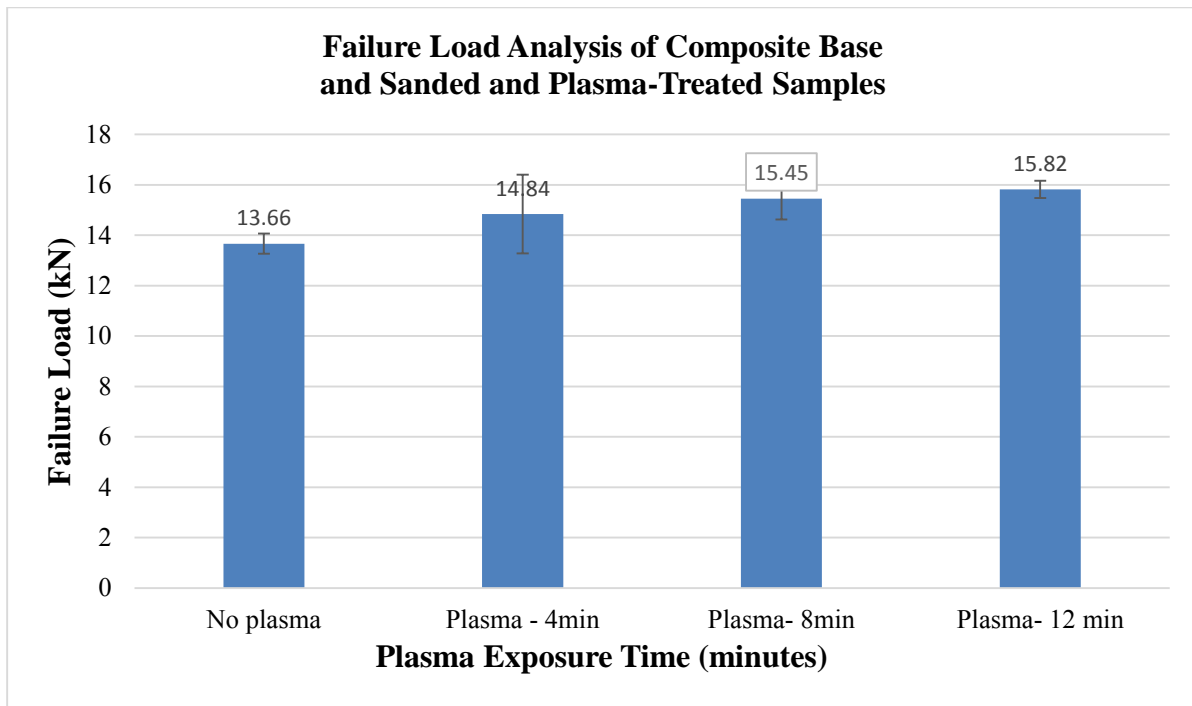


Figure 4.21. Failure load analysis of sanded and plasma-treated samples.

Table 4.14 shows the average joint strength and standard deviations of the composite-to-composite single lap joint where samples in the first set were detergent cleaned and sanded, while

samples in the other sets were detergent cleaned, sanded, and plasma treated for 4, 8, and 12 minutes. Figure 4.22 is a bar graph showing joint strength analysis with standard deviation at different plasma-exposure times.

TABLE 4.14

AVERAGE JOINT STRENGTH AND STANDARD DEVIATION FOR COMPOSITE SANDED AND PLASMA-TREATED SAMPLES

	Base (No Plasma)	Plasma 4 Minutes	Plasma 8 Minutes	Plasma 12 Minutes
Average Joint Strength	21.86	23.75	24.72	25.31
Standard Deviation	0.66	2.49	1.30	0.54

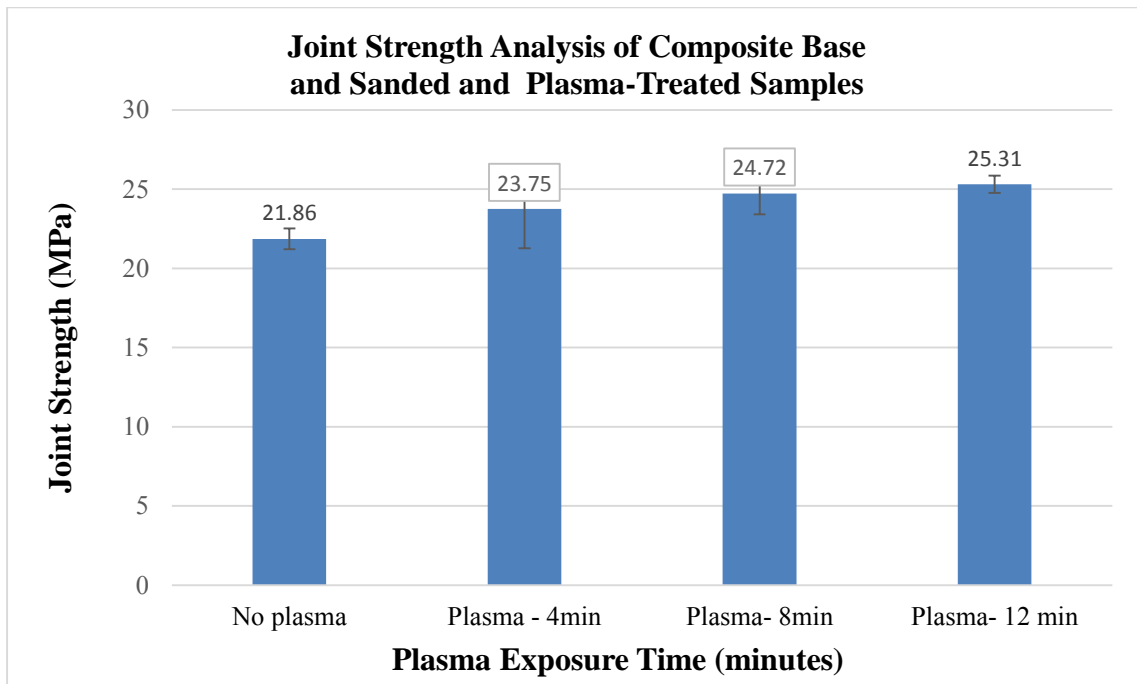


Figure 4.22. Joint strength analysis of sanded and plasma-treated samples.

It was concluded that sanding plus plasma treatment at various exposure times enhanced the joint strength and failure load compared to samples without sanding. Therefore, sanding plus plasma is an efficient way to improve the bond strength of a single lap joint between composites.

The ninth set of samples prepared were single lap joints between aluminum and composites. Both surfaces were cleaned using detergent. These samples were analyzed as base results for further comparisons. The overlap length was fixed at 25 mm. Figure 4.23 shows the failure load, that is, the load at which the joint failed. It can be seen that the nature of the graph is linear. The failure mode for all three samples tested ranged from 9 kN to 9.8 kN. The average failure load calculated was 9.46 kN. Figure 4.24 show stress versus strain graph to obtain the maximum joint strength.

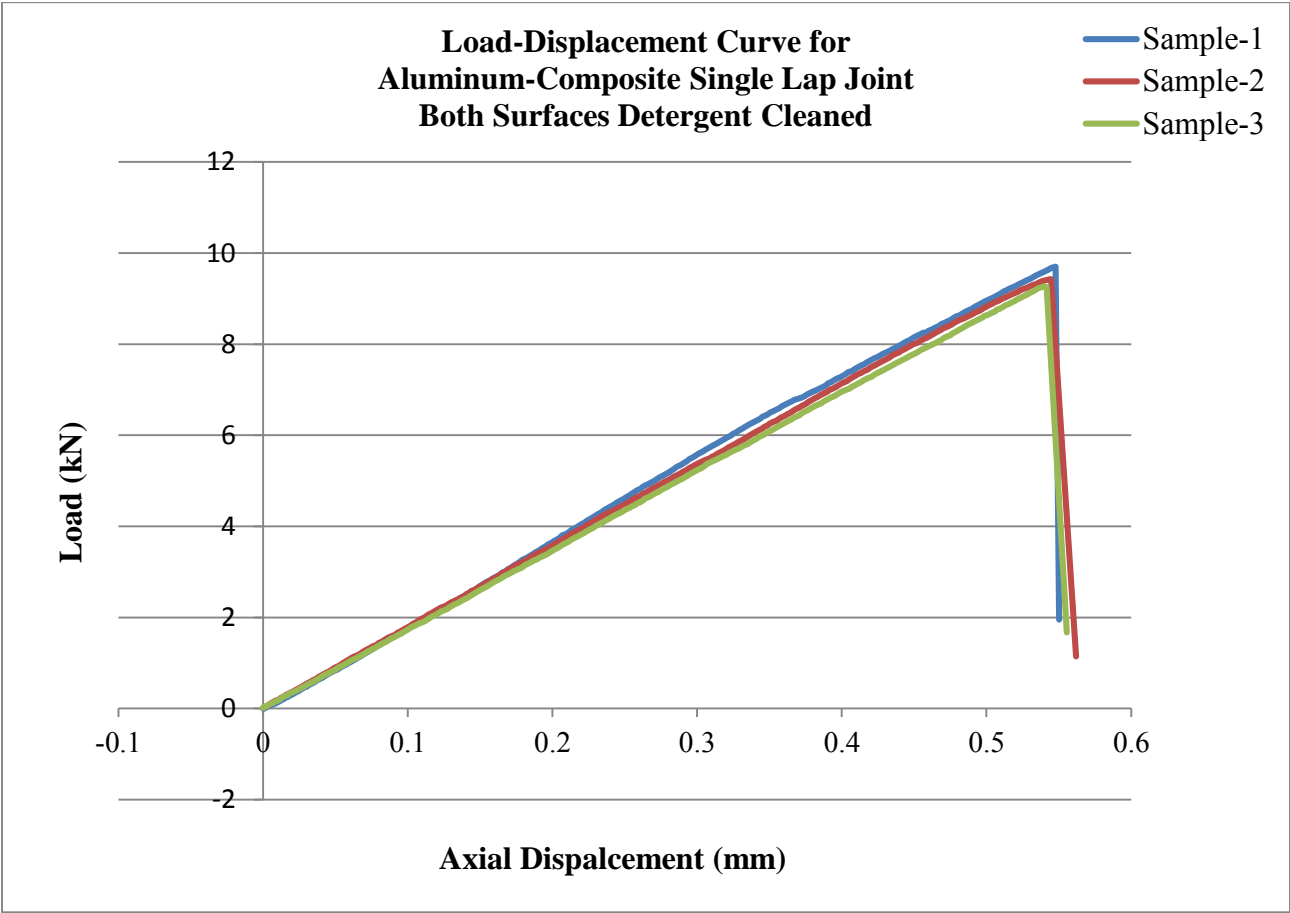


Figure 4.23. Load vs. displacement graph for ninth set of samples.

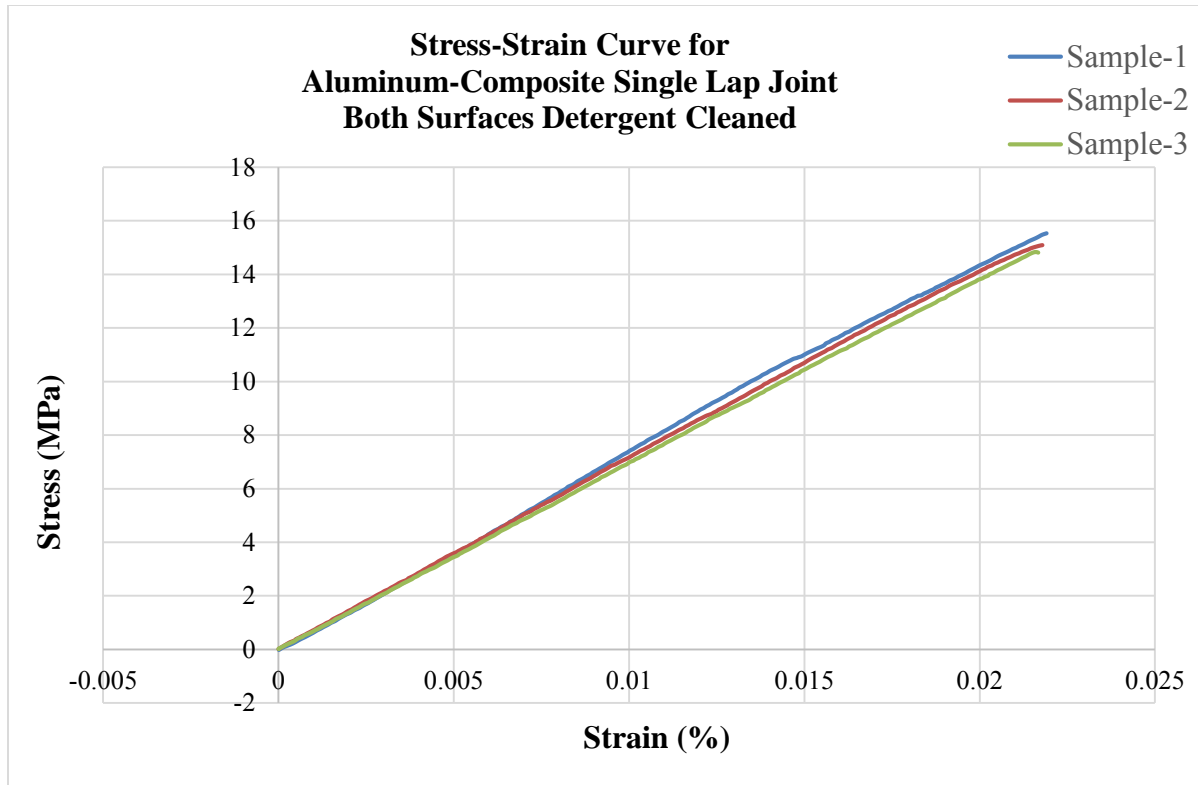


Figure 4.24. Stress vs. strain graph for ninth set of samples.

From Figure 4.24, it can be seen that the joint strength varied between 14.5 MPa and 16 MPa, with an average strength of 15.14 MPa. Table 4.15 shows joint strength and failure load when both aluminum and composite surfaces were detergent cleaned.

TABLE 4.15

JOINT STRENGTH AND FAILURE LOAD WHEN BOTH  
ALUMINUM AND COMPOSITE SURFACES DETERGENT CLEANED

Sample ID	Failure Load (KN)	Joint Strength (MPa)
1	9.71	15.53
2	9.43	15.09
3	9.25	14.81
Average	9.46	15.14
Standard Deviation	0.23	0.36

The tenth set of samples prepared were single lap joints between aluminum and composites. The composite surface was detergent cleaned, while the aluminum surface was sanded using sandpaper P 400 and then cleaned with detergent. The overlap length was fixed at 25 mm. Figure 4.25 is a bar graph representation of failure load, that is, the load at which the joint failed. It can be seen that the nature of the graph is linear. The failure mode for all three samples tested varied from 10.3 kN to 11.6 kN. The average failure load calculated was 10.9 kN. Figure 4.26 show the stress versus strain graph to obtain maximum joint strength.

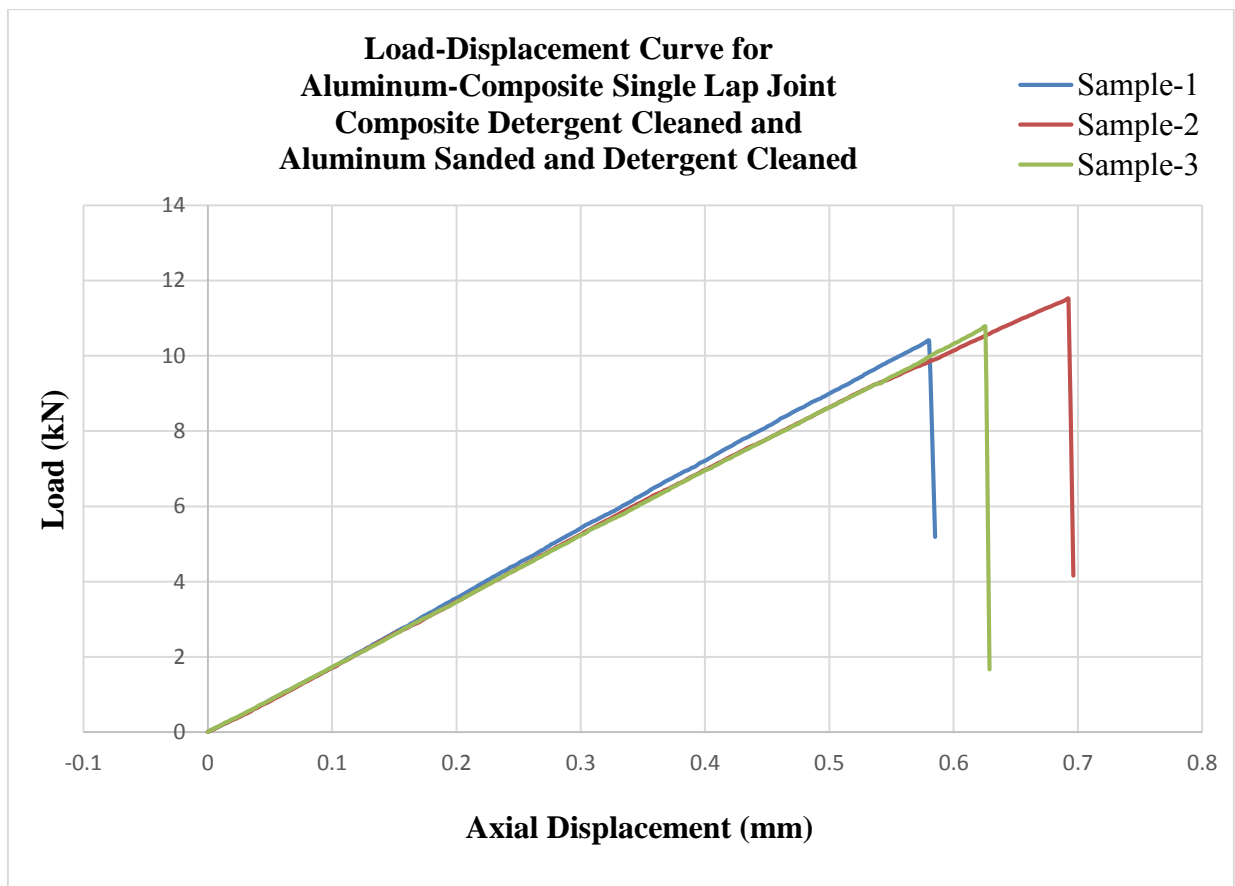


Figure 4.25. Load vs. displacement graph for tenth set of samples.

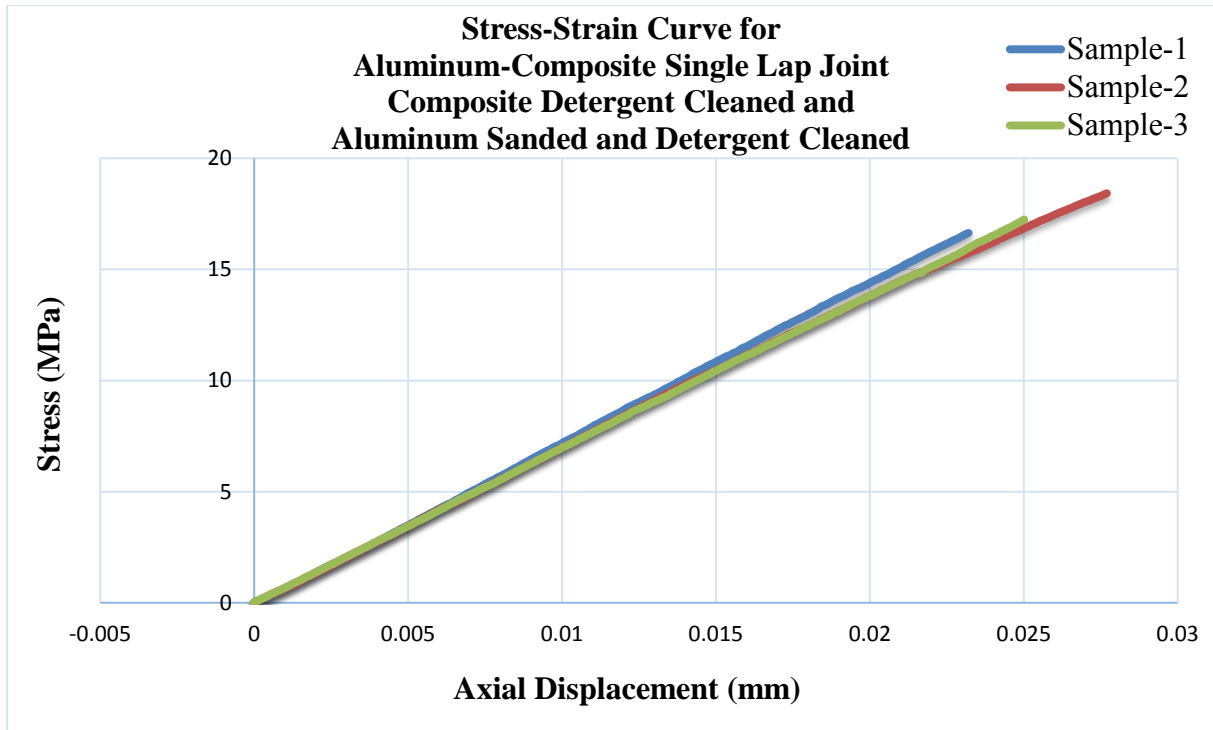


Figure 4.26. Stress vs. strain graph for tenth set of samples.

From Figure 4.26, it can be seen that the joint strength varied between 16.6 MPa and 18.5 MPa, with an average strength of 17.43 MPa. Table 4.16 shows joint strength and failure load when the composite surface was detergent cleaned and the aluminum surface was sanded and detergent cleaned.

TABLE 4.16

JOINT STRENGTH AND FAILURE LOAD WHEN COMPOSITE SURFACE  
DETERGENT CLEANED AND ALUMINUM SURFACE SANDED  
AND DETERGENT CLEANED

Sample ID	Failure Load (KN)	Joint Strength (MPa)
1	10.40	16.63
2	11.52	18.43
3	10.78	17.24
Average	10.9	17.43
Standard Deviation	0.57	0.92

The eleventh set of samples prepared were single lap joints between aluminum and composites. The composite surface was cleaned using detergent, while the aluminum surface was cleaned/etched using Alumiprep 33 solution and then coated with Alodine. The overlap length was fixed at 25 mm. Figure 4.27 is a graphical representation showing the failure load, that is, the load at which the joint failed.

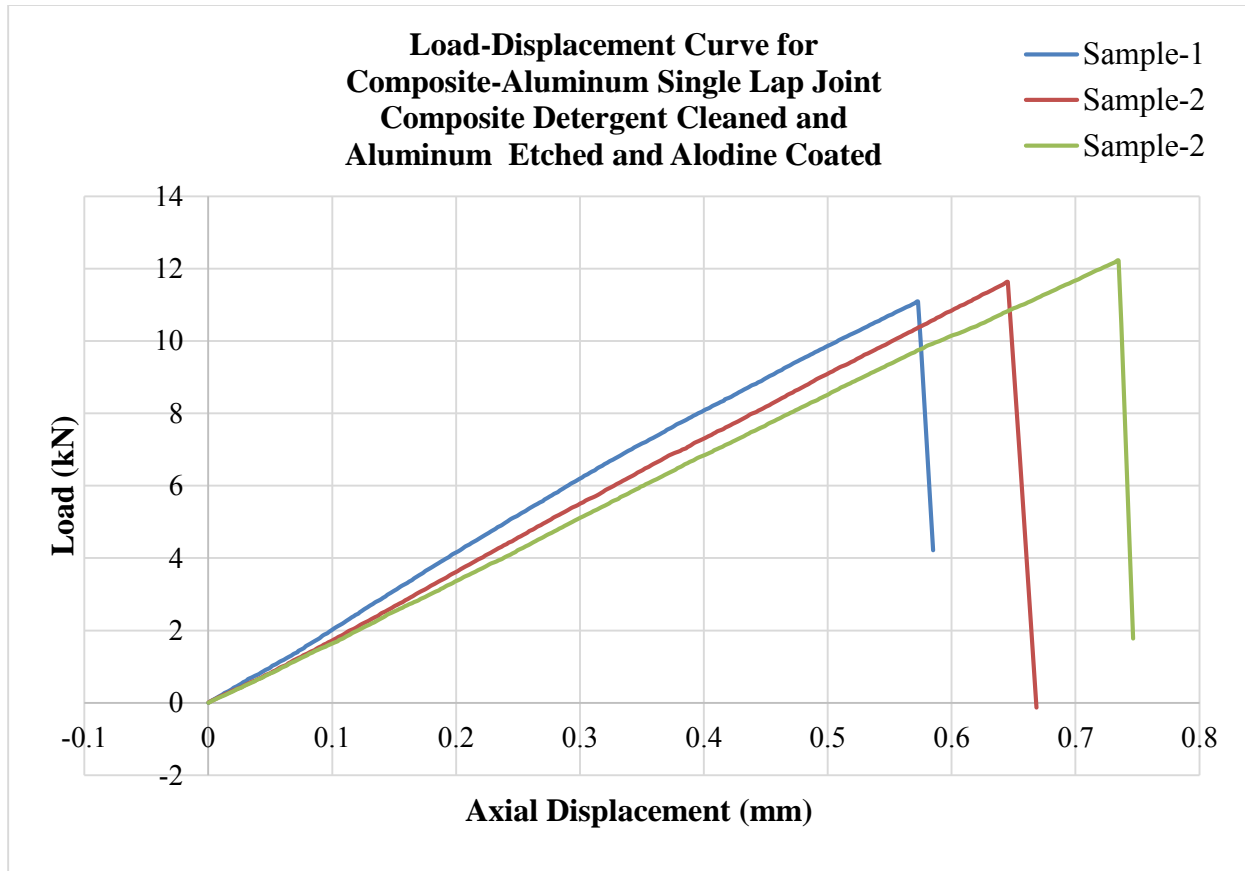


Figure 4.27. Load vs. displacement graph for eleventh set of samples

From Figure 4.27, it can be seen that the nature of the graph is linear. The failure mode for all three samples tested varied from 11 KN to 12.3 KN. The average failure load calculated was 11.64 kN. Figure 4.26 show the stress versus strain graph to obtain maximum joint strength.

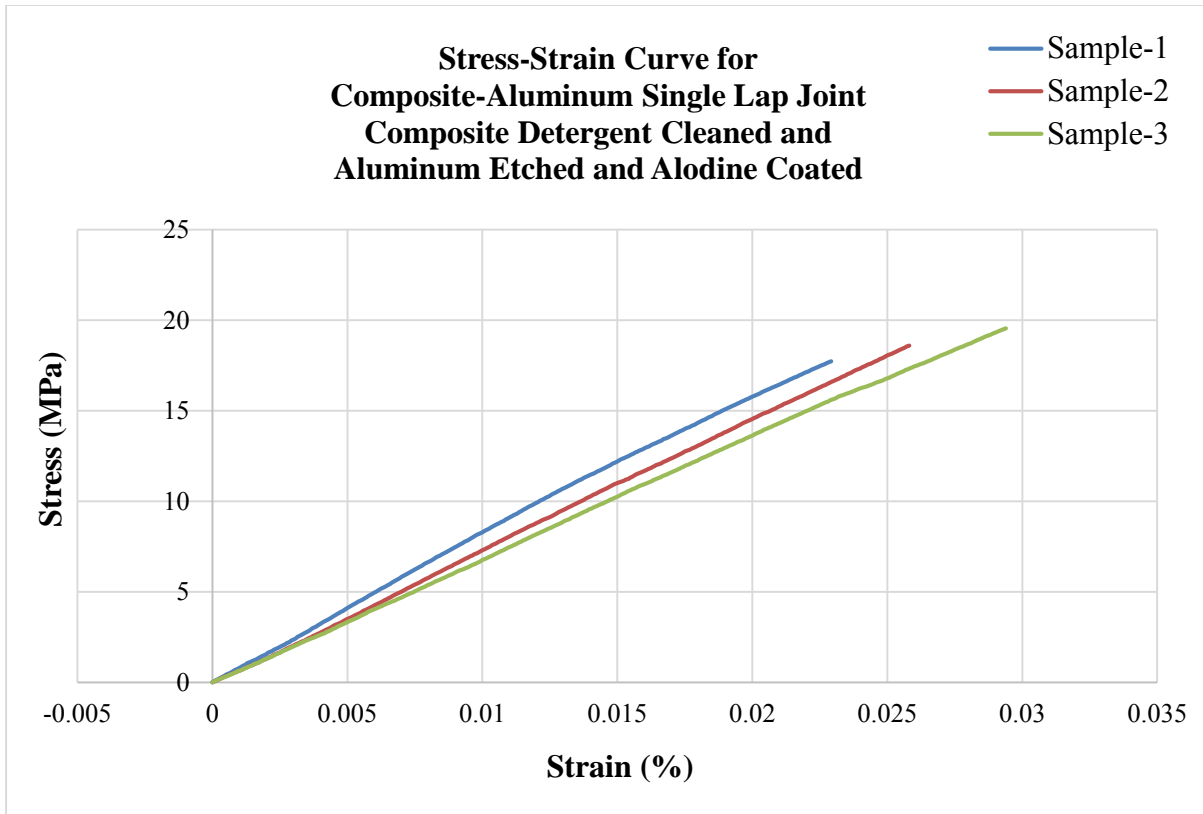


Figure 4.28. Stress vs. strain graph for eleventh set of samples.

Figure 4.28 shows that the joint strength varied between 17.5 MPa and 19.7 MPa, with an average strength of 18.63 MPa. Table 4.17 shows joint strength and failure load when the composite surface was detergent cleaned and the aluminum surface was alodine coated.

TABLE 4.17

**JOINT STRENGTH AND FAILURE LOAD WHEN COMPOSITE SURFACE DETERGENT  
CLEANED AND ALUMINUM SURFACE ETCHED AND ALODINE COATED**

<b>Sample ID</b>	<b>Failure Load (KN)</b>	<b>Joint Strength (MPa)</b>
1	11.08	17.74
2	11.63	18.60
3	12.22	19.55
Average	11.64	18.63
Standard Deviation	0.59	0.91

The twelfth set of samples prepared were single lap joints between composites and aluminum. The composite surface was cleaned with detergent, while the aluminum surface was sanded with sandpaper P 400 and then plasma treated for 4 minutes. The overlap length was fixed at 25 mm. Figure 4.29 is a graphical representation showing the failure load, that is, the load at which the joint failed.

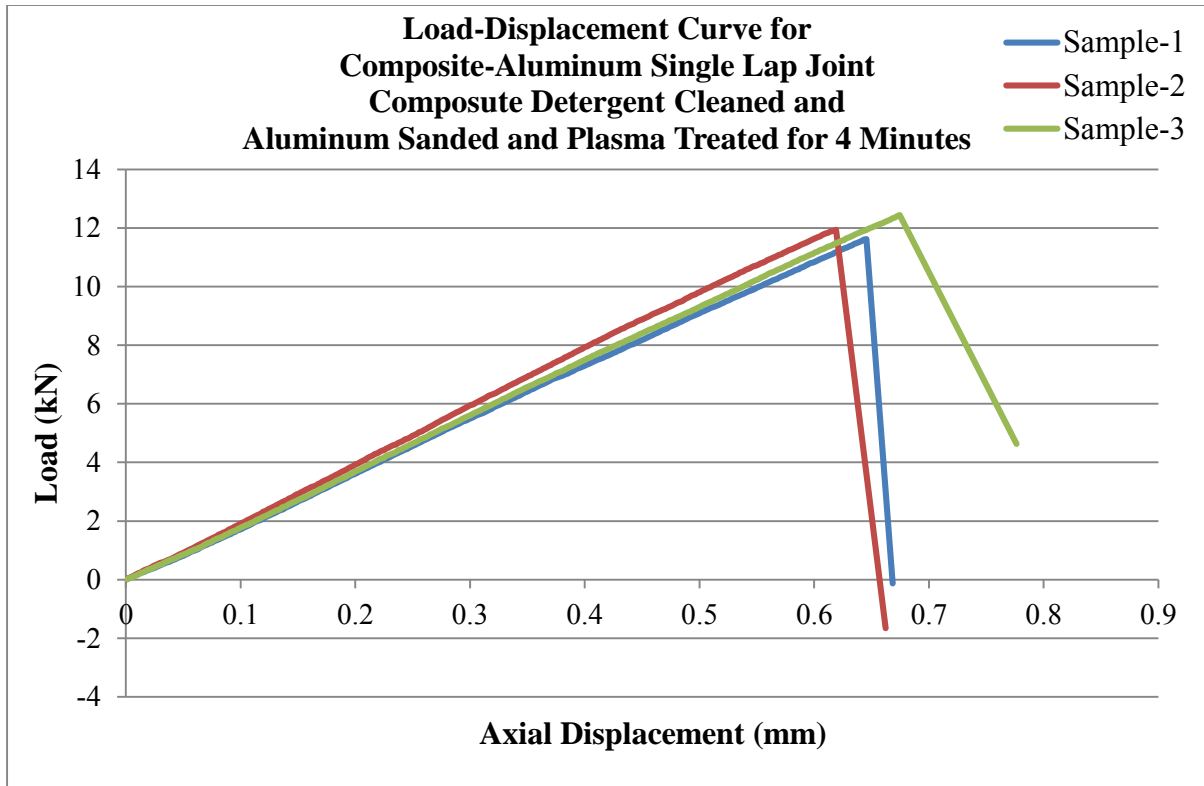


Figure 4.29. Load vs. displacement graph for twelfth set of samples.

From Figure 4.29, it can be seen that the nature of the graph is linear. The failure mode for all three samples tested varied from 11.5 kN to 12.6 kN. The average failure load calculated was 12.03 kN. Figure 4.30 show the stress versus strain graph to obtain maximum joint strength.

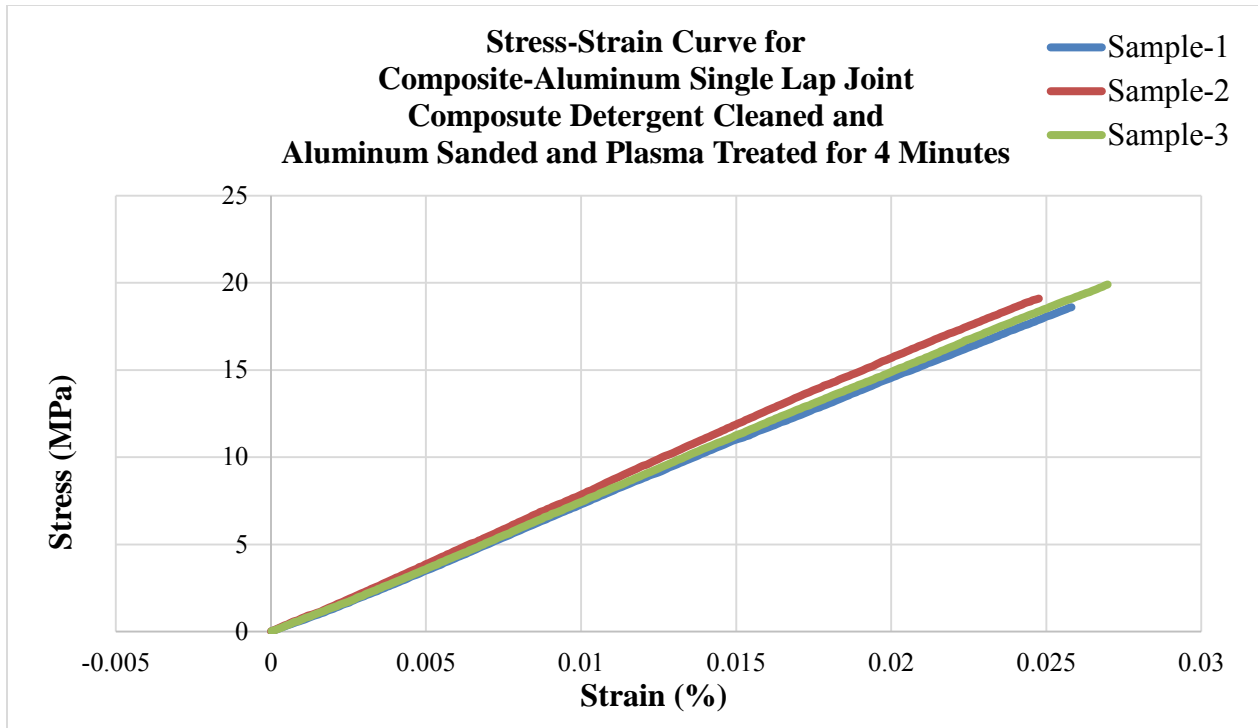


Figure 4.30. Stress vs. strain graph for twelfth set of samples.

From Figure 4.30, it can be concluded that the joint strength varied between 19 MPa and 20 MPa, with an average strength of 19.37 MPa. Table 4.18 shows joint strength and failure load when the composite surface was detergent cleaned and the aluminum surface was sanded and plasma treated for 4 minutes.

TABLE 4.18

JOINT STRENGTH AND FAILURE LOAD WHEN COMPOSITE SURFACE DETERGENT CLEANED AND ALUMINUM SURFACE SANDED AND PLASMA TREATED FOR 4 MINUTES

Sample ID	Failure Load (KN)	Joint Strength (MPa)
1	11.69	19.08
2	11.94	19.10
3	12.45	19.91
Average	12.03	19.37
Standard Deviation	0.39	0.47

The thirteenth set of samples prepared were single lap joints between composites and aluminum. The composite surface was cleaned using detergent, while the aluminum surface was sanded with sandpaper P 400 and then plasma treated for 8 minutes. The overlap length was fixed at 25 mm. Figure 4.31 is graphical representation showing the failure load, that is, the load at which the joint failed.

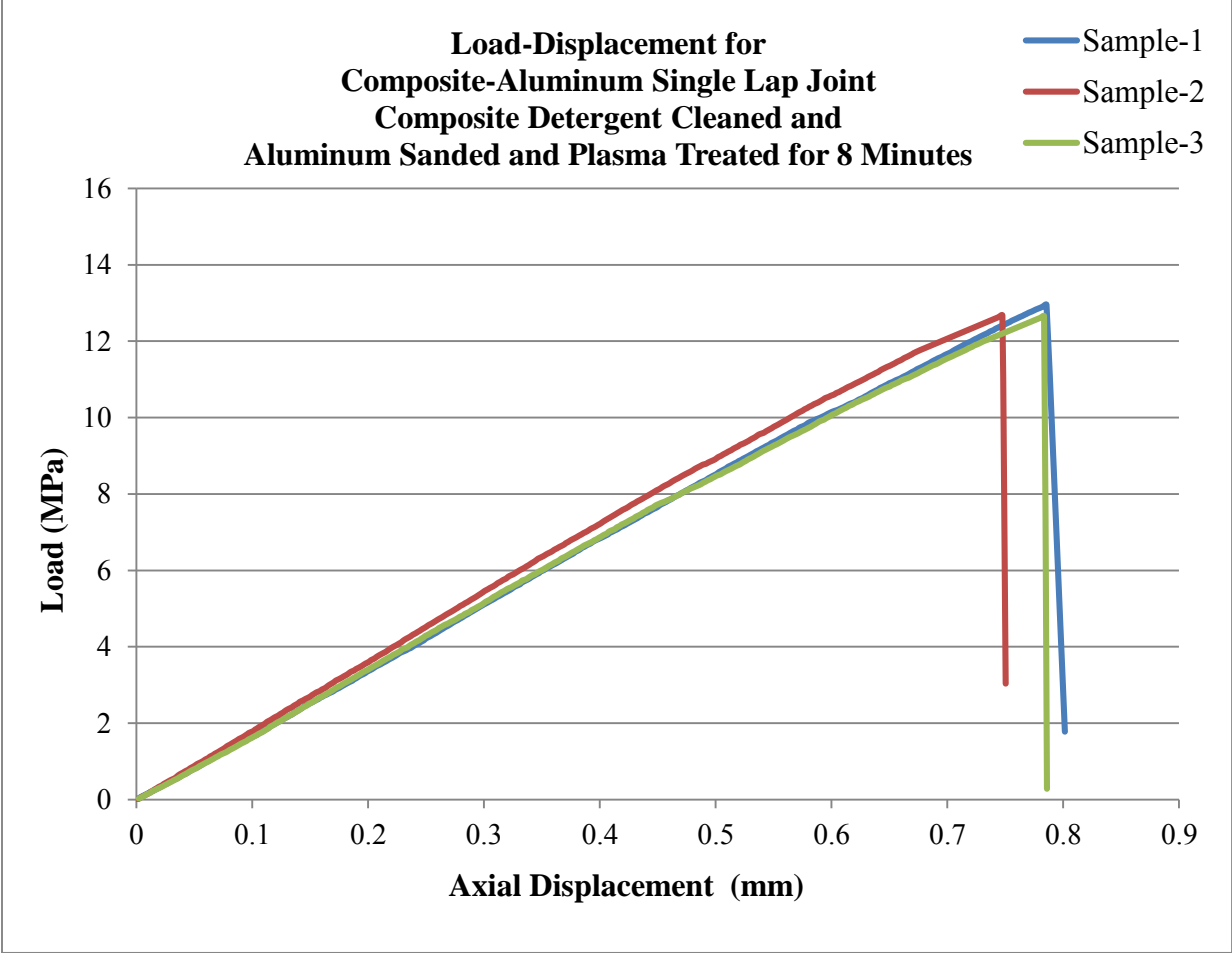


Figure 4.31. Load vs. displacement graph for thirteenth set of samples.

From Figure 4.31, it can be seen that the nature of the graph is linear. The failure mode for all three samples tested varied from 12.5 KN to 13 KN. The average failure load calculated was 12.74 kN. Figure 4.32 show the stress versus strain graph to obtain maximum joint strength.

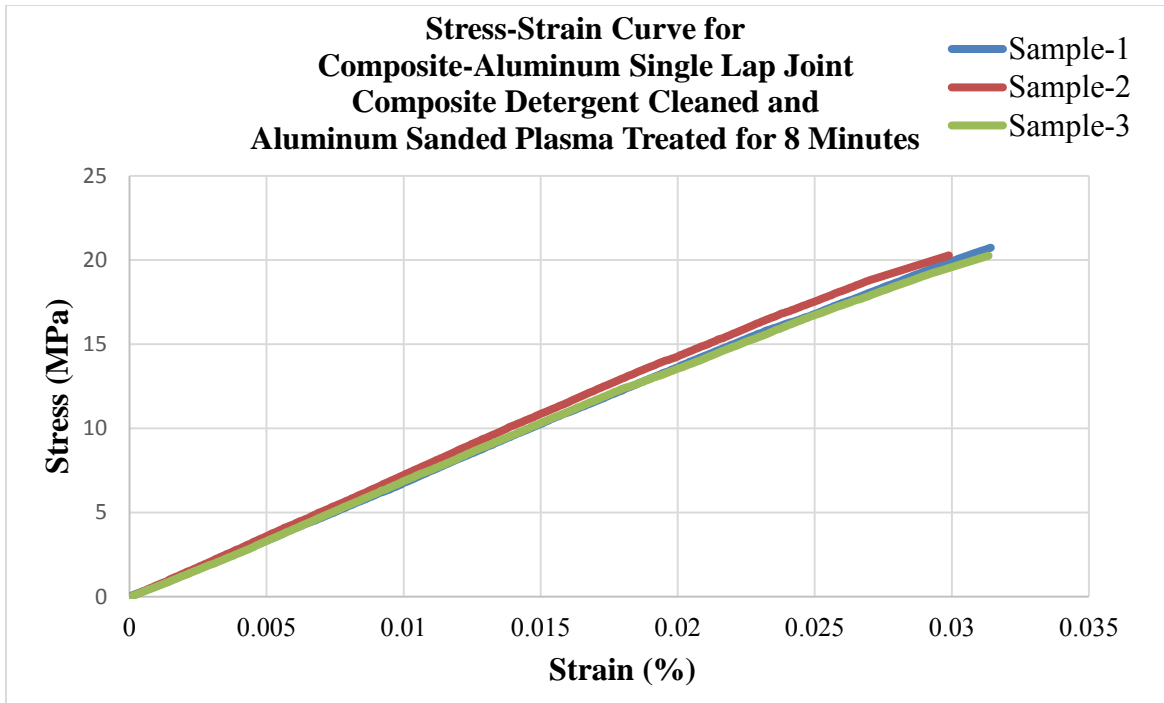


Figure 4.32. Stress vs. strain graph for thirteenth set of samples.

From Figure 4.32, it can be seen that the joint strength varied between 20 MPa and 21 MPa, with an average strength of 20.39 MPa. Table 4.19 shows the joint strength and failure load when the composite surface was detergent cleaned, while the aluminum surface was sanded and plasma treated for 8 minutes.

TABLE 4.19

JOINT STRENGTH AND FAILURE LOAD WHEN COMPOSITE SURFACE DETERGENT  
CLEANED AND ALUMINUM SURFACE SANDED AND PLASMA TREATED  
FOR 8 MINUTES

Sample ID	Failure Load (KN)	Joint Strength (MPa)
1	12.95	20.73
2	12.67	20.28
3.	12.61	20.17
Average	12.74	20.39
Standard Deviation	0.18	0.30

The fourteenth set of samples prepared were single lap joints between composites and aluminum. The composite surface was cleaned with detergent, while the aluminum surface was sanded with a sandpaper P 400 and then UV treated for 4 days. The overlap length was fixed at 25 mm. Figure 4.33 is graphical representation showing the failure load, that is, the load at which the joint failed.

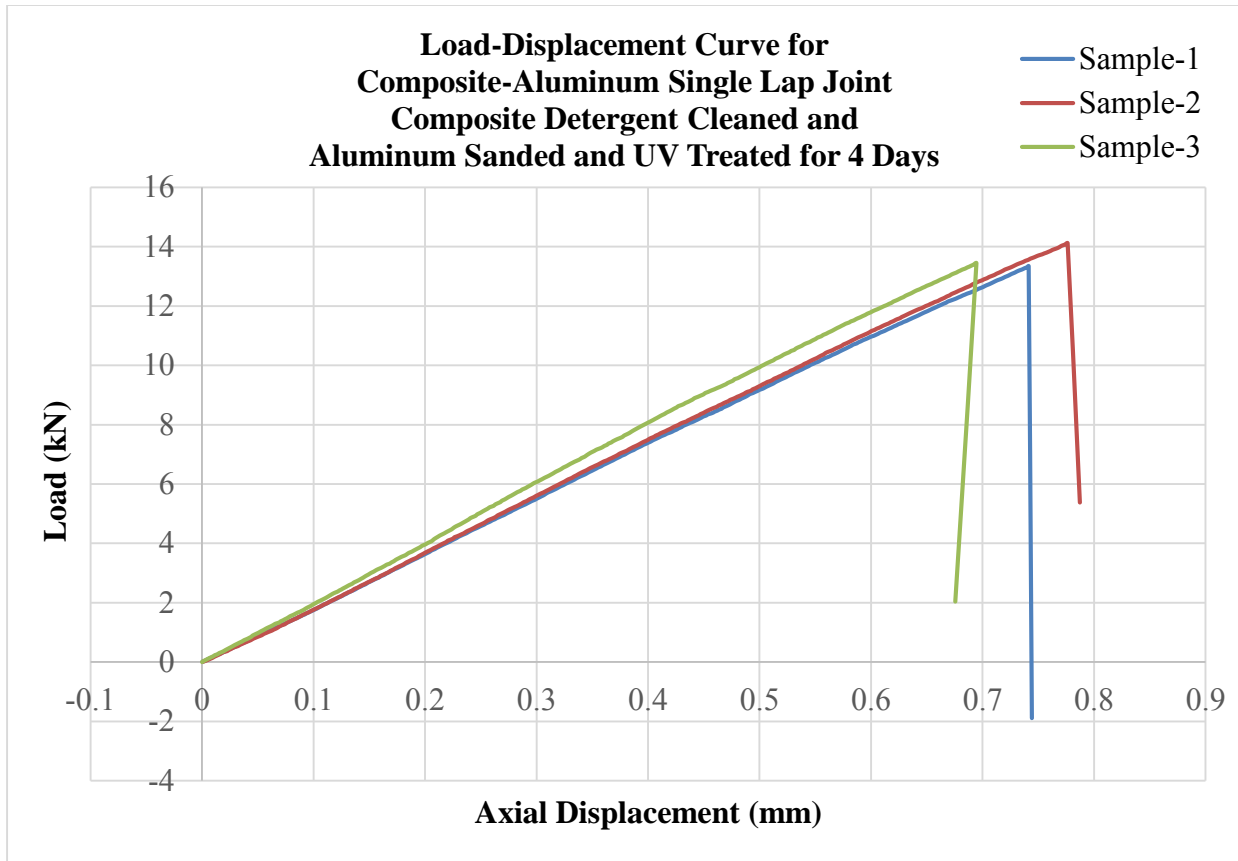


Figure 4.33. Load vs. displacement graph for fourteenth set of samples.

From Figure 4.33, it can be seen that the nature of the graph is linear. The failure mode for all three samples tested varied from 13.3 kN to 14.2 kN. The average failure load calculated was 13.65 kN. Figure 4.34 show the stress versus strain graph to obtain maximum joint strength.

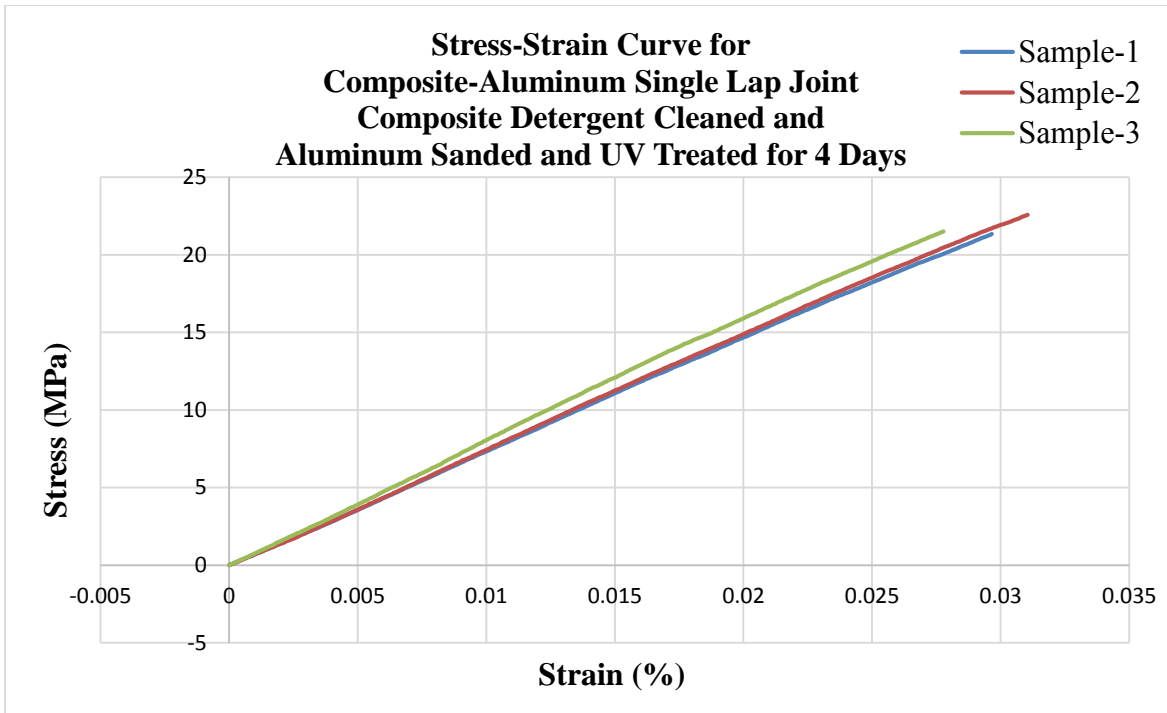


Figure 4.34. Stress vs. strain graph for fourteenth set of samples.

From Figure 4.34, it can be concluded that the joint strength varied between 21.2 MPa and 22.7 MPa, with an average strength of 21.81 MPa. Table 4.20 shows joint strength and failure load when the composite surface was detergent cleaned, while the aluminum surface was sanded and UV treated for 4 days.

TABLE 4.20

JOINT STRENGTH AND FAILURE LOAD WHEN COMPOSITE SURFACE DETERGENT CLEANED AND ALUMINUM SURFACE SANDED AND UV TREATED FOR 4 DAYS

Sample ID	Failure Load (kN)	Joint Strength (MPa)
1	13.39	21.34
2	14.12	22.59
3	13.44	21.51
Average	13.65	21.81
Standard Deviation	0.41	0.68

The fifteenth set of samples prepared were single lap joints between composites and aluminum. The composite surface was cleaned with detergent, while the aluminum surface was sanded with sandpaper P 400 and then UV treated for 8 days. The overlap length was fixed at 25 mm. Figure 4.35 is graphical representation showing the failure load, that is, the load at which the joint failed.

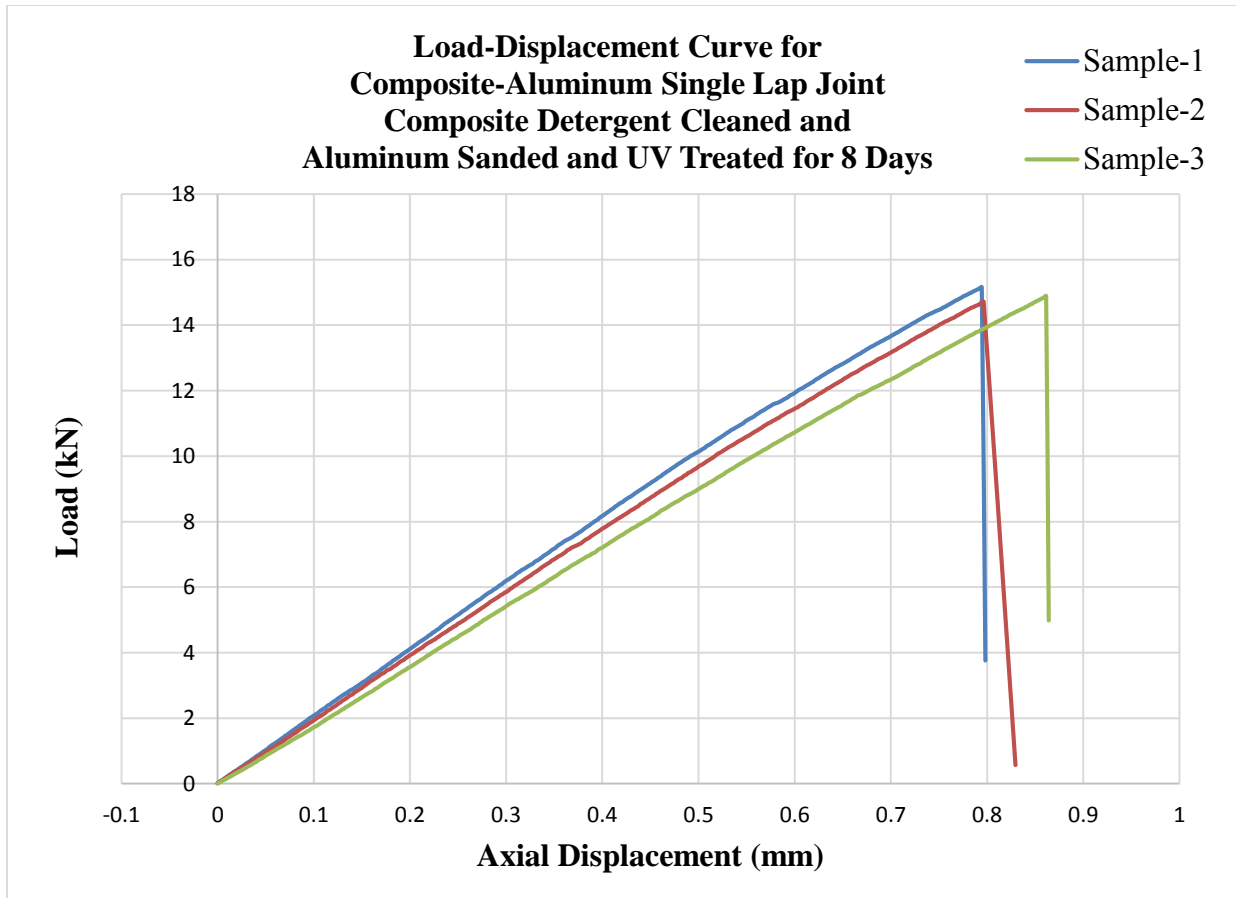


Figure 4.35. Load vs. displacement graph for fifteenth set of samples.

From Figure 4.35, it can be seen that the nature of the graph is linear. The failure mode for all three samples tested varied from 14.5 kN to 15.2 kN. The average failure load calculated was 13.65 kN. Figure 4.36 show the stress versus strain graph to obtain maximum joint strength.

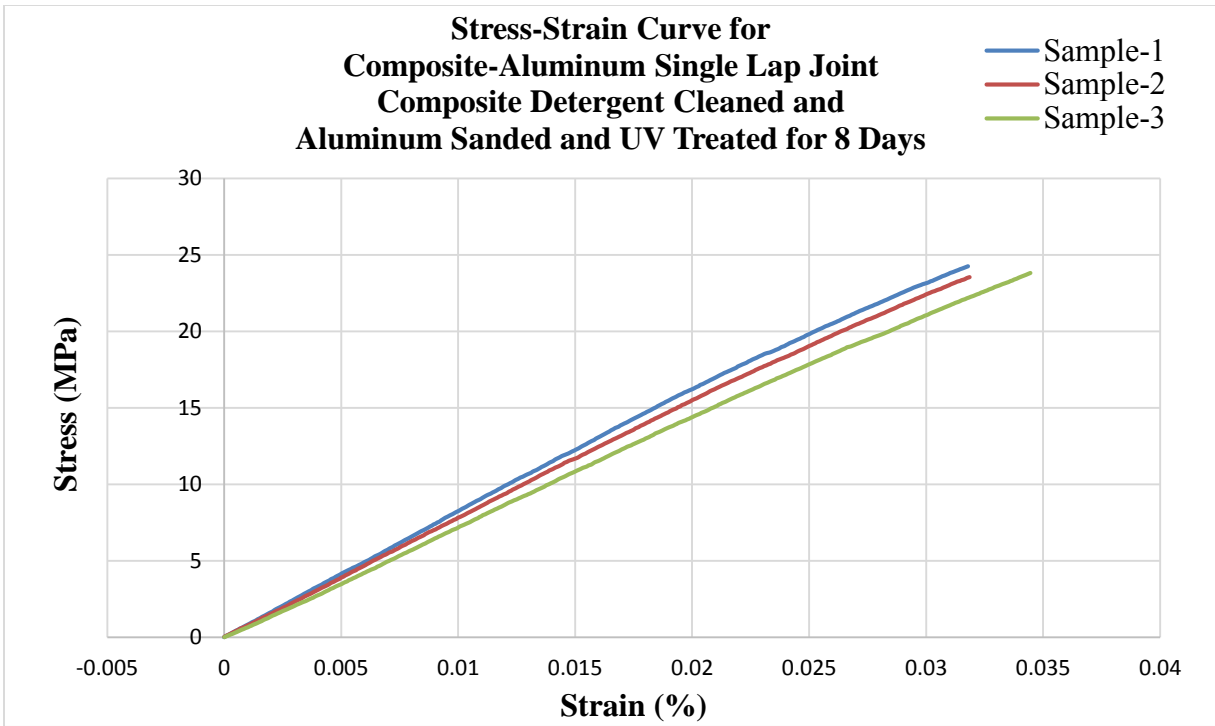


Figure 4.36. Stress vs. strain graph for fifteenth set of samples.

From Figure 4.36, it can be concluded that the joint strength varied between 23.5 MPa and 24.5 MPa, with an average strength of 23.87 MPa. Table 4.21 shows joint strength and failure load values when the composite surface was detergent cleaned, while the aluminum surface was sanded and UV treated for 8 days.

TABLE 4.21

JOINT STRENGTH AND FAILURE LOAD WHEN COMPOSITE SURFACE DETERGENT  
CLEANED AND ALUMINUM SURFACE SANDED AND UV TREATED  
FOR 8 DAYS

Sample ID	Failure Load (kN)	Joint Strength (MPa)
1	15.16	24.25
2	14.71	23.54
3	14.88	23.81
Average	14.92	23.87
Standard Deviation	0.28	0.36

Table 4.22 shows the average failure load and standard deviation calculation for different types of aluminum surface preparations.

TABLE 4.22

AVERAGE FAILURE LOAD AND STANDARD DEVIATION  
FOR DIFFERENT ALUMINUM SURFACE PREPARATIONS

<b>Serial No.</b>	<b>Surface Preparation</b>	<b>Average Failure Load (kN)</b>	<b>Standard Deviation</b>
1.	Base sample detergent cleaned only	9.46	0.23
2.	Sample sanded and detergent cleaned	10.90	0.57
3.	Sample etched and alodine coated	11.64	0.57
4.	Sample sanded, detergent cleaned, and plasma treated for 4 minutes	12.03	0.39
5.	Sample sanded, detergent cleaned, and plasma treated for 8 minutes	12.74	0.18
6.	Sample sanded, detergent cleaned, and UV treated for 4 days	13.65	0.41
7.	Sample sanded, detergent cleaned, and UV treated for 8 days	14.92	0.28

Figure 4.37 shows the variation in failure loads for different combinations of aluminum surface treatments. From these results, it can be concluded that sanding the surface plays a very important role in enhancing the quality of an adhesive bond joint. It was observed that when sanding was combined with either plasma treatment or UV treatment, the failure load was higher than individual treatments alone. Also, it can be concluded that a combination of different surface treatments can further improve the adhesive bond quality. Maximum failure load was observed when the sample was sanded and UV treated for 8 days, while the minimum failure load was observed for samples that were only detergent cleaned. Table 4.23 shows the average joint strength and standard deviation for different types of aluminum surface preparations. Figure 4.38 shows the variation in joint strength for different aluminum surface treatments.

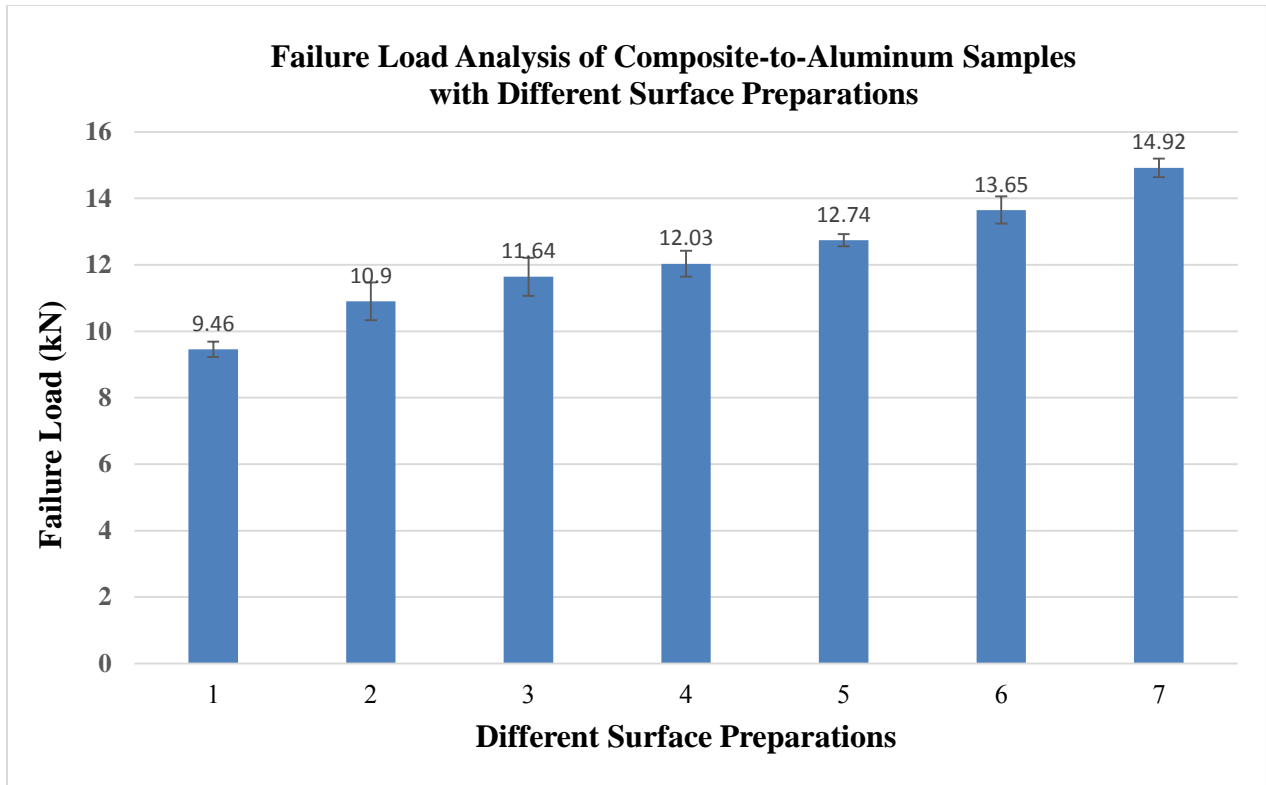


Figure 4.37. Variation in failure load for different aluminum surface preparations.

TABLE 4.23

AVERAGE JOINT STRENGTH AND STANDARD DEVIATION  
FOR DIFFERENT ALUMINUM SURFACE PREPARATIONS

Serial No.	Surface Preparation	Average Strength (MPa)	Standard Deviation
1.	Base sample detergent cleaned only	15.14	0.36
2.	Sample sanded and detergent cleaned	17.43	0.92
3.	Sample etched and alodine coated	18.63	0.91
4.	Sample sanded, detergent cleaned, and plasma treated for 4 minutes	19.37	0.47
5.	Sample sanded, detergent cleaned, and plasma treated for 8 minutes	20.39	0.30
6.	Sample sanded, detergent cleaned, and UV treated for 4 days	21.81	0.68
7.	Sample sanded, detergent cleaned, and UV treated for 8 days	23.87	0.36

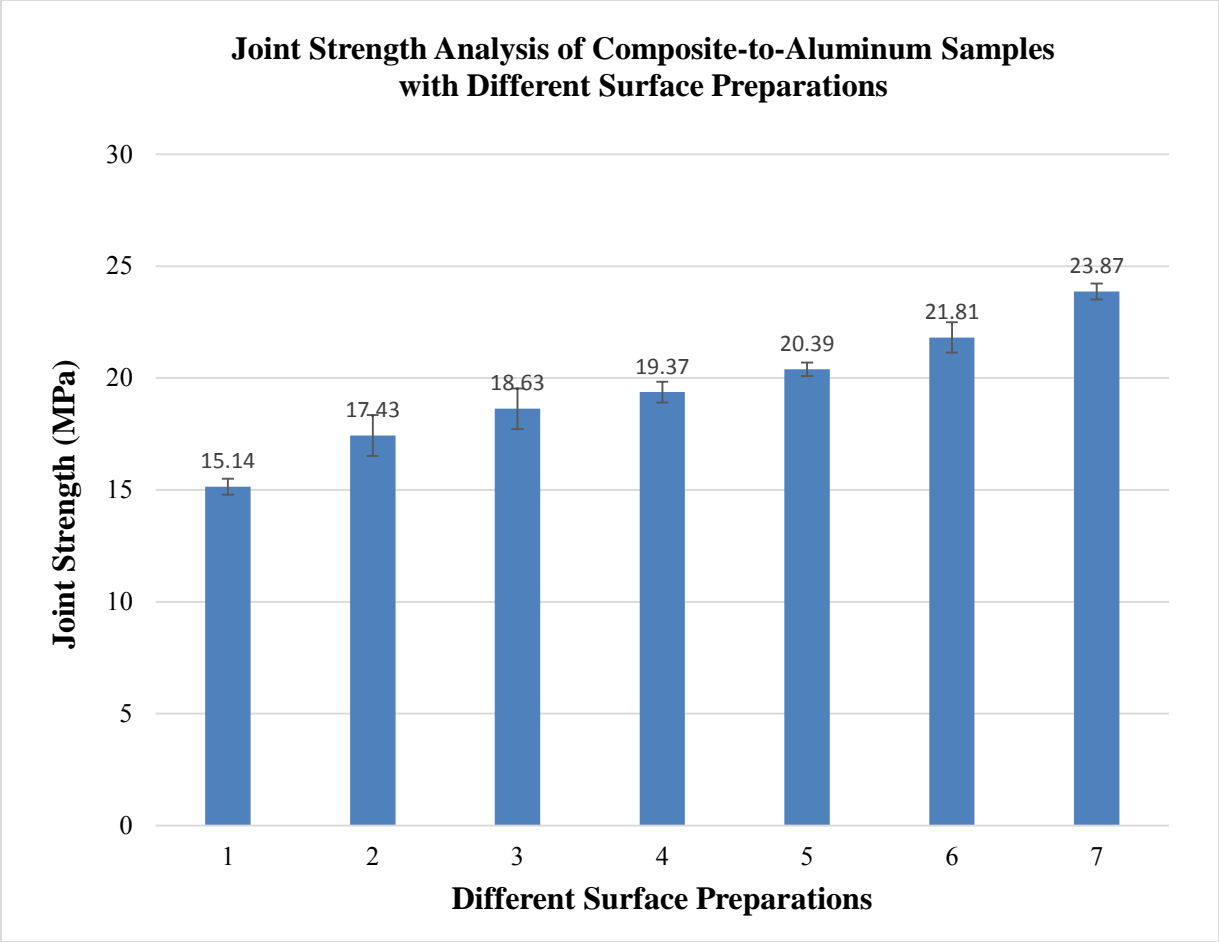


Figure 4.38. Variation in joint strength for different aluminum surface preparations.

From these results, it can be concluded that surface sanding plays a very important role in enhancing the quality of an adhesive bond joint. It was observed that when sanding was combined with either plasma treatment or UV treatment, the joint quality further improved. Also, it can be concluded that a combination of different surface treatments can further improve the bond strength. For example, the sample that was sanded and UV treated for 8 days yielded a maximum joint strength of 23.87 MPa, whereas the sample that was detergent cleaned only yielded a joint strength of only 15.14 MPa. Thus, it can be concluded that a combination of surface treatments is more effective.

After the sample testing was completed, the surfaces of the bonded areas were observed with a naked eye to determine the type of failure. Figures 4.39 and 4.40 show images of the composite-to-composite joint as well as the composite-to-aluminum joint. It can be seen that all three types of failure—adhesive failure, cohesive failure, and substrate failure—occurred. In the image on the left in Figure 4.39, it can be seen that the adhesive layer was completely ripped away from the substrate, thus indicating adhesive failure. The right-hand image in Figure 4.39 indicates both adhesive failure and cohesive failure. In Figure 4.40, the left image shows both adhesive and cohesive failure, as well as substrate failure on the composite surface. The right-hand image in Figure 4.40 again shows both adhesive and cohesive failure.

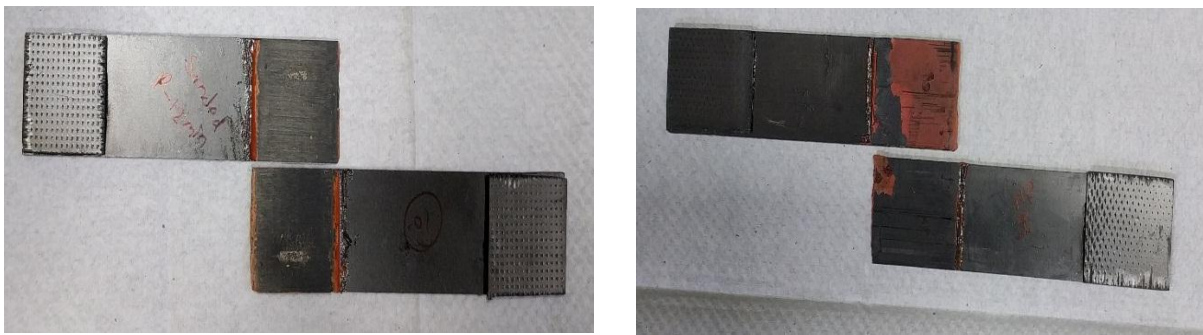


Figure 4.39. Failures observed in composite-to-composite lap joint.

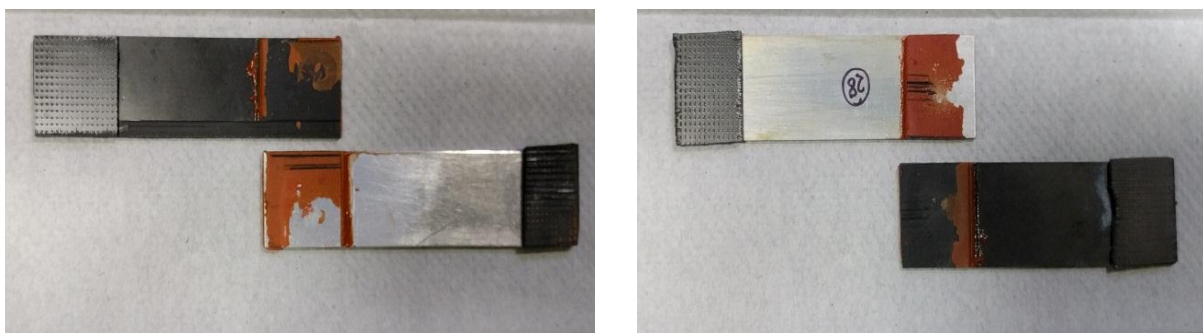


Figure 4.40. Failures observed in aluminum-to-composite lap joint.

The results obtained were then compared with previous studies, which is summarized below. According to the research conducted by Kim et al., when abrasive paper of grit size 320 was used on the composite surface, the failure load result varied between 14 kN and 15 kN for a

secondary bonded specimen, and the nature of the graph was not linear. The failure load calculated for the co-cured sample varied from 10 kN to 14 kN. The joint strength calculated was 27.6 MPa in the case of secondary bonding, while the joint strength in the case of the co-cured sample was 23.6 MPa. After using mesh paper P 400 for sanding, the joint strength was found to be 28.7 MPa [17].

In other research by Kim et al., the overlap length was kept at 25 mm for one of the samples. Here, the joint strength achieved was 23.6 MPa while the failure load was 14.7 kN [18].

Another research study by Parker and Waghorne showed that when the abrasion of the surface was done by handheld silicon carbide sandpaper of grit size 240 and 320, the joint strength achieved was 22 MPa [19].

When these results were compared to the present research, the failure load for base samples calculated was 11.51 kN, and the joint strength calculated was 18.42 MPa. When the surface was sanded using a mesh paper of grit size P 400, the failure load was 13.66 kN, while the joint strength was 21.86 MPa. For an aluminum-to-composite lap joint, a failure load of 9.46 kN was observed, while a joint strength of 15.14 MPa was achieved. When the aluminum surface was sanded, the failure load increased to 10.9 kN, while the joint strength was 15.14 MPa. Thus, it was found that the variation in results compared to previous research was due to the different types of adhesives used. Also, the grit size of the sandpaper affected the variation in failure load and joint strength. But when the surface was treated with a combination of different surface preparations, results showed an enhancement in joint strength and quality.

## CHAPTER 5

### CONCLUSION

The failure mode and joint strength of a single lap joint bonded by an adhesive was tested using different kinds of surface treatments and preparations. The primary focus of this research was to prepare a surface that has efficient wettability and adhesion so that the adhesive spreads properly on the surface, thus improving the bond strength. It was concluded that the joint strength of a composite-to-composite single lap joint was greater than that of a composite-to-aluminum single lap joint.

Sanding plays a predominant role in improving the bond quality of a joint by preparing an adequate surface. It was observed that when the surface was sanded with sandpaper, the surface to be bonded was made rougher and the surface area on the sample was increased. Thus, the oily layer on the bonding surface was removed and the surface made more reactive by increasing the mechanical interlocking. Due to an increase in the surface area, bond strength was also increased as a result of an enhancement in intermolecular forces.

Throughout this research it was observed that the failure load and joint strength were greater for specimens treated with a combination of surface preparations. In the case of a composite-to-composite lap joint, it was observed that when surface sanding was combined with plasma cleaning, the failure load and joint strength achieved were highest when compared to individual surface treatments alone. The best results were acquired when surface sanding was combined with plasma treatment for 12 minutes.

In the case of a composite-to-aluminum joint, the composite was detergent cleaned only and surface treatment was carried out on aluminum. Also, in the case of a composite-to-aluminum joint, it was observed that a combination of different surface treatments was required to raise the

bond quality. Surface sanding was also combined with plasma treatment, but when surface sanding on aluminum was combined with UV treatment, the highest bond quality was achieved. Results showed that surface sanding in combination with UV treatment for 8 days gave the greatest bond strength and failure load.

When all samples were analyzed for failure modes, it was found that the majority of samples showed both adhesive as well as cohesive failure, while some composite surfaces showed substrate failure as well.

## **CHAPTER 6**

### **FUTURE WORK**

This area of research is vast. Some different techniques and materials could be used in the future to further improve bond strength. Below are some suggestions that could be effective in achieving a bonded structure of highest quality:

- Nanomaterials could be used with an adhesive, thus enhancing its strength and resulting in a structure of high strength.
- Different overlap lengths could be used to observe the effect of bonding length on the strength of an adhesive.
- In this research, the direction of sanding was longitudinal; in the future, the direction of sanding could be changed to observe the change in bond strength.
- Research could be carried out using ceramic- and aramid fiber-based composites to observe the bond quality and strength.
- A different combination of different surface treatments could be carried out to improve bond strength.
- The joint could be designed in such a way that it would have good resistance to delamination. If this improvement could be achieved, the maximum strength of adhesive could be utilized.
- Stronger adhesives for bonding the structure more strongly could be introduced.

## REFERENCES

## REFERENCES

- [1] Sanjay K. Mazumdar, "Introduction," in *Composite Manufacturing: Materials, Product, and Process Engineering*, CRC Press LLC, 2002, pp. 1-2.
- [2] Sanjay K. Mazumdar, "Introduction," in *Composite Manufacturing: Materials, Product, and Process Engineering*, CRC Press LLC, 2002, pp. 4-10.
- [3] Alphonsus V. Pocius, "Introduction," in *Adhesion and Adhesives Technology*, Third Edition, Carl Hanser Verlag, Munich 2012, pp. 1-15
- [4] Sanjay K. Mazumdar, "Joining of composite materials," in *Composite Manufacturing: Materials, Product, and Process Engineering*, CRC Press LLC, 2002, pp. 309-312.
- [5] Susan E.M. Selke, John D. Culter, and Ruben J. Hernandez, "Adhesion, adhesives and heat sealing," in *Plastics Packaging: Properties, Processing, Applications, & Regulations*, Third Edition, Hanser Publications, 2000, pp. 185-212.
- [6] Raymond F. Wegman and James Van Twisk, "Plastics," in *Surface Preparation Techniques for Adhesive Bonding*, Second Edition, Elsevier, Inc., 2013, pp. 115-130.
- [7] J.D. Venables, Review of "Adhesion and durability of metal-polymer bonds," *Journal of Material Science*, Volume 19, Issue 8, August 1984, pp. 2431-2453.
- [8] Andrew D. Crocombe and Ian A. Ashcroft, "Simple lap joint geometry," in *Modeling of Adhesively Bonded Joints*, Springer, 2008, pp. 3-23.
- [9] Sina Ebnesajjad, "Introduction to surface preparation," in *Surface Treatment of Materials for Adhesion Bonding*, William Andrew Inc., 2006, pp. 1-23.
- [10] Sanjay K. Mazumdar, "Joining of composite materials," in *Composite Manufacturing: Materials, Product, and Process Engineering*, CRC Press LLC, 2002, pp. 313-322.
- [11] ChemQuest Group, "Surface treatment," URL: [http://www.adhesives.org/docs/default-document-library/surfaceprep\\_adhesives-org.pdf](http://www.adhesives.org/docs/default-document-library/surfaceprep_adhesives-org.pdf) [cited July, 2016].
- [12] Alphonsus V. Pocius, "The surface preparation of adherends for adhesive bonding," in *Adhesion and Adhesive Technology*, Third Edition, Carl Hanser Verlag, Munich 2012, pp. 181-200.
- [13] Alphonsus V. Pocius, "The surface preparation of adherends for adhesive bonding," *Adhesion and Adhesive Technology*, Third Edition, Carl Hanser Verlag, Munich 2012, pp. 211-212.
- [14] MAC SST-50 EDC-Aluminum Coating Options, Alodine-Cerakote-HAIII, URL: <http://www.candlepowerforums.com/vb/showthread.php?312700-MAC-SST-50-EDC-> [cited July 2016].

## REFERENCES (continued)

- [15] Y. Kawamura, K. Toyoda, and S. Namba, "Effective deep ultraviolet photoetching of polymethyl methacrylate by an excimer laser," *Applied Physics Letters*, Volume 40, Issue 5, 1982, p. 374.
- [16] Askeland, P. A. and Drzal, L. T., "Adhesion Science for the 21<sup>st</sup> Century, Proceedings of the 23rd Annual Meeting of the Adhesion Society, Myrtle Beach South Carolina, 2000, pp. 180, [cited July 2016].
- [17] Kwang-Soo Kim, Jae-Seok Yoo, Yeong-Moo Yi, and Chun-Gon Kim, "Failure mode and strength of uni-directional composite single lap bonded joints with different bonding methods," *Composite Structures*, Volume 72, issue 4, April 2006, pp. 477-485.
- [18] T.-H. Kim, J.-H. Kweon, and J. H., Choi, "An experimental study on the effect of overlap length on the failure of composite to aluminum single lap bonded joints," *Journal of Reinforced Plastics and Composites*, Volume 27, No. 10, 2008, pp. 1071-1081.
- [19] J.-H. Kweon, J. W. Jung, T. H. Kim, J. H. Choi, and D. H. Kim, "Failure of carbon composite to aluminum joints with combined mechanical fastening and adhesive bonding," *Composite Structures*, Volume 75, Issue 1-4, September 2006, pp. 192-198.
- [20] L. W. Crane, C. L. Hamermesh, and L. Malls, "Surface treatment of cured epoxy graphite composites to improve adhesive bonding," *SAMPE Journal*, Volume 12, 1976, pp. 6-9.
- [21] B.M. Parker and R.M. Waghorne, "Surface pre-treatment of carbon fibre-reinforced composites for adhesive bonding," *Composites*, Volume 13, Issue 3, July 1982, pp. 280-288.
- [22] European Agent, RDR Aerospace Ltd, Magnolia Plastics Inc., Magnolia 6380 A/B, URL: [http://www.google.com/url?q=http://www.rdr-aerospace.co.uk/magnolia\\_data/MagnoliaStructural.pdf&sa=U&ved=0ahUKEwjvuonFwJ7OAhVr5YMKHT2EAyMQFggUMAA&usg=AFQjCNEAVKfvGUZ1z84J8qm-bH7d5WY2gQ](http://www.google.com/url?q=http://www.rdr-aerospace.co.uk/magnolia_data/MagnoliaStructural.pdf&sa=U&ved=0ahUKEwjvuonFwJ7OAhVr5YMKHT2EAyMQFggUMAA&usg=AFQjCNEAVKfvGUZ1z84J8qm-bH7d5WY2gQ) [cited July 2016].
- [23] Magnolia Plastics Inc., Technical Data Sheet, Magnobond 6380 A/B, URL: [http://www.bivas.co.il/image/users/75693/ftp/my\\_files/TDS+Magnobond+6380.doc](http://www.bivas.co.il/image/users/75693/ftp/my_files/TDS+Magnobond+6380.doc) [cited July 2016].
- [24] Henkel, Surface Technologies, Technical Bulletin No. 234449, Revision 09/15/2006, URL: <https://henk0008.home.xs4all.nl/Turco/TURCO%20ALUMIPREP%2033.pdf> [cited July 2016].
- [25] Henkel, Technical Process Bulletin No. 235110, Alodine® 1201, Revision 01/08/2004, URL: <https://www.aircraftspruce.com/catalog/pdf/alodine1201tds.pdf> [cited July 2016].

## REFERENCES (continued)

- [26] OnlineMetals.com, Custom Metal and Plastics Supply, 2024-T3 Clad Aluminum Sheet, URL: [http://www.onlinemetals.com/merchant.cfm?id=752&step=2&top\\_cat=60](http://www.onlinemetals.com/merchant.cfm?id=752&step=2&top_cat=60) [cited July 2016].
- [27] UCL Eastman Dental Institute, Biomedical and Tissue Engineering Department, URL: <http://www.ucl.ac.uk/eastman/research/departments/biomaterials-and-tissueengineering/facilities/goniometry> [cited July 2016].
- [28] Institute of Organic Chemistry and Biochemistry AS CR, “KSV-CAM 101,” URL: <http://www.uochb.cz/web/structure/1146.html> [cited July 2016].
- [29] Michael J. Hoke, “Adhesive Bonding of Composites,” URL: [http://www.cozybuilders.org/Oshkosh\\_Presentations/AbarisCompositeBondingOshkosh2005.pdf](http://www.cozybuilders.org/Oshkosh_Presentations/AbarisCompositeBondingOshkosh2005.pdf) [cited July 2016].